FUNDAMENTAL PROPERTIES OF FLOTATION FROTHERS AND THEIR EFFECT ON FLOTATION

by

FRANCISCO MELO

B.Sc., University of Concepcion, 2001

A THESIS SUBMITTED IN PARTIAL FULFILLMENT OF
THE REQUIREMENTS FOR THE DEGREE OF

MASTER OF APPLIED SCIENCE

In

THE FACULTY OF GRADUATE STUDIES

MINING ENGINEERING

THE UNIVERSITY OF BRITISH COLUMBIA

March 2005

ABSTRACT

In the present work, five different flotation frothers were tested in order to evaluate their performance in the flotation of two coal samples in terms of their effect on the entrainment of fine particles.

The experimental program included the characterization of the investigated frothers by means of surface tension measurements, dynamic foamability index (DFI), critical coalescence concentration (CCC) and water recovery tests in aqueous solutions. The experiments also included both forward and reverse batch flotation tests in the presence of the tested reagents.

The results indicate that, while there is a clear relationship between water recovery in a two-phase system and the fundamental properties of the frothers, expressed in terms of DFI, the trend observed in the batch flotation tests in the presence of coal for the same frothers is different. This indicates that characterization of flotation frothers in a two-phase experiment is not adequate since the water transport results obtained in the two-phase and three-phase experiments were different.

The reverse flotation tests revealed that dodecyl trimethyl ammonium bromide (DTAB), which is used as a collector for mineral matter and as a frother, generates froths characterized by low water contents and high stability, which promote the entrainment of unwanted particles to the froth collection zone. It was also observed that when polyacrylamide (PAM) was used in addition to the coal depressant (dextrin) and DTAB, the selectivity of the process slightly improved. However, in the presence of PAM, the rates of transfer of water and solids to the froth also increased, which translated into a higher degree of entrainment of coal particles in the froth product.

The selectivity of the coal reverse flotation process and the reagent consumption, at this point of the development of this technology, constitute a problem which remains unsolved.

TABLE OF CONTENTS

LIST OF FIGURES

LIST OF TABLES

ACKNOWLEDGMENTS

The completion of this work would not have been possible without the expert assistance of Dr. Janusz S. Laskowski.

I would also like to thank Dr. Dee Bradshaw for allowing me to spend one month at the Chemical Engineering Department of the University of Cape Town.

Thanks are also due to Dr. Fernando Concha A., for giving me the opportunity of studying with Dr. Laskowski in Canada.

To my family in Chile, thanks for the love, patience and encouragement to accomplish this goal.

Endless thanks to the Jara Family. Their constant support and love made everything easier.

Special thanks to Dr. Marek Pawlik for his continuous advice and help since my first day in this Department.

1. INTRODUCTION.

From a geological point of view coal may be classified as a sedimentary rock consisting of organic components with a minor proportion of mineral constituents. Coals vary in composition and properties in accordance with the extent of the alteration of the original plant material from which they were derived. This degree of alteration of the plant material defines the different varieties of coal, commonly referred to as lignite, sub-bituminous coal, bituminous coal, semi-anthracite and anthracite.

Coal processing embraces a number of unit operations, including blending and homogenization, size reduction, size classification, beneficiation (cleaning) and dewatering. Among all these unit operations, the cleaning stage is the one that governs the total cost of coal preparation. Coal cleaning methods include mostly gravity separation processes, although in the case of metallurgical coals, flotation is commonly used for processing of the fine fractions, as shown in Figure 1b; in the case of thermal coals, the fine fractions are normally rejected without any treatment and only the intermediate and coarse size fractions are cleaned (Figure 1a).

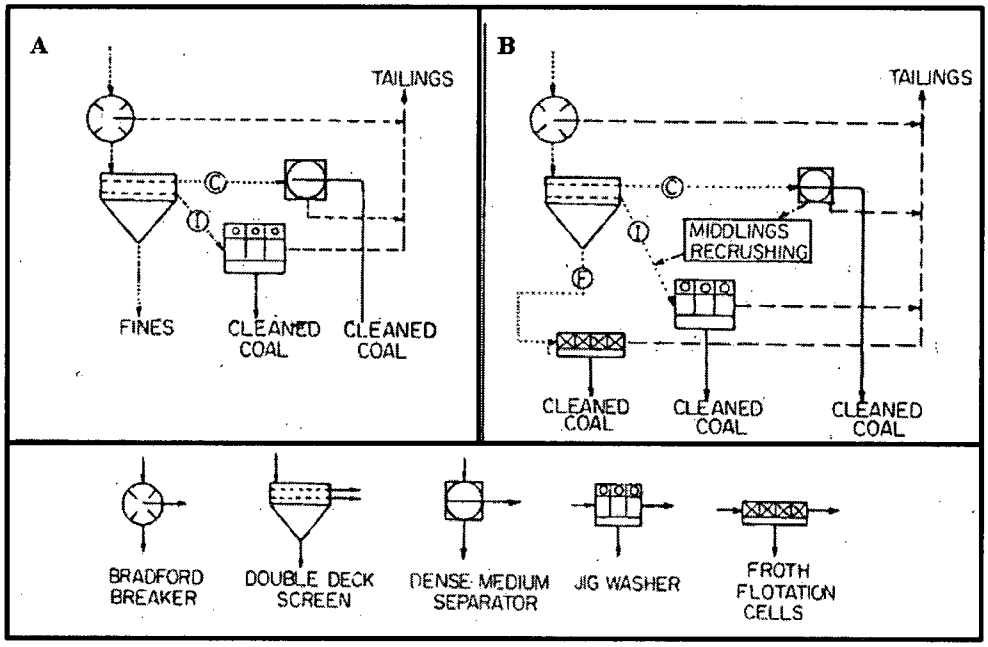

Figure 1: Flowsheets for coal processing. A) Typical process flowsheet for thermal coal plants. B) Typical process flowsheet for metallurgical coal plants.

1.1. Flotation Frothers and their Effect on Entrainment.

In coal preparation, the overall results of the beneficiation of fine particles by flotation are affected, as in any other flotation, by a number of phenomena that affect the quality of the final product. Among them, entrainment is probably one of the most important ones, since its effect is greatly enhanced by the high yields of floating material involved in coal flotation. In this mechanism, the solid particles, irrespective of their surface properties, report to the froth product suspended in the lamellae of water that surround the bubbles. This process is controlled by the water recovery in the froth and it is well known that the higher the amount of water recovered in the concentrate, the higher the degree of entrainment.

The frother type is one of the major factors that affect the water recovery in flotation. This variable, along with the characteristics of the solids, primarily define not only the water content in the froth, but also the stability of the froth, and therefore, the effect of frothing agents on the entrainment of unwanted particles is paramount.

Flotation frothers have been referred to as "powerful" or "selective" for a long time, and only recently a more scientific basis of comparison has arisen through the use of the *dynamic foamability index* (DFI), which characterizes the stability of the foam, and the *critical coalescence concentration* (CCC), which allows to assess the effectiveness of the frother in reducing bubble size.

Although these two indices provide a well founded criterion for the selection and comparison of flotation frothers, they have never been used to relate the characteristics of the frothers to their performance in flotation.

1.2. Coal Reverse Flotation.

The high yields of floating material in coal flotation not only enhance the detrimental effect of non-selective mechanisms such as entrainment and entrapment, but also constraint the use of column cells in coal flotation, due to their limited carrying.

The coal reverse flotation process, in which mineral matter is floated and coal is depressed, seems to be a good alternative to overcome the problems previously mentioned. Moreover, this technology allows to make the coal cleaning process compatible with the

subsequent stage of preparation of Coal Water Slurries (CWS) in the seam-to-steam strategy. However, this new approach also poses problems that need to be addressed, such as the lack of drainage of unwanted particles from the froth, the high reagent consumption and the high froth stability.

1.3. Scope of Work.

In this work, the properties of five different flotation frothers are firstly studied in aqueous solutions and then related to the entrainment of particles in the forward flotation of two different kinds of coals. In addition, since in the reverse flotation of low-rank coal dodecyl trimethyl ammonium bromide (DTAB) is used as a collector for gangue and also as a frother that generates metastable (dry) froths, the performance of this reagent and its effect on the entrainment of coal particles is also assessed.

2. OBJECTIVES.

i) To study the relationship between fundamental properties of flotation frothers and the recovery of particles, varying in wettability, by entrainment in the flotation of two coals of different ranks.

ii) To compare the effect of frothers on the amount of water recovered in two-phase and three-phase systems.

iii) To study the effect of DTAB on the degree of entrainment of coal particles in the reverse flotation of a low-rank coal.

3. LITERATURE REVIEW.

3.1. Flotation Frothers.

3.1.1. General Description and Classification.

Frothers play an important role in flotation. Since they have a direct impact on the characteristics of the froth, and therefore affect variables related to the entrainment of unwanted particles, the proper selection of these reagents is paramount for the overall flotation performance.

It is accepted that frothers:

a) Reduce bubble size.
b) Stabilize the froth.

Flotation frothers must also meet some requirements in order to assure their industrial applicability. The most important ones are summarized below:

a) It must be readily dispersible within the medium.
b) It must have an inert structure that does not interfere and is compatible with the quality and function of the other reagents used in froth flotation.
c) It must not be affected by changes in the pH of the medium in the flotation cell
d) The froth removed containing valuable mineral must easily disengage to allow further treatment.
e) It must be economical, available and have no negative environmental impacts when used on a large scale.

These requirements apply mostly to the flotation of sulfides and other minerals. Coal flotation however, as pointed out by Wheeler (1994), differ in several aspects with the flotation of sulfides (Table 1) and therefore, the guidelines to be followed for a proper selection of flotation frothers need to be expanded.

Table 1: Differences between coal and ore flotation.

Factor	Coal	Ore
Spec. gravity of floated solids	1.2-1.4	3-7
Max. particle size in floated solids (mm)	1	0.3
Average flotation time (min)	3-8	10-30
Concentrate yield (%)	65-85	5-20
Percent of total floated in first 2 cells	60-80	10-20
Feed tonnage per bank (tons/hour)	30-150	100-300
Tons floated in first 2 cells	12-102	0.5-12

As shown in Table 1, the yields involved in coal flotation are considerably higher compared to the flotation of most other ores. It is clear then that the frother must generate a froth capable of supporting a great amount of material. Polypropylene glycol based frothers produce strong froths that do not collapse easily. This is especially important in column flotation.

Frothers in coal flotation should also be able to interact with collectors to enhance collector adsorption on the coal particle surface. This combined adsorption improves kinetics, final recovery and decreases reagent consumption (Wheeler, 1994).

There are 3 main groups of frothers used in the industry.

a) Alcohols.

This type of frothers presents a limited solubility in water and their molecular structure usually includes 5 to 8 carbon atoms in hydrocarbon chain. Methyl-Isobutyl-Carbinol (MIBC), which is widely used in the industry, belongs to this category.

This group includes three sub-categories: aliphatic, cyclic and aromatic alcohols.

b) Alkoxy-Type Frothers.

This type of frothers is usually more selective and powerful than alcohols. Since high concentrations of these frothers do not affect significantly the structure of the froth, they are not widely used on an industrial scale.

c) Polyglycol Frothers.

This group includes compounds whose solubility in water can vary from totally miscible to partially soluble, depending on the ratio of hydrophobic to hydrophilic group in the frother molecule.

This category of frothers presents great flexibility when it comes to selecting compounds with different molecular weights and chemical structures, thus allowing a better control of the flotation rate and selectivity.

The most common frothers in this group are known under the trade name of "Dowfroth". These frothers are capable of floating coarser particles than the corresponding alcohol frothers. The latter are more selective for finer particles

It is worth pointing out that due to the hydrophobic nature of the coal surface, frothers adsorb not only at the gas/liquid interface, but also onto coal. Adsorption of frothers on coal has been investigated by several researchers. Furstenau et al. (1982) studied adsorption of MIBC and α-terpineol onto a high-volatile bituminous coal. Adsorption of MIBC was also studied by Miller et al. (1983).Gurses et al. (1992) investigated adsorption of cresols, and adsorption of phenol onto coals varying in rank was studied in the 50's (Eveson, quoted after Laskowski, 2001). There are not data on adsorption of polyglycol frothers on coal.

Table 2: Classification of flotation frothers.

	Name	Formula	Solubility in H_2O
(1)	**Aliphatic alcohols**	**R–OH**	
	Methyl isobutyl carbinol (MIBC)	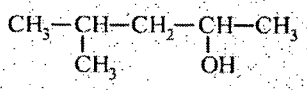	Low
	2-ethyl hexanol	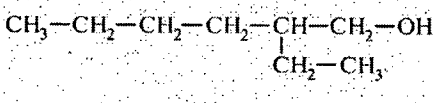	Low
	diacetone alcohol	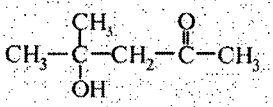	Very good
	2,2,4-trimethylpentanediol 1,3-monoisobutyrate (TEXANOL)	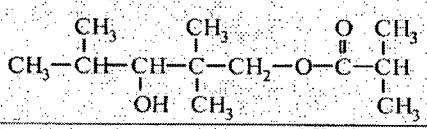	Insoluble
(2)	**Cyclic alcohols**		
	α–terpineol (Active constituent of pine oil)	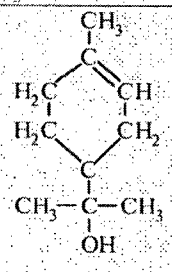	Low
	Cyclohexanol	$C_6H_{11}OH$	Low
(3)	**Aromatic alcohols**		
	cresylic acid (Mixture of cresols and xylenols)	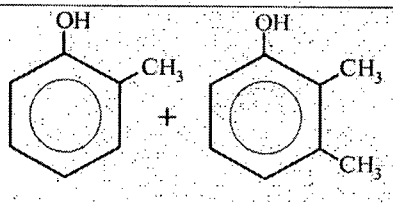	Low
(4)	**Alkoxy-type frothers**		
	1,1,3-triethoxybutane (TEB)	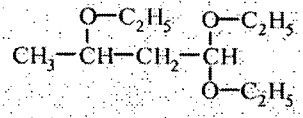	Low
(5)	**Polyglycol-type frothers**	**$R(X)_nOH$, R=H or C_nH_{2n+1}, X=EO, PO or BO**	Very good or total
	DF 250	$CH_3(PO)_4OH$	Total
	DF1012	$CH_3(PO)_{6.3}OH$	32%
	Aerofroth 65 DF 400	$H(PO)_{6.5}OH$	Total
	DF-1263	$CH_3(PO)_4(BO)OH$	Very good

3.1.2. Fundamental Properties of Flotation Frothers and Evaluation of Frother Performance.

Although the importance of frothers is widely acknowledged, their classification based on a consistent criterion has been difficult. For a long time, terms such as "powerful" and "selective" have been used to describe frother properties (Laskowski, 2003).

In the following Sections, some parameters useful for a proper characterization of frothers are presented.

3.1.2.1. Dynamic Foamability Index (DFI).

The dynamic foamability index is a method of characterisation of frothers that was proposed by Czarnecki et al (1982). The test involves passing a gas through a sintered disc and into the test solution of known frother concentration. The total gas present in the system (solution + foam) is determined for each corresponding gas flow rate. Above a given flow rate, a linear relationship (Figure 2) is seen to develop between the foam height and the gas flow rate. The slope of such a curve is referred to as the retention time (equation 1), whose physical meaning may be thought of as the average lifetime of a bubble, from growth to rupture.

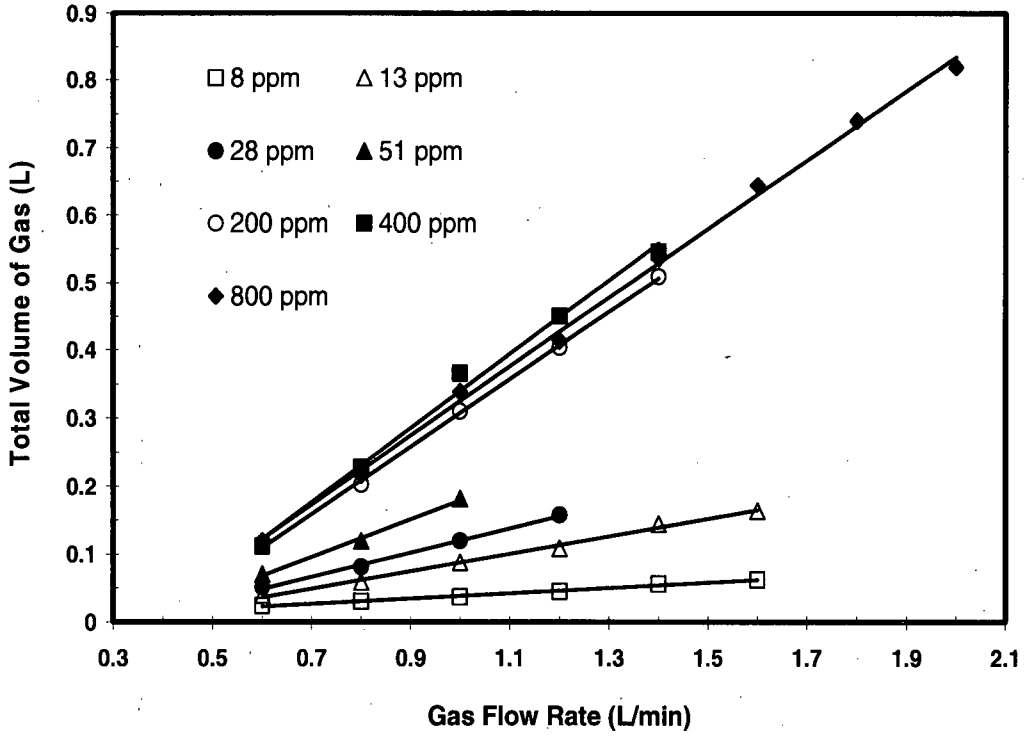

Figure 2: Linear part of the curve volume versus gas flow rate (retention time) for MIBC at different concentrations.

$$rt=\frac{\Delta V}{\Delta Q} \qquad (1)$$

where:

rt = Retention time, [s]

V= Total volume of gas in the system, [L]

Q= Gas flow rate, [L/s]

The retention time values increase with increasing concentration of frothers, and reach a maximum value at a certain concentration. The retention time versus frother concentration curves are therefore expected to have an inverse exponential shape. The parameter DFI is defined as the limiting slope of this curve, for $c \rightarrow 0$:

$$DFI=\left(\frac{\partial rt}{\partial C}\right)_{C\rightarrow 0} \qquad (2)$$

A non-graphical method for the calculation of the DFI has been proposed, in order to diminish the error involved in determining the slope for $c \rightarrow 0$ from the retention time versus concentration plot. It consists of fitting the following expression for a set of values of rt for various concentrations:

$$rt=rt_{\infty}\left[1-\exp(-kc)\right]+2.4 \qquad (3)$$

where:

rt = Retention time, [s]

rt_{∞} = Limiting value for rt when $c \rightarrow \infty$

k = Constant

The inverse exponential equation can be expanded to a power series to give $rt-2.4=DFI \cdot c$, from where the DFI can be evaluated.

As will be seen in the following Sections, the DFI, in combination with the critical coalescence concentration (CCC), provides a useful tool for characterizing frothers.

3.1.2.2. Critical Coalescence Concentration (CCC).

Frothers reduce bubble size by reducing coalescence between bubbles. The concentration above which bubble coalescence is entirely prevented is referred to as critical coalescence concentration, which is characteristic for each frother (Cho et al., 2002)

For concentrations higher than the CCC, the bubble size is no longer affected by the frother concentration and becomes dependent on the sparger's geometry.

The CCC can easily be determined for a given frother by measuring the bubble size as a function of the frother concentration (Figure 3).

It was shown that this property can be used to calculate the ratios of frothers of different characteristics in the blends (Laskowski et al., 2003).

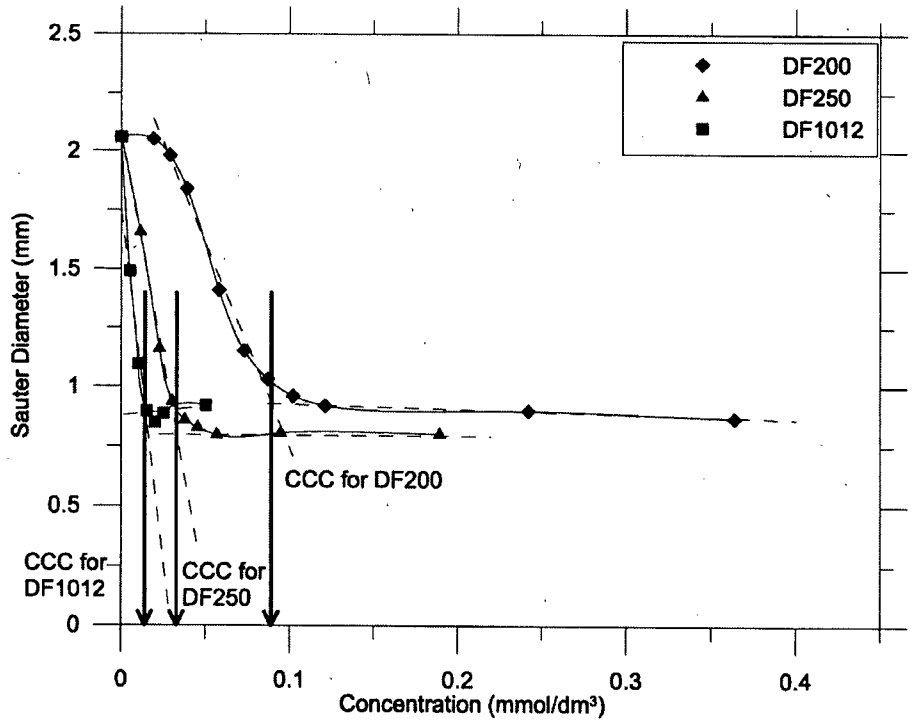

Figure 3: Graphical determination of the Critical Coalescence Concentration for three different frothers (From Laskowski et al., 2003)

3.1.2.3. *The DFI-CCC Curve as Tool for Characterization of Flotation Frothers.*

Laskowski et al. (2003) proposed a relationship between DFI and CCC values to classify frothers. They showed that powerful frothers are more efficient in reducing bubble size (low CCC values) and also produce more stable foams (high DFI values). This kind of reagents will tend to give higher recoveries and will perform well in flotation of coarser feeds, while flotation of fine particles in their presence will not be selective. On the other hand, more selective frothers are characterized by higher CCC and lower values of DFI. This suggests that a continuous decreasing exponential curve may be used to fit the relationship between DFI and CCC for flotation frothers, as shown in Figure 4. Powerful frothers appear in the upper-left corner of the diagram, while selective frothers are located in the lower-right corner.

This relationship provides a well founded scientific basis to characterize frothers. This also suggests that these reagents should be commercially offered along with the CCC and DFI values (Laskowski, 2003)

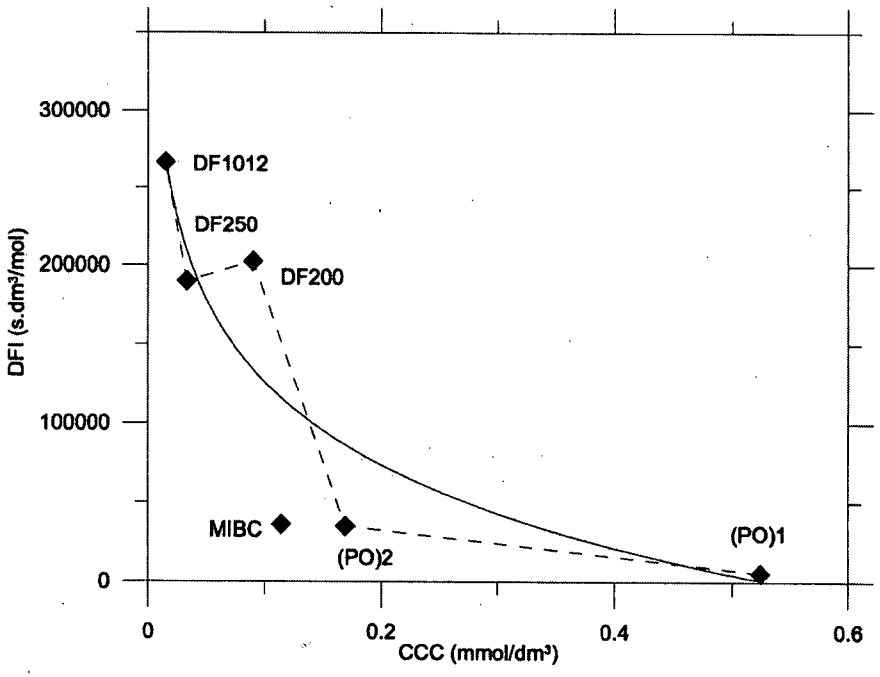

Figure 4: Relationship between DFI and CCC values for some frothers (From Laskowski et al., 2003)

3.1.2.4. The Hydrophile – Lipophile Balance Number (HLB).

The HLB number can be used to evaluate hydrophobic/hydrophilic properties of frother molecules (Laskowski, 1998)

If the chemical structure of a given frother is known, then the HLB number can be calculated using the following equation:

$$HLB=7+\sum(\text{Hydrophile group no.})+\sum(\text{Lipophile group no.}) \qquad (4)$$

The lower the HLB number, the more hydrophobic is the frother molecule and hence it is less water soluble.

The HLB number has the disadvantage of not accounting for molecular mass. Two frothers of similar HLB numbers, but of different molecular mass, will produce different types of froths, and therefore different final grades and recoveries should be expected. To overcome this inconvenience, Laskowski (1998) showed that by plotting the calculated values of the HLB number versus the molecular weight for a given group of frothers, this parameter can indeed be used for their characterization.

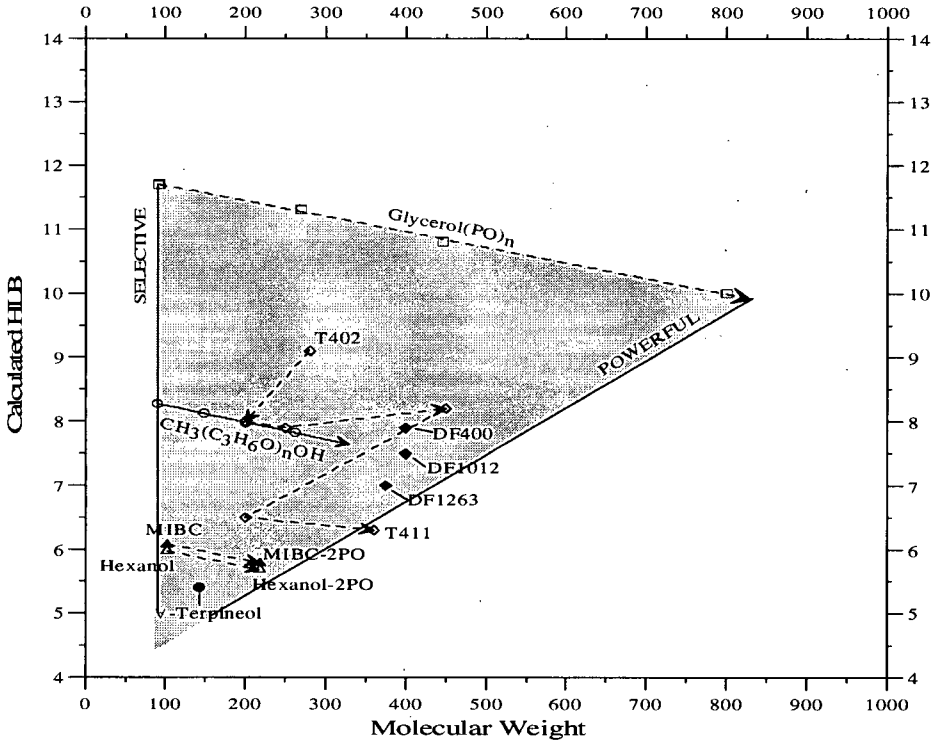

Figure 5: The HLB-Molecular Weight diagram for flotation frothers (Laskowski, 2003)

3.1.3. Effect of Frothing on Flotation.

It is known that sufficiently hydrophobic coals can be floated with a frother only. Malysa et al. (1987) conducted this kind of experiments in a Denver flotation cell in order to investigate the effect of frothing on flotation. These authors used frothers of known frothability indices (butanol, pentanol and hexanol) and two coals that do not require a collector. The results are shown in Figure 6. It is clear that flotation with hexanol gave the best results in comparison with the other tested alcohols. The results were re-plotted in terms of yield vs DFI x c. The resulting plot showed that all the experimental points converged on two curves for the two tested coals (Figure 7), which indicates that when highly hydrophobic solids are floated without a collector, the results depend only on frothability. This suggests that the flotation results can be normalized with respect to frother concentration.

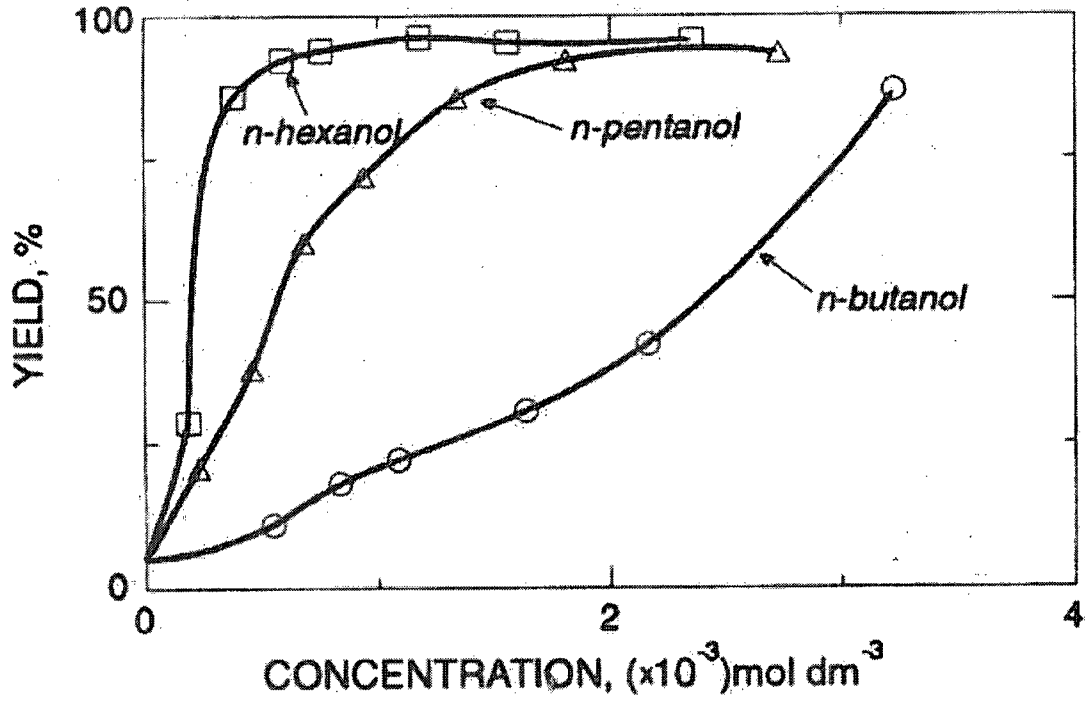

Figure 6: Relation between the froth product yield and concentration of different frothers for a bituminous coal (from Malysa et al., 1987)

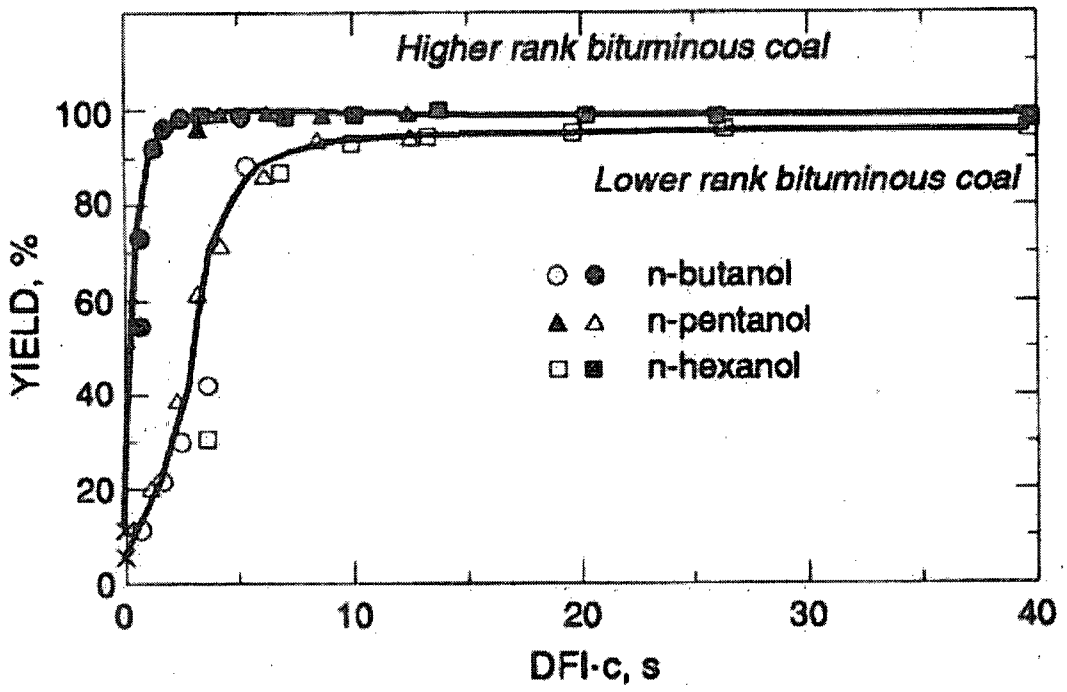

Figure 7: Relationship between the froth product yield (%) and DFI x C for two different coals (high volatile A bituminous and high volatile C bituminous) (from Malysa et al., 1987)

3.2. Foams and Froths: Stability and Structure.

For a long time the terms foam and froth were considered synonymous. Nowadays, it is accepted that these are two different systems. A foam is a two-phase system, formed by liquid and gas. The stability of this system is primarily dependent on the type and concentration of the frother used. On the other hand, a froth is a much more complicated system, which includes not only the liquid and gas, but also solid particles. In this case, the stability is determined by the frother and the characteristics of the solids, such as size and surface properties.

As far as structure is concerned, frothers also play a key role. Dependent on the type of frother, foams may greatly vary in their appearance and water content. In general, two different types of foams have been identified:

i) Unstable Foams: Unstable foams (or wet foams) are characterized by spherical bubbles separated by thick liquid walls. Dilute solutions of flotation frothers typically yield this kind of foam. (Kitchener and Cooper, 1959)

Wet foams can only exist while a gas is being pumped through the foaming solution and they quickly collapse as soon as the gas supply is stopped.

In this kind of foam, the water content may be as high as 40 % (Malysa, 1998) and decreases with height. Thus, the upper layer of wet foams contains the least amount of water.

It is interesting to point out that in dynamic unstable foams, which are characteristic for flotation, the "temporary stability" of the foam observed when a gas is passing through the foaming solution results from elasticity forces, which apparently increase with frother concentration up to a given point. The maximum value that these stabilizing forces can achieve is known as the "Marangoni Elasticity Modulus".

ii) Metastable Foams: Metastable or dry foams are characterized by bubbles with polyhedral shapes which are separated by planar or only slightly curved liquid films. These foams can persist for a considerable period of time even if no gas is being pumped through the foaming solution

Powerful frothers such as DF-1012 yield metastable foams, whereas more selective frothers like MIBC produce unstable foams (Laskowski et al., 2003). According to this, Rahal et al's (2001) conclusion that the type of frother does not affect the structure of the froth, was probably drawn from testing frothers that produced only one type of foam.

While the DFI describes well the properties of unstable (wet foams), the same index is not equally effective for the characterization of stable foams. In order to overcome this problem, Iglesias et al. (1995) proposed an alternative method to assess frother properties. These authors claim that the monitoring of the changes in foam volume (measured in terms of the height of a foam column) as a function of time in systems with smooth decay can also be used as a measure of foam stability. According to the procedure that they proposed, the solution to be tested is introduced into a glass column and a pre-humidified nitrogen is bubbled from the bottom through a hypodermic needle (1.5 mm diameter) at a constant flow rate of 140 ml/min. The system is then allowed to reach a dynamic equilibrium state, which takes place when the rate of foam breakage at the top exactly compensates the rate of foam formation at the bottom layer of the foam column. When this happens, the foam column height attains a stable value. The gas flow is then closed and the foam column height (H) is monitored versus time (t).

Iglesias et al., (1995) conducted this experiment on a number of different foaming solutions. They found that if the results are plotted in terms of a dimensionless height H/H_0, where H_0 is the initial height of the foam column, versus log $(t/t_{1/2})$, where $t_{1/2}$ is the time at which the column height is half the original height, the experimental data for all the tested solutions follow a single straight line (Figure 8), which indicates that the differences between the properties of the foaming solutions analyzed with this procedure can be translated to the H_0 and $t_{1/2}$ values.

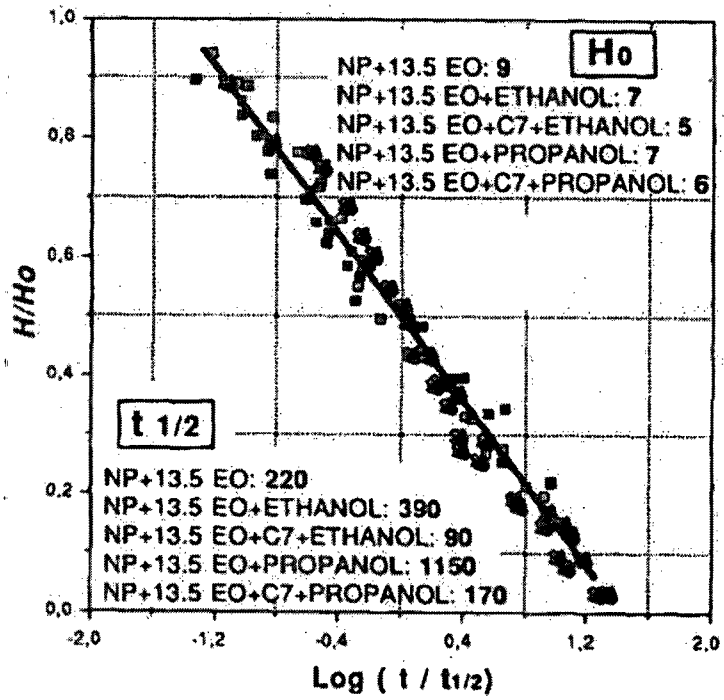

Figure 8: Dimensionless plot and characteristic parameter values (H_0 and $t_{1/2}$) for different foaming solutions (From Iglesias et al., 1995)

This method provides combined information on foamability and stability and it cannot separate the two.

3.3. Flotation Kinetics.

Flotation kinetics is related to interactions between particles and bubbles. The most traditional kinetic model is based on the analogy between a chemical reaction that involves collision between molecules:

$$A + B \rightarrow C$$

where A and B are reactants and C is the product of the reaction, and a flotation mechanism that includes collisions between hydrophobic particles and air bubbles in the pulp volume:

Solid particle + Bubble → Particle-bubble aggregate

This analogy is questionable since flotation is a physical solid-solid separation process that involves more than one important transport mechanism (Figure 9) as opposed to a simple chemical reaction.

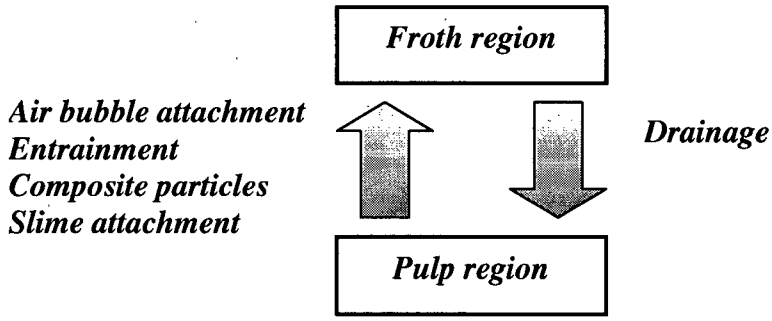

Figure 9: Transfer of material between pulp and froth regions in a flotation cell.

Although the modeling of flotation is complex due to the several transport phenomena occurring simultaneously, it is intrinsically a rate process, since particles reach the concentrate launder at a rate which is proportional to the concentration of those particles in the pulp (Lynch et al. 1981).

If it is assumed that the bubble surface is in excess in a flotation cell, then the flotation kinetics can be modeled by a first order reaction. The general rate equation can be written as:

$$-\frac{dC}{dt} = kC^n, \text{ where n =1 (first order reaction)} \quad (5)$$

Let us assume that C is the floatable mineral concentration remaining in a cell at time t, C_0 the initial concentration (at t = 0), and k the flotation rate constant. Then, the integration of equation (5) leads to:

$$C = C_0 e^{-kt} \quad (6)$$

Writing recovery in terms of concentrations:

$$R = \frac{C_0 - C}{C_0} \quad (7)$$

Letting R be R_∞ at t = t_∞, and combining equations (7) and (8) one arrives at:

$$R = R_\infty \left(1 - e^{-kt}\right) \quad (8)$$

In terms of percent recovery, equation (8) can also be written as:

$$\ln\left(\frac{100 - R}{100}\right) = -kt \quad (9)$$

or using decimal logarithms:

$$\log(100 - R) = \log 100 - \frac{kt}{2.3} \quad (10)$$

The plot of equation (10) gives a straight line as shown in Figure 10.

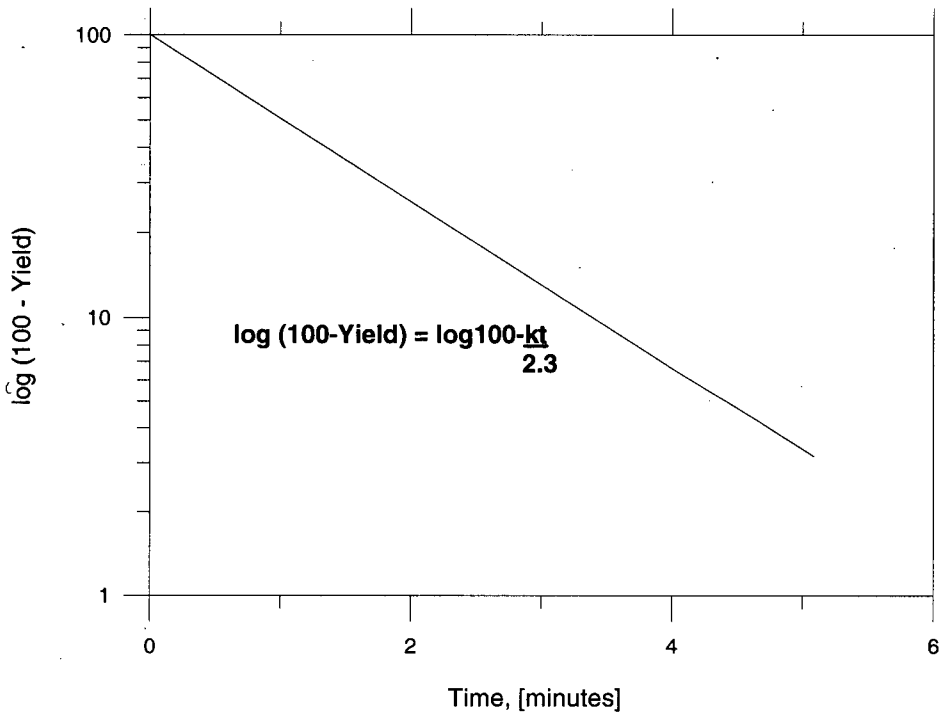

Figure 10: Semi-log plot used to calculate the flotation rate constant

In general, the flotation rate constant is a complex function depending on many variables, including particle and bubble sizes, reagent concentration and flotation cell hydrodynamics. The first order model generally predicts correctly the flotation kinetics, although in some cases the order of the process may vary. In fact, it is not unusual that the flotation kinetics varies for different components of the feed. In such cases, the particles in the pulp do not possess identical flotation properties but a continuous range of rate constants. When this happens, equation 6 becomes:

$$C = C_0 \int_0^{\infty} \exp(-kt)\, f(k)\, dk \qquad (11)$$

where *f(k)* represents a continuous distribution of rate constants. It is clear that the determination of this function is not trivial and therefore, the applicability of equation (11) is limited.

In order to simplify the problem, the first order approach can still be used separately to model the kinetics of the components which float first (fast floating components) and those which float more slowly (slow floating components). This idea is schematically illustrated in Figure 11, which represents the remaining fraction of solids in a flotation cell as a function of time, in a semi-log plot.

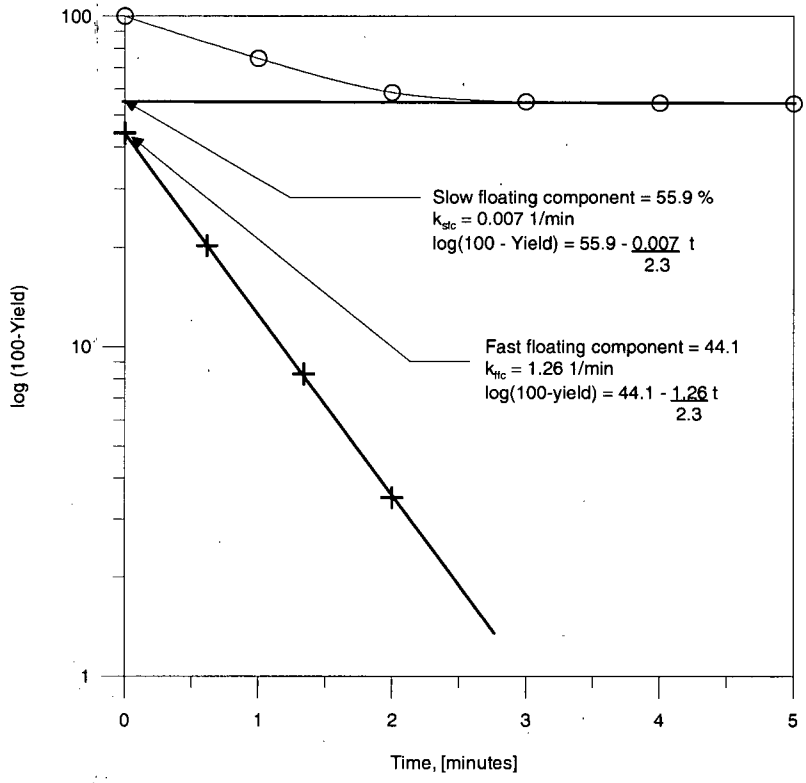

Figure 11: Determination of flotation rate constants for fast and slow floating components.

It is clear that the curve does not follow a straight line and therefore, equation (10) cannot be used. However, the curve can be split into two portions that can be represented by equations similar to equation (10). The straight line that runs through the experimental points after long enough time represents the flotation of the slow floating component of the feed. The intersection of this line with the vertical axis indicates the amount of this component present in the feed. The slope of this straight line can be used to determine the flotation rate constant (k_s) for this component.

It is worth pointing out that the particles with low flotation rate constants can cause severe problems. A certain amount of slow floating particles is always present in all size

fractions, although this proportion is particularly high in coarse sizes, due to the presence of composites or excessively coarse liberated particles (Lynch et al., 1981)

The same procedure applies to the fast floating component. The amount of this component in the feed is calculated from the difference between 100 and the amount of slow floating component previously determined. Since at all times the summation of the fast and slow floating components must equal the remaining amount of solids in the cell, which can be directly read off the curve, the equation that represents the kinetics of the fast floating component can be determined and from the slope of this curve, the flotation rate constant (k_f) for this component can be calculated.

It is clear that, once the flotation rate constants for the fast and slow floating components have been calculated, the remaining amount of solids in the cell at any given time can be calculated using the following equation:

$$100 - \Sigma Y = C_f + C_s = (100 - \phi)\exp(-k_f t) + \phi \exp(-k_s t) \qquad (12)$$

where Y is the yield of floating material, C_f and C_s are the yields of the fast and slow floating components remaining in the cell after time t, φ is amount (%) of slow floating component present in the flotation feed, and k_f and k_s are the flotation rate constants for the fast and slow floating components.

3.3.1. Froth Overloading and its Effect on the Kinetics Model in Coal Flotation.

In coal flotation, the froth might sometimes become immobile due to the high concentration of coal particles in it. This phenomenon, referred to as "froth overloading", has an important effect on the rate of flotation of the particles into the launder.

As pointed out by Lynch et al., a froth may be overloaded with regard to one component but not overloaded with regard to others, which basically means that the flow rate of one component into the concentrate launder may be significantly lower compared to the theoretical value that one would expect based on kinetic considerations. At the same time, the flow rates of other components may approximate the theoretical values. It is clear then that different models

should be used to describe processes where coal follows a normal kinetic relationship, and processes in which overloading occurs. In the latter case, since the flow rate of solids to the concentrate launder is directly related to the flow rate of water to the concentrate (Lynch et al., 1981), an appropriate model should include a component which describes the behavior of the water.

3.4. Entrainment in Froth Flotation.

The mechanical transportation of hydrophilic gangue minerals in flotation is caused by different mechanisms, including entrapment, entrainment, recovery via composite particles and slime coatings.

Entrapment occurs when part of the gangue remains entrapped by floatable particles in the froth and become recovered to the froth product. This mechanism is usually enhanced in flocculated (or coagulated) and highly mineralized froths (Kirjavainen, 1996).

The recovery of gangue minerals due to composite particles is a problem in fine grained ores. A certain amount of composite particles is always present since there is a compromise between mineral liberation and optimum particle size in flotation (Kirjavainen, 1996).

Slime formation is a consequence of excessive grinding, which leads to low flotation rates and to the recovery of unwanted material.

It is generally accepted that entrainment is the primary mechanism for the recovery of fully liberated gangue particles. In this mechanism, the particles suspended in the pulp of a flotation cell are mechanically carried up into the froth suspended in the water between the bubbles, regardless of the particle surface properties.

3.4.1. Factors Affecting Entrainment.

The mechanical flotation of gangue is strongly affected by the amount of water transferred to the froth product and therefore, factors affecting froth characteristics and the recovery of water have an impact on entrainment. The following Sections deal with the effect on the entrainability of gangue particles of each one of the process variables involved in a given flotation process.

3.4.1.1. Recovery of Water.

Many authors have reported that the recovery of gangue particles by entrainment is strongly related to the recovery of water (see for example, Smith and Warren [1989], K.Rahal et al. [2001], Savassi et al. [1997]). In general, the higher the recovery of water, the higher the degree of entrainment. This should be carefully considered when it comes to selecting proper reagents for a given flotation process. Different chemicals modify in different ways the structure of the froth, changing its tendency to recover water, and therefore, changing the degree of entrainment.

3.4.1.2. Particle Size.

In general, it has been observed that the finer the particle, the more likely it is to be recovered by entrainment.

In order to quantify the effect of particle size on entrainment, Johnson et al. (1974) defined classification factors as follows:

$$CF^i = \frac{\text{mass free gangue of size i in unit mass water in concentrate}}{\text{mass free gangue of size i in unit mass water in pulp}} \qquad (13)$$

$$CFM^i = \frac{\text{recovery rate of gangue of size i into concentrate}}{(\text{flow rate of gangue of size i in feed})(\text{fraction water recovered})} \qquad (14)$$

Although both CF^i and CFM^i attempt to measure the degree of entrainment taking into account the particle size, they are usually different, but still they show a clear trend as the particle size increases. The reported values for CF^i for particles finer than 10 microns are in the range 0.5 to 0.8, while for particles of about 50 microns, the values fall in the range from 0.02 to 0.2, showing that coarse particles (in the range of 50 microns and bigger) are not recovered by entrainment.

The actual size where entrainment is no longer significant is dependent on the froth properties. (Savassi et al., 1997)

Englebrecht and Woodburn (1975) showed the effect of particle size on the entrainment. They conducted a number of flotation tests measuring the recoveries of water, silica and pyrite from a feed containing a mixture of finely ground silica and pyrite. They found that, above a minimum water recovery, the relationship between gangue recovery and water recovery is linear; however, the straight line for large particles did not pass through the origin, intercepting the x-axis (Figure 12). For fine particles, a directly proportional relationship (passing through the origin) was found.

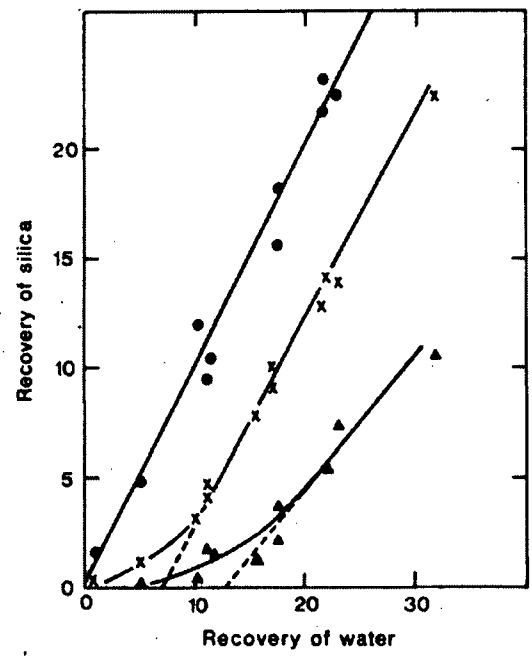

Figure 12: Recovery curves for silica. Upper curve < 12 μm, middle curve 23.3-32.3 μm, lower curve > 41.6 μm (Englebrecht and Woodburn, 1975)

The lower sedimentation velocity associated with fine particles of low densities is also responsible for a higher degree of entrainment. Particles with higher densities will settle out of the froth avoiding entrainment.

3.4.1.3. Froth Structure.

The structure of the froth, which is primarily defined by the type and concentration of frother, collector concentration, air flow and content of hydrophobic particles (Savassi et al., 1997), may have a pronounced effect on the degree of entrainment of fine particles since it is closely related to the drainage of water from the froth to the pulp. Above the pulp/froth interface, spherical bubbles promote the drainage of water. However, as the froth height increases, the bubbles can no longer preserve their spherical shape and they begin to deform to a polyhedral structure from which the water drainage is much lower. It is clear that in the former case the structure of the froth enhances the rejection of unwanted particles from the froth collection zone, whereas in the latter, this effect is less significant.

It is worthy of mention that there is experimental evidence that indicates that in coal flotation, the beneficiation process stops at froth depths where the structure of the bubbles begins to change from close-packed spheres to the polyhedral form.

3.4.1.4. Froth Height.

In general, thick froths enhance the rejection of hydrophilic gangue particles from the froth, thus improving selectivity. Savassi et al. (1997) showed that an increase in the froth depth leads to an increase in the froth residence time of air, with more drainage of coarser particles and, therefore, a lower degree of entrainment. Laplante et al. (1989) also showed that, at constant water recovery, hydraulic entrainment is minimized by increasing both gas rate and froth depth.

It is worth mentioning that, as pointed out by Laplante et al.(1989), plant froths vary in thickness, depending on the objective of a given flotation stage. In cleaner circuits for instance, upgradability is stressed and thick froths (up to 40 cm) are used, which yields low water recoveries and contributes to selective rejection of non-sulfide gangue. On the other hand, in scavenger flotation, same as in rougher flotation, recovery is the main objective and thin froths (< 3cm) are used.

In the flotation of industrial minerals, such as potash and phosphates, thin froths are required to float coarse particles. In these cases, in which entrainment is significant due to the low thickness of the froth, wash water can be used to enhance both the stability of the froth and the selectivity of the process.

3.4.2. Methods to Measure Degree of Entrainment.

3.4.2.1. The Empirical Partition Curve.

The degree of entrainment in a flotation cell is defined by the ratio:

$$ENT = \frac{\text{mass transfer of entrained particles to the concentrate}}{\text{Mass transfer of water to the concentrate.}} \qquad (15)$$

As pointed out before, the degree of entrainment is dependent on the particle size. This relationship resembles a classification function whose form depends on the operating conditions in the flotation system being investigated. Figure 13 shows schematically this type of curves.

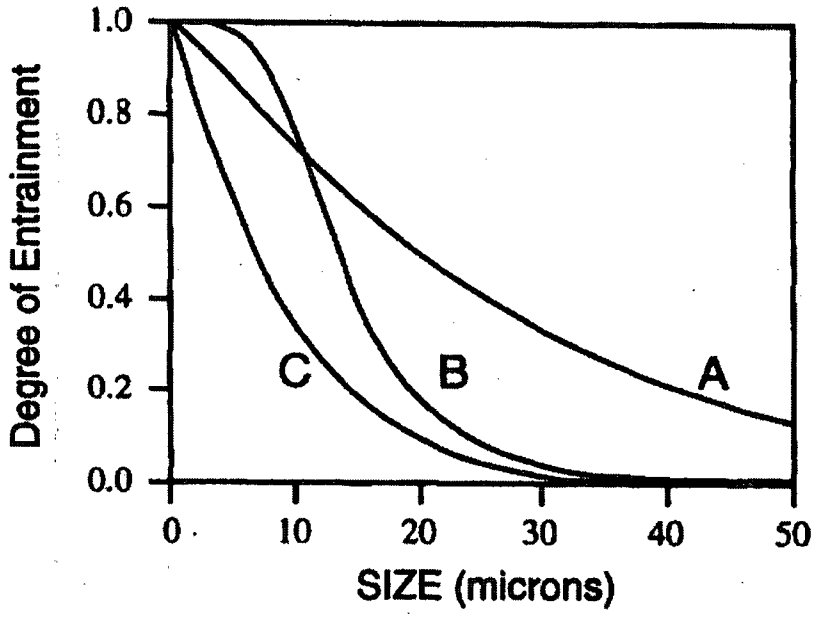

Figure 13: Partition curves for different degrees of entrainment of particles, (Savassi, 1998).

Curve A represents a flotation system with a comparatively high degree of entrainment throughout the particle size distribution; curve B represents a flotation system with a high degree of entrainment for the fine particle size range, whereas curve C represents a flotation system with a comparatively low degree of entrainment throughout the size distribution.

It is convenient to use a continuous curve to represent the different types of curves mentioned above. Savassi (1998) proposed the following empirical partition curve to describe the variation of the degree of entrainment throughout the particle size distribution in a flotation cell operated at fixed conditions:

$$ENT_i = \frac{2}{\exp\left[2.292\left(\frac{x_i}{\xi}\right)^{adj}\right] + \exp\left[-2.292\left(\frac{x_i}{\xi}\right)^{adj}\right]} \quad (16)$$

$$adj = 1 - \frac{\ln\left(\frac{1}{\delta}\right)}{\exp(x_i/\xi)} \quad (17)$$

Where:
x_i = Particle size i.
ξ = Entrainment parameter (Particle size for which the degree of entrainment is 20 %)
δ = Drainage parameter.

It is clear that the empirical partition curve given by equation (16) should meet the following boundary conditions:

$$\begin{aligned} x_i \to \infty &\Rightarrow ENT_i \to 0 \\ x_i \to 0 &\Rightarrow ENT_i = 1 \\ x_i = \xi &\Rightarrow ENT_i = 0.20 \end{aligned} \quad (18)$$

Additional restrictions are required in order to ensure the physical meaning of the partition curve. These restrictions are given by the following equations:

$$\frac{d(ENT_i)}{d\,x_i} < 0,\ x_i > 0 \quad (19)$$

$$\frac{d^2(ENT_i)}{d\,x_i^2} > 0\ ;\ x_i > x_{int} \quad (20)$$

Equation (19) states that the degree of entrainment must decrease continuously as the particle size increases; equation (20) states that the curvature of the partition curve is always positive above a certain particle size (x_{int}), which defines the region of coarse particles.

The empirical partition curves reviewed in this section have proved to be a good tool for fitting the relationship between the degree of entrainment and the particle size of a tracer mineral species in a flotation cell operated at fixed conditions and for predicting this relationship in the same cell operating at varying conditions.

To use the partition curve as a predictive tool for a given flotation system, auxiliary equations describing the relationship between the parameters of the curve and the operating conditions of the system being investigated (like froth residence time of air, solids content of the pulp, addition rate of chemicals, etc.) must be developed. Once this is done, the partition curve can be used for predicting the recovery by entrainment under different operating conditions.

3.4.2.2. Trahar's Method.

This method allows to decouple the effects of true flotation and entrainment by performing two tests, with and without collector addition (Trahar, 1981). The basic assumption is that at a given water recovery in both tests, the same amount of solids is recovered by entrainment (i.e., the degree of entrainment is the same).

Figure 14 shows the results obtained by Trahar using this method. He conducted flotation tests with siderite using first only frother and then frother and collector. He attributed the recovery-size curve obtained in the first case (frother) to entrainment; the subtraction of this curve from the recovery-size curve obtained with frother and collector provides the recovery curve due to "true flotation".

It can be seen from Figure 14 that as the particle size decreases, the recovery due to entrainment increases, accounting for a significant part of the overall recovery curve.

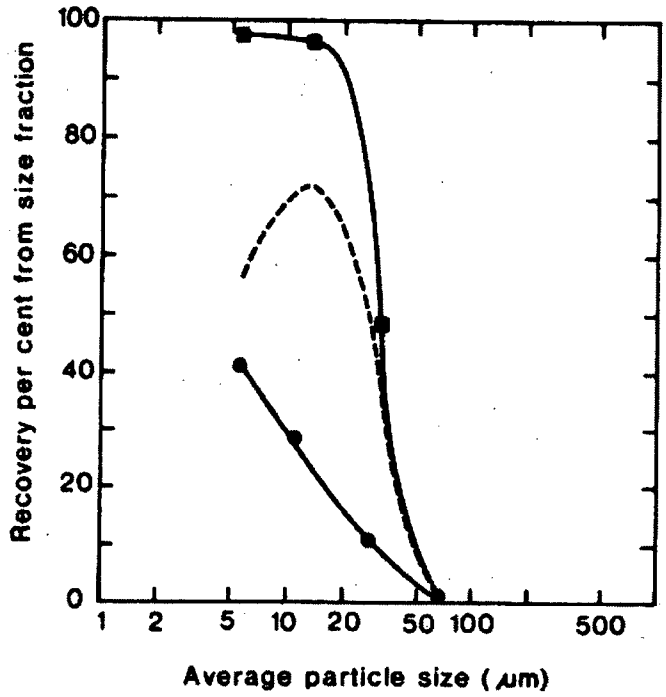

Figure 14: Recovery of siderite as a function of particle size. Recovery with frother only (lower curve), recovery with collector and frother (upper curve) and recovery due to true flotation (dotted line). (From Trahar, 1981)

The main criticism of this method is the fact that its basic assumption (same degree of entrainment in both tests) may not be true, since the absence of collector in one of the tests may change the structure of the froth, and therefore it is likely that the degree of entrainment is different in both experiments. (Savassi, 1998)

3.4.2.3. Warren's Method.

Englebrecht and Woodburn reported from continuos laboratory flotation tests that the recovery of valuable hydrophobic pyrite (R_v) is dependant on the recovery of water, as well as size and chemical environment (pH and reagents).

They found (Figure 15) that only in the case of ultrafine particles the straight line passed trough the origin. For larger sizes, the line intercepts the vertical axis.

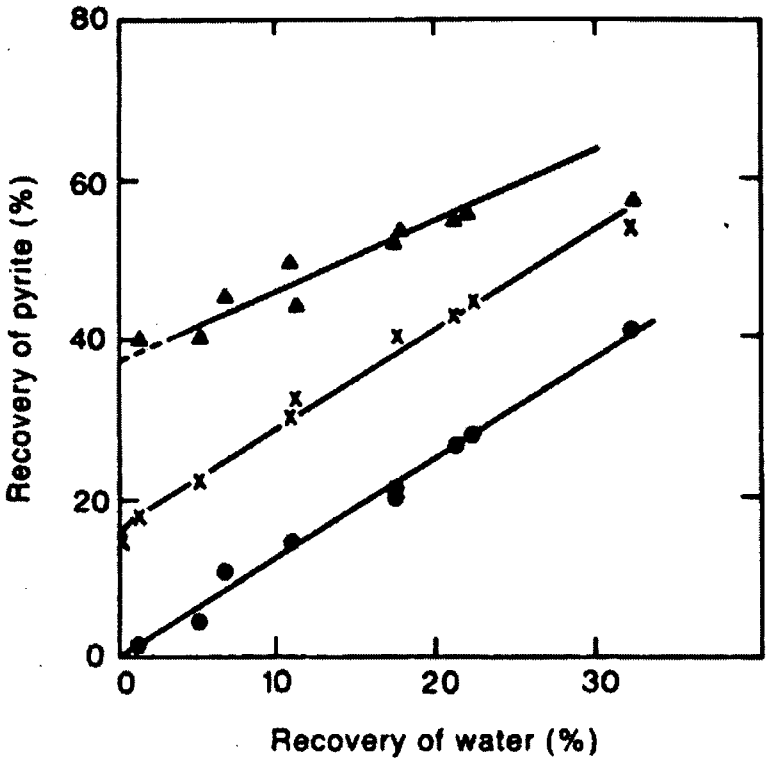

Figure 15: Recovery curves for sized fractions of hydrophobic pyrite. Upper curve 20.7-26.6 μm, middle curve 10-14.7 μm, lower curve < 7.7 μm. (Englebrencht and Woodburn, 1975)

Warren reported similar results and proposed the following equations to describe the behavior of hydrophobic valuable particles and hydrophilic gangue particles:

$$R^i_v = F^i_v + e^i_v R_w \qquad (21)$$

$$R^i_g = e^i_g R_w \qquad (22)$$

Where:

F_v^i: Intercept of the extrapolated line on the mineral recovery axis.

e^i_v, e^i_g : Entrainment factors for hydrophobic valuable minerals and hydrophilic gangue minerals, respectively.

According to equation (21), the overall recovery R^i_v compromises two parts: F^I_v, independent of water recovery ("true flotation") and $e^i_v R_w$, which is related to the recovery of water (entrainment)

The experimental procedure consists of carrying out a number of batch tests changing the recovery of water in each one of them, by modifying the froth height or the rate of removal. The recoveries of valuable or gangue material are plotted against the recovery of water and then the equations (21) or (22) are fitted to the curves.

3.5. Coal Reverse Flotation (CRF).

3.5.1. The Conflict Between Flotation as Beneficiation Method and the Preparation of Coal Water Slurries (CWS): The Importance of Coal Reverse Flotation.

The flow characteristics of CWS are critical for their proper handling. They depend on both coal surface properties and coal particle size distribution. While with simple modifications of the flotation circuit, a bi-modal size distribution can be achieved, which can improve the characteristics of the material used to prepare CWS (Laskowski, 1999), the modification of the coal surface properties in the cleaning stage in order to facilitate the subsequent preparation of CWS is not simple. Strongly attractive hydrophobic forces operating between hydrophobic particles in water promote aggregation, thus raising the yield stress and making the system behavior more non-Newtonian (Pawlik et al., 2004)

Flotation is commonly used to clean fine coal. Flotation of bituminous (metallurgical) coals is easy and it can be achieved using only a frother. On the other hand, lower rank coals are less hydrophobic and more difficult to float and they require, in addition to frother, the use of collectors. Moreover, the reduction of the hydrophilic mineral matter content (ash) during the cleaning process increases even further the hydrophobicity of the final product (clean coal).

Since the chemical additives used to reduce viscosity of CWS operate by making coal surface hydrophilic (in order to reduce the attractive hydrophobic interactions) and by increasing the electrical charge of the particles, thus promoting repulsive forces (Pawlik et al., 1997), it is clear that the flotation reagents are not compatible with viscosity reducers. Hence the reverse flotation, in which collectors are used to render the gangue particle surfaces hydrophobic, appears to be a good alternative for the cleaning of low rank coals.

3.5.2. Advantages of CRF.

In conventional flotation (forward flotation), the coal is floated whereas the mineral matter (gangue) reports to tailings. However, the high concentrate yield (which can be as high as 70 to 80%), enhances the mechanical transport of gangue particles to the concentrate (mainly due to entrainment and entrapment), increasing the ash content of the clean product.

One viable solution to control entrainment is the use of column flotation technique (Figure 16). It consists of a tall column (8 to 12 m high) of square or circular cross section. The lower part of the column contains a quiescent pulp zone in which the ore particles move downwards, counter-current to a swarm of rising air bubbles that are introduced at the base of the pulp. The froth is continuously washed down with water from the top of the column, at a flow rate which results in a net downward flow of water in the column, called positive bias. The water flow provides the mechanism for the drainage of the entrained particles back to the pulp. In addition, the wash water also enhances the stability of the froth.

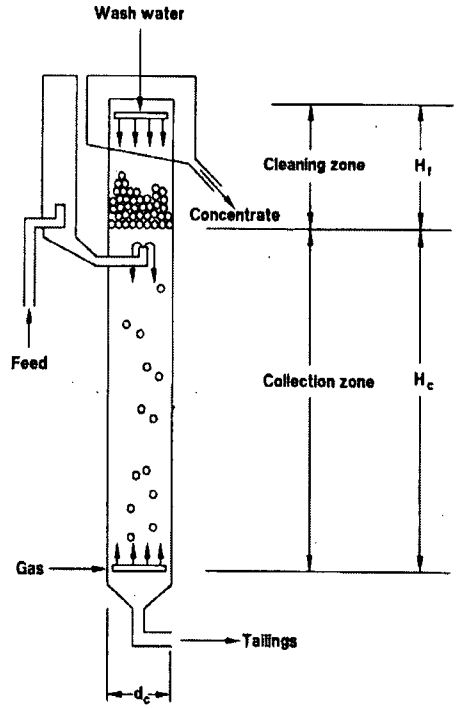

Figure 16: Schematic of column flotation cell.

Although the use of this technique has proved to be effective in reducing entrainment, the high mass recovery in forward coal flotation poses a problem due to the limited carrying capacity of flotation columns.

In the reverse coal flotation, the gangue is floated while the valuable material is collected as tailings. Since the gangue material accounts for approximately the 30 % of the feed, the yield is much lower. This fact should allow for a better use of column cells in coal flotation.

In forward flotation, the relatively small gangue particles and composite particles are easily entrained along with the coal particles in the concentrate, increasing the ash content of the clean product. In reverse flotation, in which coal is depressed and recovered in tailings, the gangue particles and some middling particles are collected and thus removed with the concentrate, along with a certain amount of entrained coal particles.

The reverse flotation presents a number of advantages in comparison to forward flotation. Stonestreet (1991) identified 4 main factors:

a) Reduction of Mass Recovery.

The gangue material makes up a smaller proportion of the feed, usually around 15 to 30 %. Since this is the component that is being floated in the reverse flotation, the concentrate yield is drastically reduced, allowing the use of higher pulp densities in the feed.

b) Reduction of the Entrainment.

Due to the high yield in forward flotation, a considerable amount of gangue may be entrained affecting the quality of the clean product. In the reverse flotation, because of the smaller mass flux and the coarser size of the coal particles, some coal particles will be entrained but to a much lesser extent than the entrainment of gangue in forward flotation.

Therefore, better results can be expected in reverse flotation in terms of the final grade of the clean product.

c) Application to Column Cell Technology.

The reduction of yield in reverse flotation allows to overcome the problem associated to the limited carrying capacity of flotation columns, allowing the use of higher feed rates and pulp densities and thus improving the overall performance.

d) Uniformity of Gangue Floatability.

Coal gangue minerals appear to have well defined structures and, therefore, the flotation of these minerals is likely to be more consistent than the forward flotation of highly heterogeneous coal.

In spite of its apparent advantages, CRF is a process which is still under development. The entrainment of particles, although lower in reverse flotation than in forward flotation, can still be considerable due to the excessive stabilization of the froth caused by the reagents involved in the process. In addition, preliminary tests have shown that the reagent consumption can be very high, which puts at risk the economic feasibility of the process.

3.5.3. Reagents Used in CRF.

3.5.3.1. Dodecyl-Trimethyl Ammonium Bromide.

DTAB has been extensively used in the development of the reverse flotation technology. From the chemical point of view, it belongs to a group of quaternary amines, which are strong electrolytes that exhibit a very high solubility in water. As such their speciation in aqueous solutions is independent of pH, as opposed to primary amines, and thus only one type of ionic species (the quaternary ammonium cation) exists throughout the pH range.

In the research conducted by Pawlik (2003), the role of DTAB in the reverse flotation process was closely studied. He found that this reagent renders silica surface hydrophobic through its adsorption at the air-silica interface. His results also revealed that DTAB cannot be used as a depressant for high rank coals, since only at very high concentrations this reagent is able to render the coal surface hydrophilic. Figure 17 summarizes the wettability studies that back up these conclusions. The curve shows advancing and receding contact angles measured on quartz, LS43 coal and F4 (hydrophobic) coal. It can be seen that, although the contact angles measured on F4 in presence of DTAB continuously decrease as the concentration of the amine increases, the resulting hydrophilicity is not low enough to depress the coal. This effect is only observed at concentrations close to the critical micelle concentration, in which the contact angles eventually fall to zero. Below the critical micelle concentration, DTAB acts simply as a frother due to the adsorption at the air-water interface. The froth formed in the presence of this quaternary amine is extremely stable and dry.

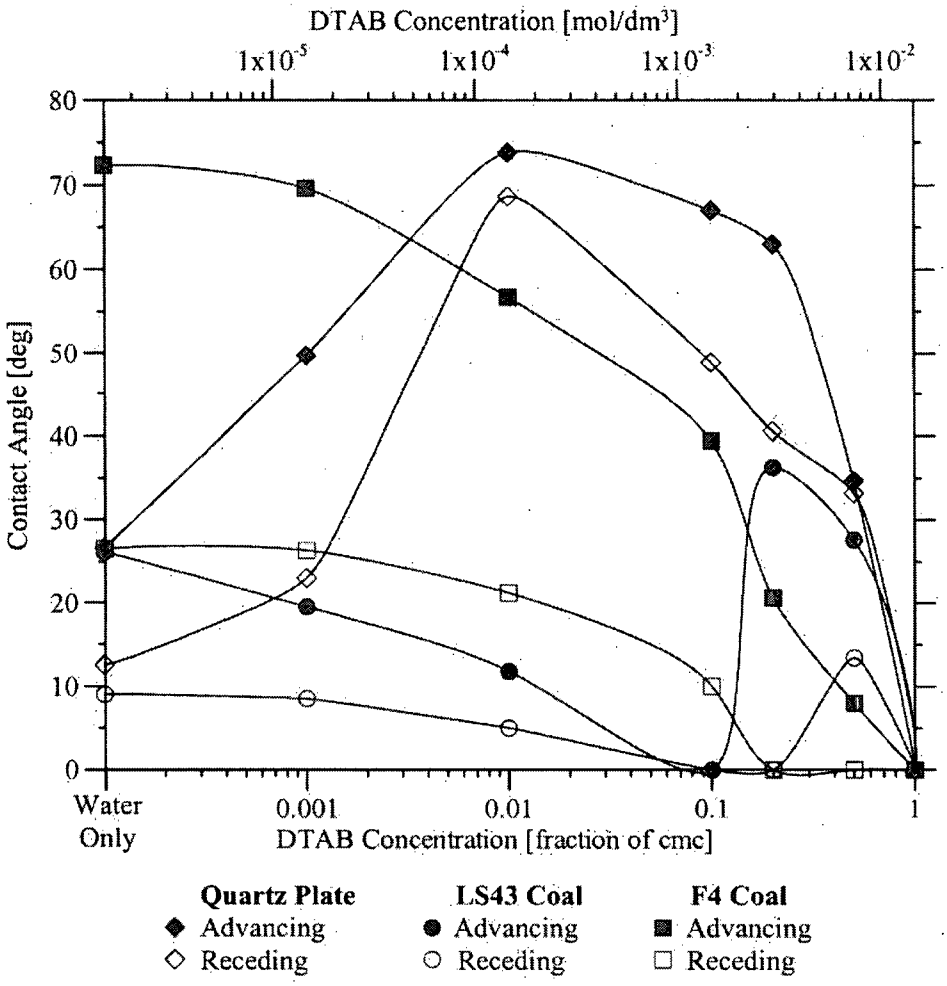

Figure 17: Contact angles measured on coals and quartz in the presence of DTAB (from Pawlik, 2003).

In the same work by Pawlik it was demonstrated that naturally hydrophilic coals strongly adsorb DTAB (Figure 18), which explains the reason behind the high consumption of this reagent in the reverse flotation of low-rank coals.

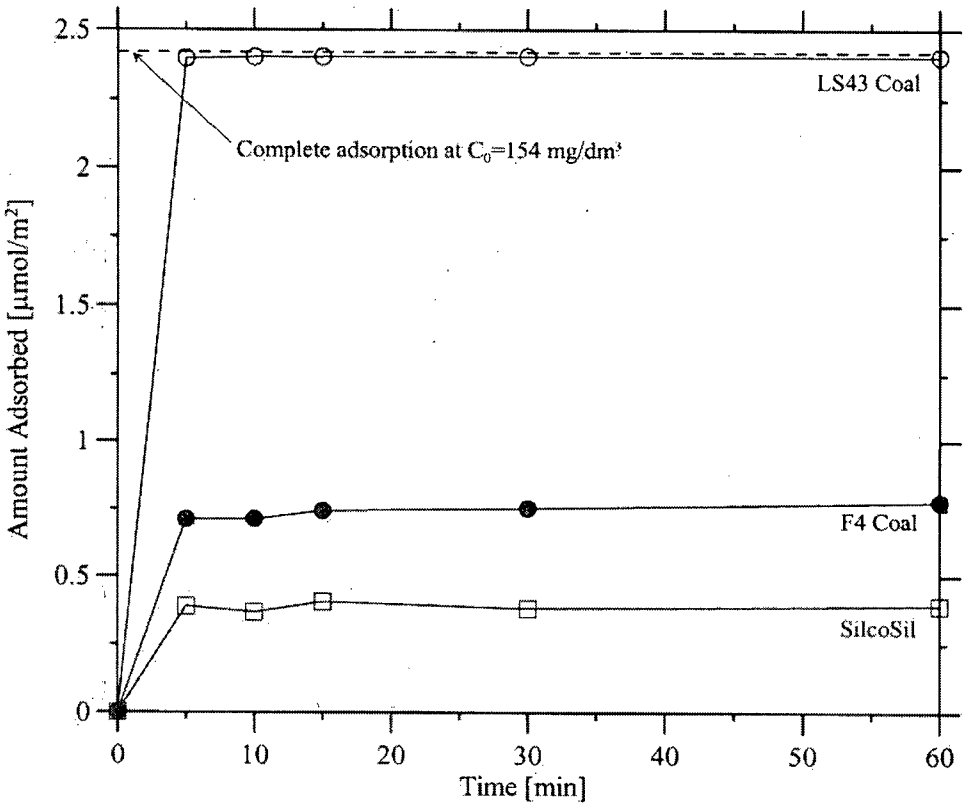

Figure 18: Adsorption kinetics of DTAB onto LS43 Coal (hydrophilic), F4 Coal (hydrophobic) and Silica. (From Pawlik, 2002)

3.5.3.2. Depressants.

Water-soluble polymers used as flocculant are strong flotation depressants (Laskowski, 2002). As shown in Table 3, in addition to the size enlargement effect, this kind of reagents produces hydrophilic flocs.

Polysaccharides are also used as depressants in the flotation of ores containing inherently hydrophobic minerals such as graphite, talc, molybdenite and coals. A good example is the use of guar gums as depressants of talc in the flotation of platinum ores in South Africa.

According to some studies quoted by Pawlik (2002), Starch and Dextrin, which belong to the same class of polysaccharides, have also been successfully used as selective coal depressants.

Table 3: Classification of the aggregation phenomena as a function of solid wettability and type of chemical additive (from Laskowski, 2002)

Solid wettability	Resulting properties	Type of additive		
		Hydrophilic flocculent	Hydrophobic latex	Emulsified oil
Hydrophilic solids	Size enlargement	Yes	No	No
	Floc wettability	Hidrophilic	-----	-----
	Mechanism	Adsorption-bridging	-----	-----
Slightly hydrophobic solids	Size enlargement	Yes	-----	Slight
	Floc wettability	Hidrophilic	-----	Hydrophobic
	Mechanism	Adsorption-bridging	-----	Bridging by immiscible liquid
Hydrophobic solids	***Size enlargement***	***Yes***	Yes	Yes
	Floc wettability	***Hydrophilic***	Hydrophobic	Hydrophobic
	Mechanism	***Adsorption-bridging***	Hydrophobic coagulation	Bridging by immiscible liquid

4. EXPERIMENTAL.

4.1. Introduction.

Although the CCC and the DFI have been extensively used to characterize frothers, it is not clear how these indices are related to flotation. Since the entrainment of fine particles was shown to be caused by the presence of water in the froth, in this research the ability of frothers to recover water was tested in the absence and presence of solid particles.

The experimental program of this project was split into two parts. Firstly, different frothers were characterized in terms of DFI and CCC, as well as by means of surface tension measurements. In addition, the amount of water present in the foam formed when air is bubbled through a solution containing a given concentration of these frothers, in the absence of solids, was also measured. This may provide valuable information on the relationship between the nature of the frother and its ability to carry water on to the foam.

The rates of water recovery obtained from these tests (water-frother system) were then compared to the rates of water recovered in the presence of solids, to study the correlations.

The second part of the experimental program involved batch flotation tests. A highly hydrophobic coal (medium-volatile bituminous coal) and a hydrophilic coal (sub-bituminous coal) were used to conduct these experiments. Forward and reverse flotation tests were carried out in order to study the effect of the different reagents utilized in both processes on the entrainment of unwanted particles.

A kinetic analysis was undertaken to study the correlation between frother properties and flotation rate constants in reverse and forward flotation.

4.2. Materials.

4.2.1. Reagents.

4.2.1.1. Frothers.

Five different frothers were used to conduct the experiments (Table 4). The frothers were added as a 1 g/L solution, which were prepared with distilled water at room temperature.

Table 4: Frothers tested in this research

Frother	***Molecular weight (g/mol)***
MIBC	102
DF-200	206
DF-1012	400
α-terpineol	142
Diacetone alcohol	116

4.2.1.2. Diesel Oil.

Diesel oil was used as collector in the forward flotation of a sub-bituminous coal (LS-20) Prior to addition, this reagent was emulsified as described in Section 4.3.3.2.

4.2.1.3. Dextrin.

A sample of dextrin (Tapioca Dextrin 12 by A.E. Staley Manufacturing Co.) was utilized as a coal depressant.

Stock solutions of up to 2 g/L were prepared according to the following procedure: The total amount of solids is placed in 500 mls. of distilled water in a 1 liter flask. The content is vigorously stirred and heated to 60 degrees until all the solids are dissolved (between 15 to 20 minutes). Finally, the flask is filled to the 1 liter mark.

4.2.1.4. Dodecyl-Trimethyl Ammonium Bromide (DTAB).

A 99%-pure sample of DTAB, obtained from Acros Organics, was used in the reverse flotation tests as a collector for mineral matter and as a frother.

Due to the high solubility of this amine, stock solutions of up to 10 g/L were prepared with distilled water.

4.2.1.5. Polyacrylamide (PAM).

Polyacrylamide (Cytec Canada Inc.), was used in the reverse flotation tests to prevent the adsorption of DTAB onto coal. Preliminary tests indicated that the preparation of the PAM solution has an important effect on the overall flotation results; when polyacrylamide is prepared in distilled water only, it acts solely as a flocculant, whereas when the PAM solution is prepared using NaOH, it increases the yield of froth product and improves the selectivity of the reverse flotation process. This effect is associated to the degree of anionicity of the polymer, which can be controlled by boiling PAM with NaOH in solution at different time intervals (Ding, 2004).

Stock solutions of this reagent were prepared by mixing 0.5 g of PAM with 1 g of NaOH in 100 ml of distilled water.

4.2.2. Coal Samples.

Two coals samples varying in rank were used in this project:

- A high rank, bituminous coal sample (F4), was obtained from the Fording Mine, in South-eastern, BC.
- Low rank coal (LS-20) was provided by the Luscar Sterco mine in Alberta

Both samples of coal were crushed and pulverized to produce a feed of about 80-90% passing 150 microns.

The proximate analysis for these two coals is presented in Table 5. According to the ASTM Coal Classification System, F4 Coal can be classified as a medium-volatile bituminous coal, while LS-20 corresponds to a sub-bituminous coal.

Table 5: Proximate analysis for F4 and LS-20

Coal	Moisture (%)	Ash (%)	Volatile Matter (%)	Volatile Matter, d.m.m.f.(%)	Fixed Carbon, d.m.m.f. (%)
F4	0.68	11.18	23.54	26.7	73.3
LS-20	3.64	34.6	27.48	44.5	55.5

Since ash content in the F4 coal was low, this sample was blended with silica, in order to increase its ash content up to about 30 %. The particle size distribution of the silica used to make this mixture is presented in Appendix 5.

Figure 19 and shows the particle size distribution for the two samples used in this research.

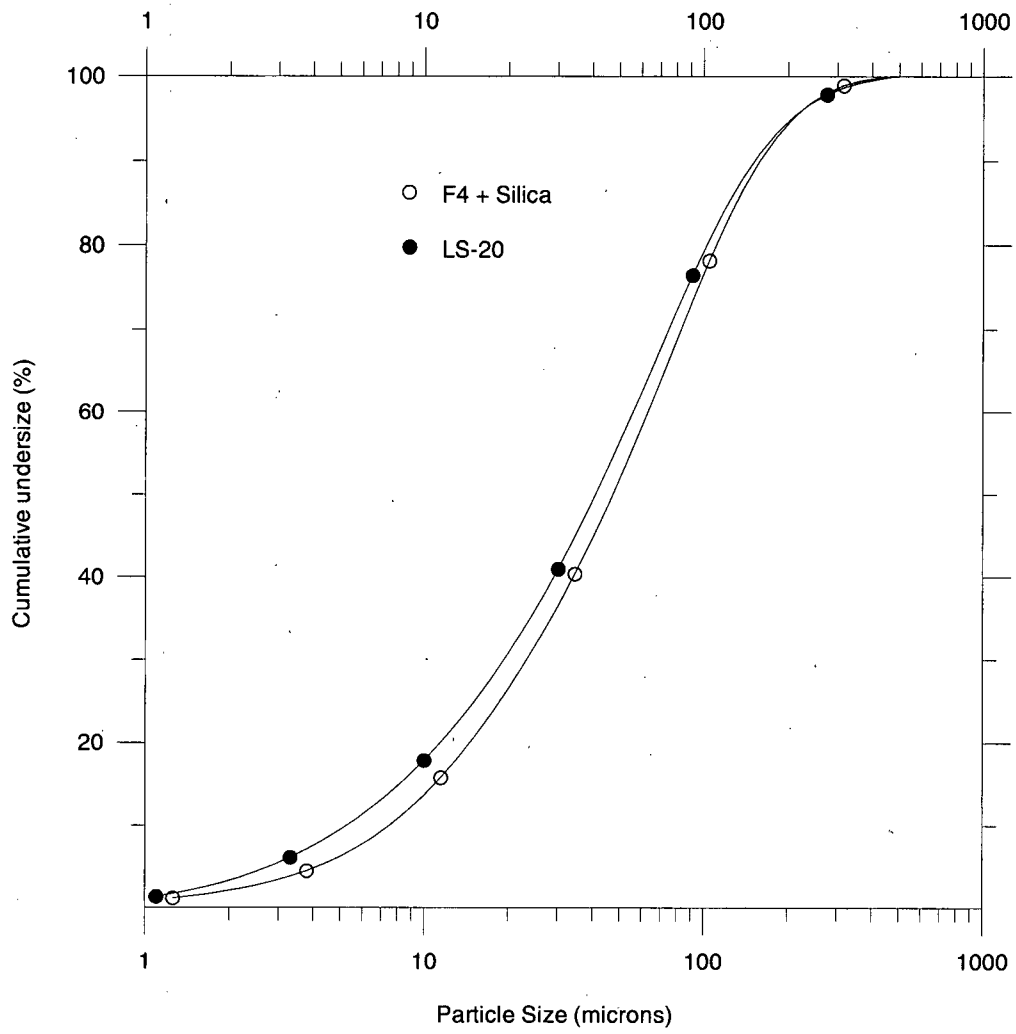

Figure 19: Particle size distribution for F4 (artificial mixture) and LS-20

4.3. Equipment and Methods.

4.3.1. Measurement of Dynamic Foamability Index (DFI).

The experiments were conducted in a glass column of 45 mm diameter and 90 cm height. A sintered disc is installed at the bottom part of the column. Foam is generated by pumping air through it. The experimental setup is schematically shown in Figure 20.

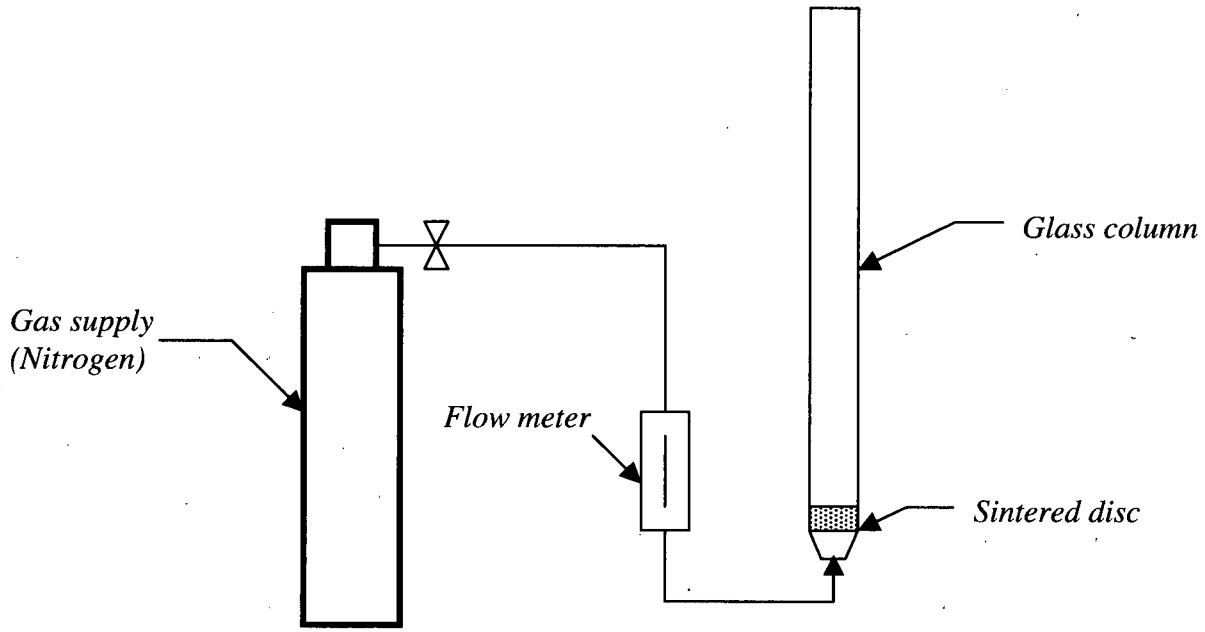

Figure 20: Setup for measurement of Dynamic Foamability Index

As it was already mentioned in Section 3.1.2.1., the DFI is defined as the limiting slope of the retention time versus concentration curve, as c → 0 (Equation 2). To determine the retention time for a given frother concentration, the column is filled with the solution to be tested and then gas is pumped through it at flow rates that range from 0.6 up to 2.4 L/min. The total volume of gas present in the system (foam + solution) is measured and plotted as a function of the gas flow rate. Above a given flow rate, a linear relationship should be observed between these two variables. The slope of this linear trend corresponds to the retention time.

Finally, the retention times are plotted against concentration, which gives a curve like the one shown in Figure 21. From this curve, the DFI can be determined graphically.

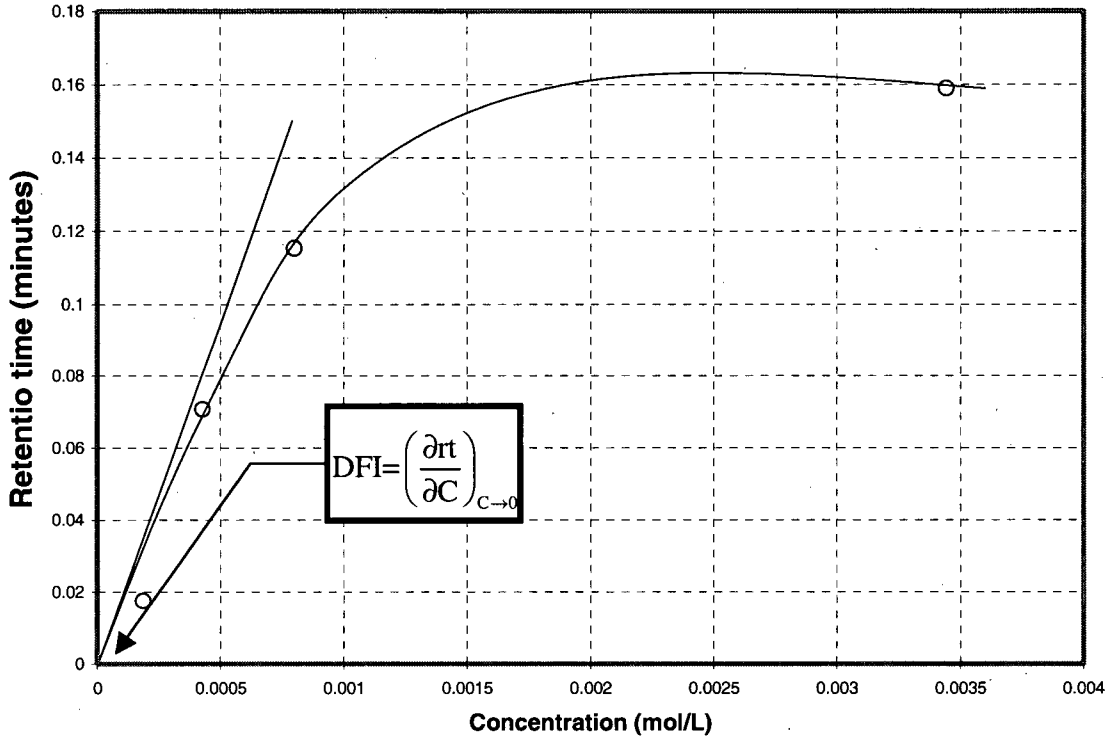

Figure 21: Graphic determination of DFI from retention time versus concentration curve.

4.3.2. Measurement of Water Recovery (Two-Phase System).

All the frothers used in this study were tested in order to measure their ability to recover water in a simple system consisting of water and frother only. The tests were conducted in a 3-liter Open Top Leeds flotation cell.

For each frother, a number of concentrations were tried. The procedure followed to carry out the test for each concentration is described below:

- Weigh out 5 containers and number them from 1 to 5.
- Fill flotation cell with tap water to approximately 2.9 L.
- Set the agitator to 1200 rpm.
- Add the required volume of frother from stock solution (1g/L) to the cell and complete the volume to 3 liters with tap water.

- Condition for 5 minutes.
- Open the air valve and set the air flow rate to 4 L/min.
- "Float" water for five minutes. Scrap the foam off every 15 seconds (4 times per minute) and collect the water in the trays previously weighed.
- Weigh out each tray (tray + water recovered).

All the tests are conducted adjusting the foam height to 1 cm, which allows to recover water even when weak frothers are tested.

4.3.3. Batch Flotation Tests.

All the flotation tests were conducted at 10 % solids in a 3-liter Open Top Leeds flotation cell. The froth height was set to a convenient thickness in each case and it was closely controlled during the performance of each test. The pulp level was maintained constant at all times by adding water as required.

In both forward and reverse flotation, the concentrates were collected every one minute in separate trays (previously weighed) over a period of five minutes. The froth was scrapped off every 10 seconds.

Five bottles filled with water were also weighed out before conducting each test. The water in these bottles was used to wash off the froth attached to the scrapper when collecting the concentrates. After each test, the water remaining in each bottle was weighed in order to determine the amount of "wash water" added to each tray. When analyzing the data, this amount was subtracted from the water recovered from the cell in each tray.

The concentrates were dried in an oven at 90 ^{0}C for 24 hours. A sample of tailings was collected in each test for mass balance calculations.

All the tests were carried out at natural pH to reflect industrial conditions.

4.3.3.1. Flotation of F4 Coal.

The forward flotation tests were carried out on the F4 coal using frother only due to the high hydrophobicity of this sample. Four concentrations of each of the frothers tested in this research were tried, namely $3.3x10^{-3}$, $5.5x10^{-3}$, $7.7x10^{-3}$ and $1.1x10^{-2}$ g/L, which correspond to 30, 50 70 and 100 g/t, respectively.

310 grams of the F-4 coal were mixed with 2 liters of tap water in the flotation cell for 15 minutes, stirring the pulp at 1300 rpm. Such a conditioning time was required to ensure that all the coal gets completely wet. The froth height was set to 3 cm as preliminary tests indicated that this thickness allows proper collection of the floating material. A very thin froth makes difficult to collect the concentrate and to maintain the pulp level due to the high yields observed in the flotation of this kind of coal, whereas a thick froth does not allow to collect all the material that is actually floating.

Once the conditioning is completed, the cell is filled up to 3 liters and the impeller set to 1000 rpm. Then the frother is added from a stock solution and is conditioned only for thirty seconds to avoid its adsorption onto coal particles. The flotation tests were conducted at an air flow rate of 5 L/min.

4.3.3.2. Flotation of LS-20 Coal.

a) Forward Flotation.

Similarly to the case of forward flotation of F4, four concentrations were tried for each frother, namely $1.1x10^{-2}$, $1.6x10^{-2}$ and $2.2x10^{-2}$ g/L. In addition, Diesel oil was used as oily collector to enhance the selectivity of the flotation of LS-20.

The froth height was set to 1 cm since the yields are significantly lower compared to the flotation of F-4.

The test is conducted by preparing a 10% solids pulp in the cell. The pulp is conditioned for 5 minutes at 1300 rpm. Then, the impeller is set to 1000 rpm. Once this is done, the Diesel oil is added as an emulsion, which is prepared according to the following procedure:

- The total amount of Diesel oil required for each test is placed along with 50 mls. of water in a blender.
- One half of the total volume of frother required to conduct the test is also added to the blender.
- The content of the blender is vigorously mixed at high speed for one minute.
- The emulsion is then quickly transferred to the flotation cell, and conditioned for 15 seconds.
- The remaining amount of frother is then added to the cell and conditioned for another 15 seconds.

After the addition of the emulsion and the remaining amount of frother to the cell, the air flow rate is set to 5 L/min to start floating for 5 minutes.

b) Reverse Flotation.

To carry out the reverse flotation tests, the pulp is conditioned in the cell for 5 minutes at 1300 rpm. After this initial conditioning period, the impeller speed is decreased to 1000 rpm. Then the coal depressant (dextrin) is added and conditioned for three minutes, followed by the addition of DTAB. The latter reagent is not conditioned at all in order to minimize its adsorption on the coal surface and the test starts as soon as it is added.

Due to the high DTAB consumption observed in these experiments, additional tests were conducted in the presence of polyacrylamide (PAM), since there is experimental evidence that indicates that when this reagent is used the amount of DTAB needed in the process can be reduced (Ding, 2004). When this polymer was utilized, it was added after the coal depressant, followed by five minutes of conditioning. The amine (DTAB) was then added to the cell (without any conditioning) to start the test.

4.3.4. Particle Size Measurements.

The particle size distributions of the coal samples were determined using a laser diffraction based instrument (Mastersizer 2000) that allows to carry out measurements, in a range from 0.02 to 2000 microns, on different sample types, including emulsions, suspensions and dry powders.

4.3.5. Surface Tension Measurements.

Surface tension measurements were conducted for each tested frother by means of a Du Nouy ring tensiometer.

The measurement procedure for each frother included the preparation of several solutions in distilled water, with concentrations ranging from 10^{-5} to 10^{-2} mol/L.

All the solutions were prepared at room temperature and stirred for 5 minutes before conducting the measurement.

Preliminary calibration measurements performed on distilled water and pure methanol revealed good reproducibility and accuracy of the measurements (+/-1mN/m). No correction factors were applied to the measured values.

4.3.6. Ash Content Determination.

Ash determination analyzes were run on a regular basis throughout this work. These analyzes were conducted by burning a known amount of coal in a crucible at 750 ^{0}C for three hours. The remaining residue is then carefully weighed out to calculate the ash content according to the following equation:

$$\% \text{ Ash} = \frac{[\text{Residue remaining after burning (g)}]}{[\text{Initial weight of coal (g)}]} * 100$$

5. RESULTS.

5.1. Frother Characterization.

5.1.1. Surface Tension Measurements.

Figure 22 shows the surface tension versus concentration curves for all the tested frothers. Since DTAB also plays the role of frother in reverse flotation, the curve for this amine is also included.

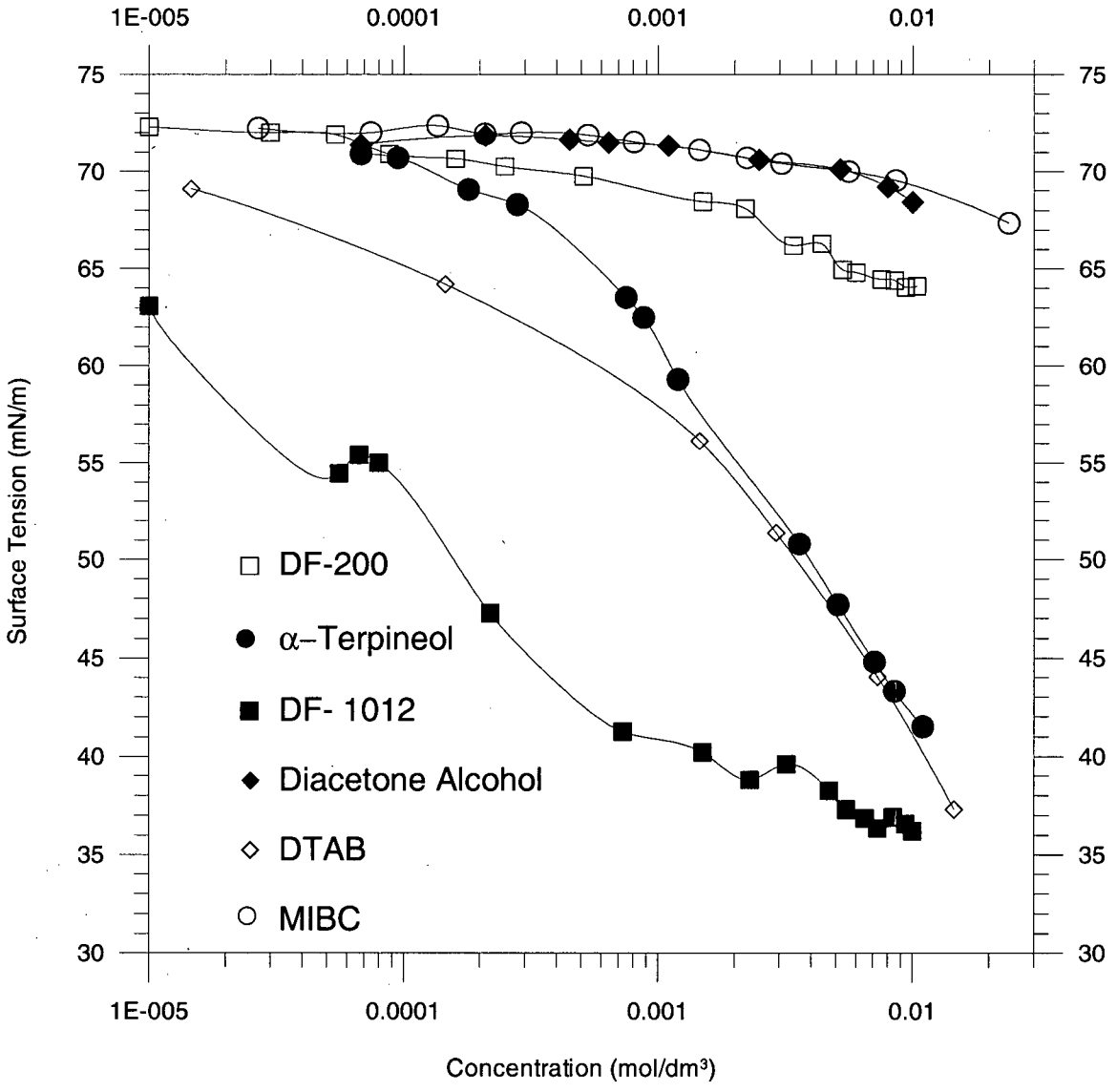

Figure 22: Surface tension curves for all the tested frothers.

Figure 22 clearly shows that DF-1012, α-terpineol and DTAB are quite surface active, whereas MIBC and diacetone alcohol reduce only slightly the surface tension of distilled water. DF-200 falls in between these two groups.

5.1.2. Dynamic Foamability Index (DFI).

Table 6 shows the values of the dynamic foamability indices for all the tested frothers.

Table 6: Dynamic foamability indices for all the tested frothers

Frother	DFI, [sdm^3/mol]
DF-1012	267000
DF-200	196000
α-terpineol	138000
MIBC	37000
Diacetone alcohol	12000

The values presented in Table 6 were extracted from references, except those for diacetone alcohol. Appendix 2 shows the curves used in the calculation of the DFI for this frother.

5.1.3. Foam Structure.

In general, spherical bubbles were observed in the foams generated in the presence of the flotation frothers investigated in this work, as shown in Figure 23 for the case of MIBC. This structure is significantly different compared to the one observed for DTAB solutions in terms of both appearance and stability. Figure 24 shows the foam generated from a DTAB aqueous solution. It can clearly be seen that the shape of the bubbles is different in comparison with the structure shown in Figure 23.

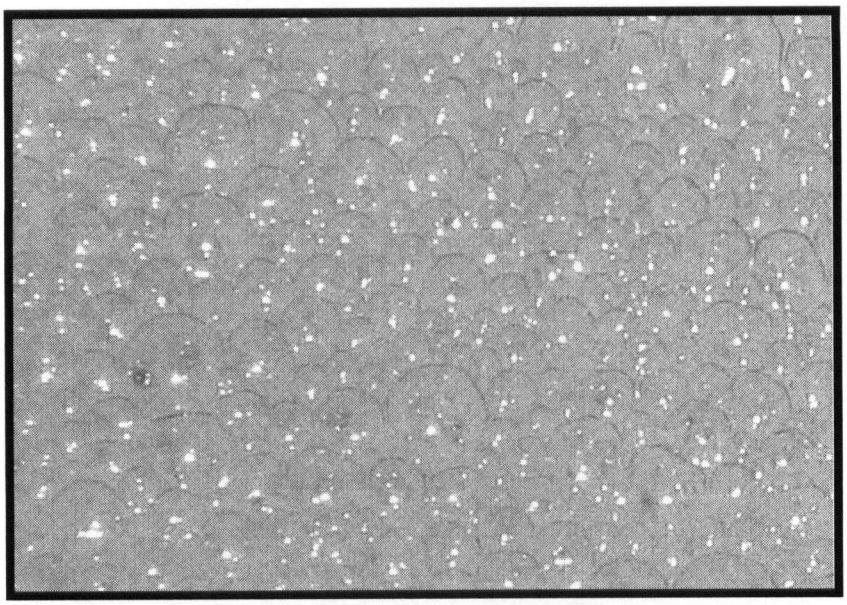

Figure 23: Foam generated from a MIBC aqueous solution (12 ppm, gas flow rate = 4 L/min)

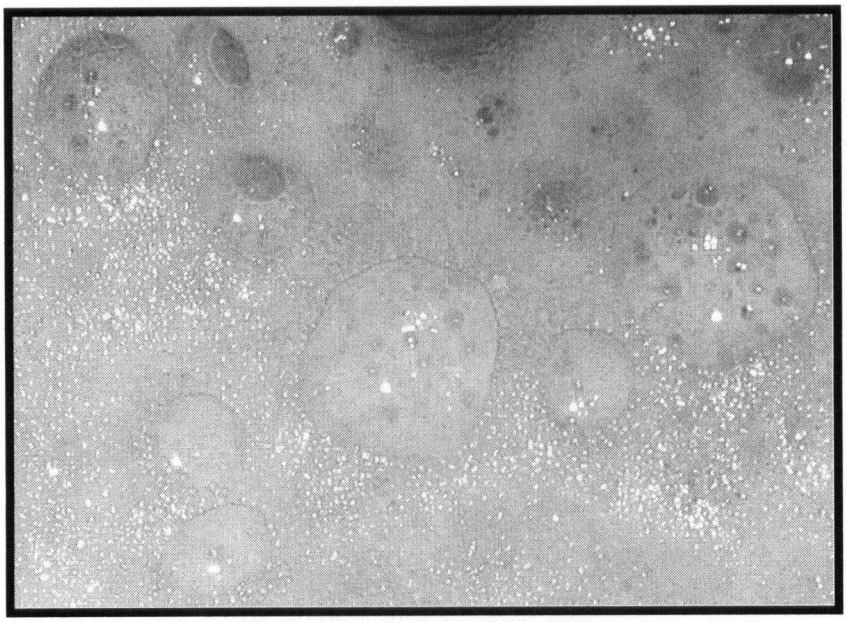

Figure 24: Foam generated from a DTAB aqueous solution (12 ppm, gas flow rate = 4 L/min)

The difference in stability between the two types of foams could be observed when the gas supply is cut off. In the case of the flotation frothers, the foam quickly collapses whereas in the case of DTAB the foam persists for a considerably longer period of time before collapsing after the gas supply is stopped.

It is worth mentioning that this difference in stability should also be reflected in terms of the DFI values. It is clear that DTAB should have the highest DFI among all the tested frothers. Unfortunately, this parameter could not be measured for the case of DTAB, since the foam generated when following the experimental procedure described in Section 4.3.1. consistently ascends along the column without reaching an equilibrium state that allows to measure the total volume of gas in the system.

5.1.4. Measurements of Water Recovery in a Two-Phase System.

Tests to measure the amount of water recovered in a flotation cell containing frother solutions were carried out according to the procedure described in Section 4.3.2. Figures 25 to 29 show the curves obtained from these tests.

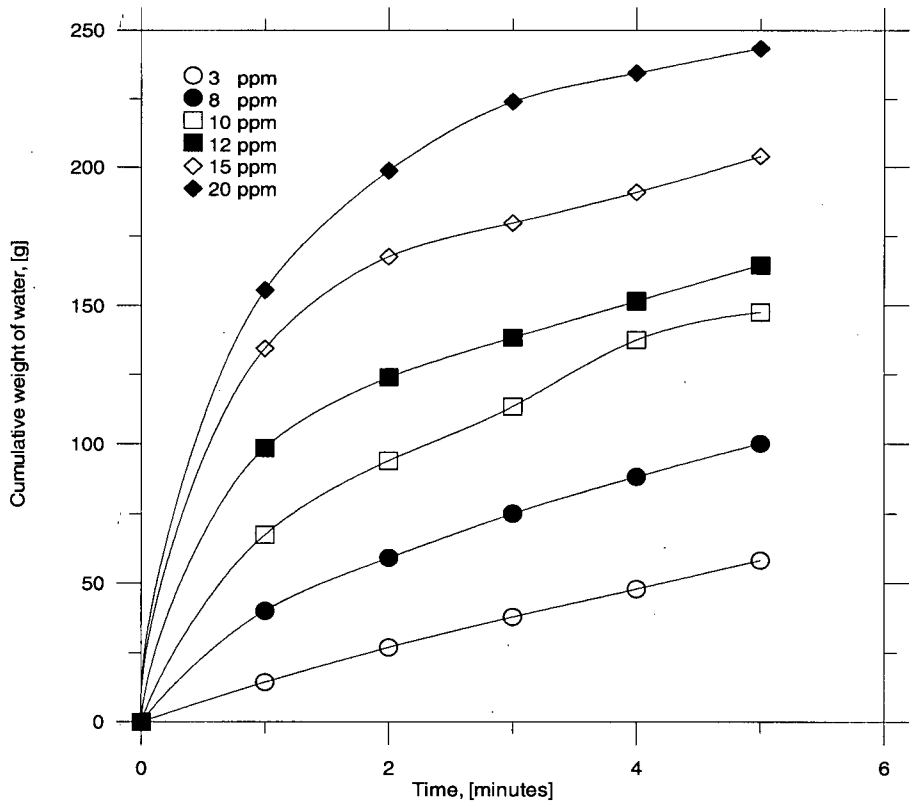

Figure 25: Cumulative water recovery versus time for MIBC solutions (gas flow rate = 4 L/min)

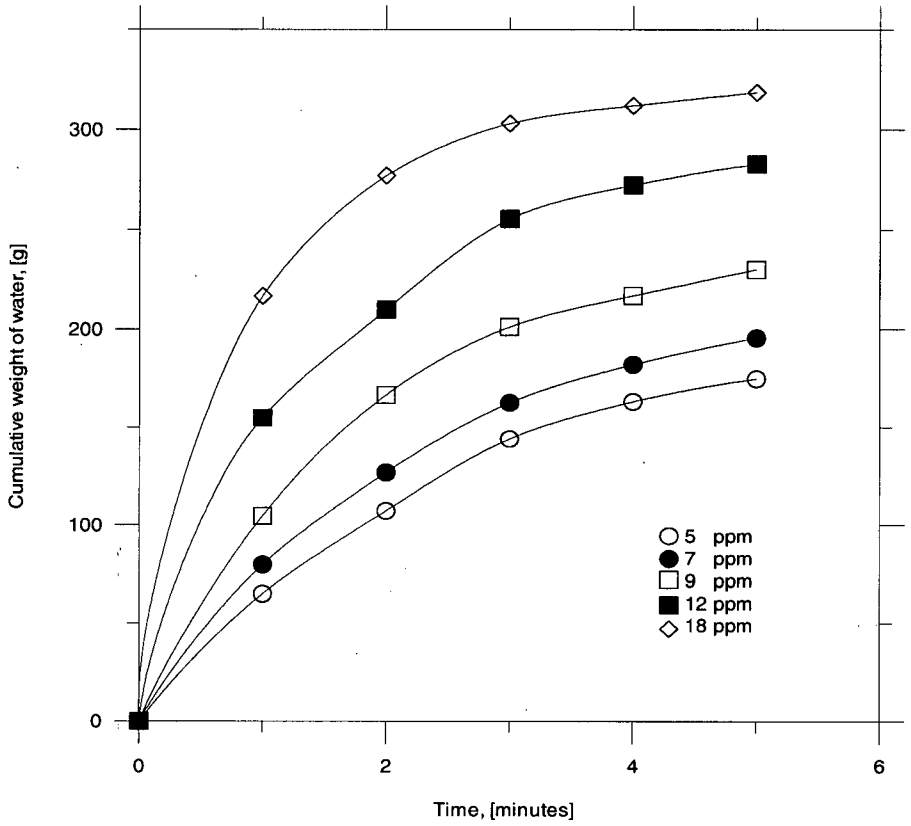

Figure 26: Cumulative water recovery versus time for α-terpineol (gas flow rate = 4 L/min)

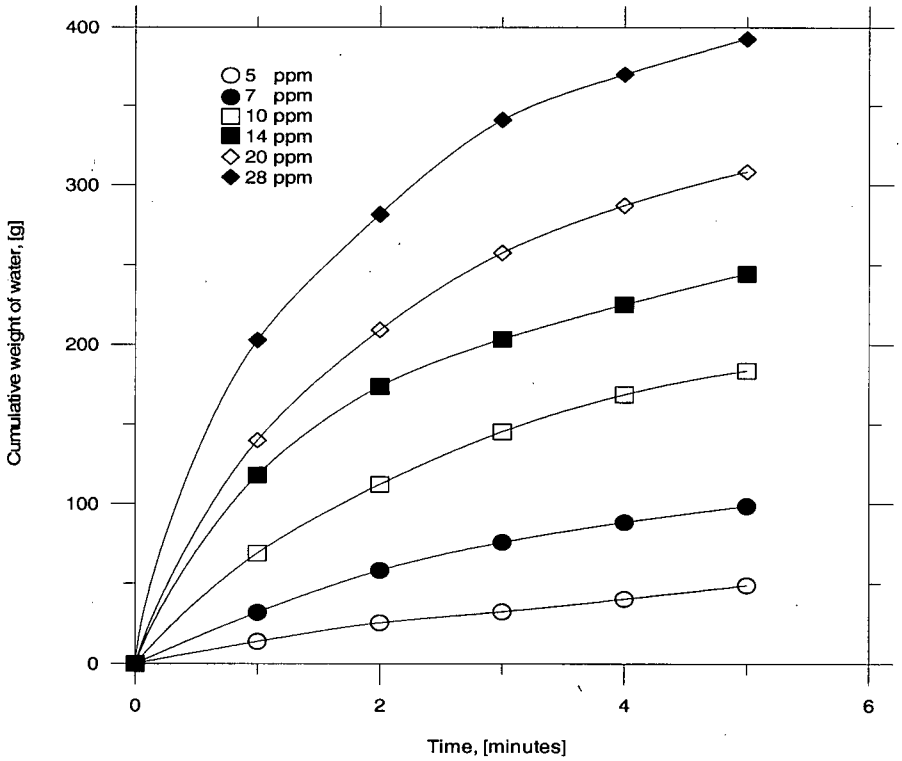

Figure 27: Cumulative water recovery versus time for DF-200 solutions (gas flow rate = 4 L/min)

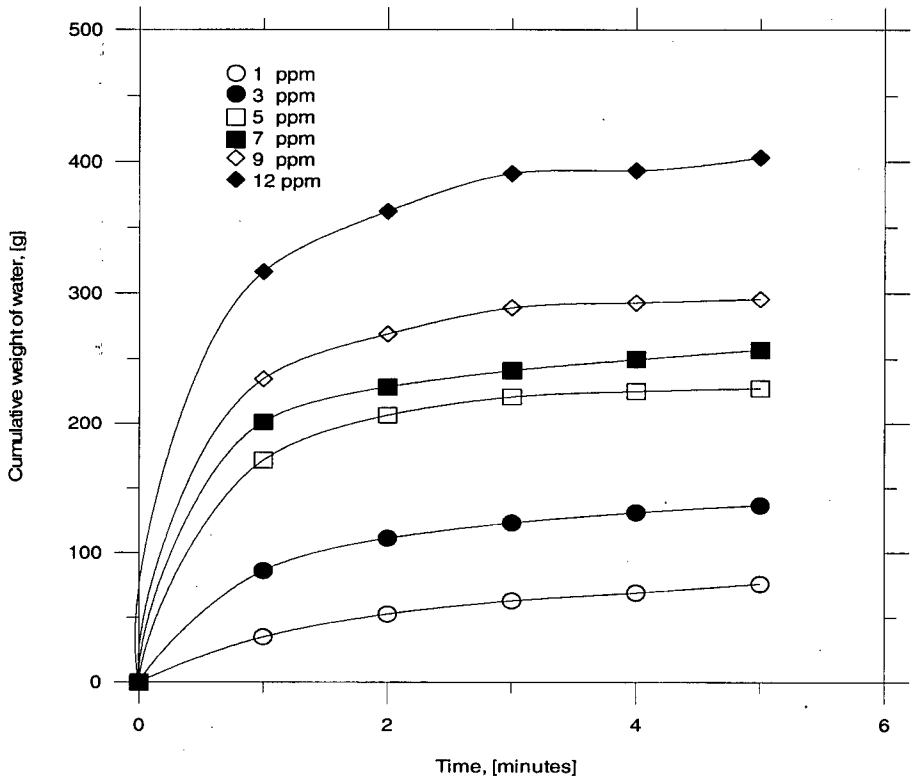

Figure 28: Cumulative water recovery versus time for DF-1012 solutions (gas flow rate = 4 L/min)

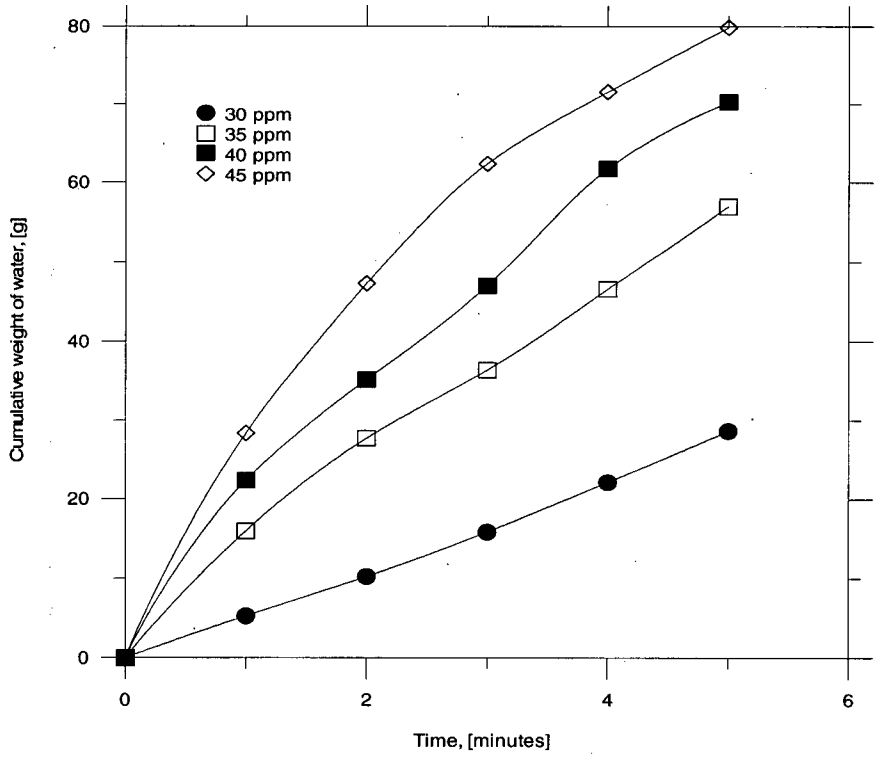

Figure 29: Cumulative water recovery versus time for diacetone alcohol solutions (gas flow rate = 4 L/min)

In order to facilitate the interpretation and comparison of the results obtained for the different frothers, it is necessary to translate each curve into a single value that represents the performance of the frother in terms of water recovery. This value should also be related to the frother concentration in the system, which decreases continuously during the test, as the water is floated out of the cell. It is clear that only at the beginning of the test, the actual concentration of frother is known.

In this work, the initial rate of water recovery was calculated for each test as a measure of the performance of the frother, since this parameter can be directly related to the actual frother concentration in the cell. The calculation was done taking into account the slope of the cumulative water recovery versus time curve at five different time intervals (from minute 0-1, 1-2, 2-3, 3-4 and 4-5) and assigning the resulting values to the middle point of each time interval. Then, the calculated rates were plotted against time and the curve obtained was extrapolated to "time zero" to determine the initial rate.

Figure 30 shows the curve rate of water recovery versus time for MIBC. The curves obtained for the other frothers are presented in Appendix 4.

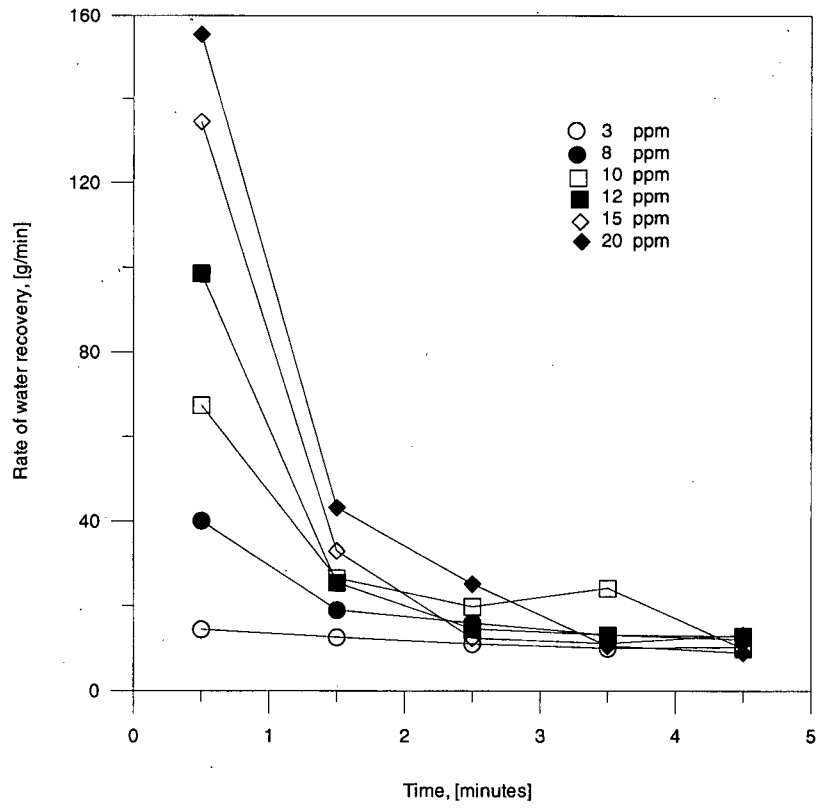

Figure 30: Rate of water recovery versus time for MIBC solutions at different concentrations.

The extrapolation of each curve in Figure 30 to "time zero" yields a set of values for the initial rate of water recovery at different concentrations. The same set of data can be obtained for all the tested frothers and plotted in one graph. This is shown in Figure 31. If a straight line is fitted to each curve in this graph, the slope of such a line can be used as a "water recovery constant" to characterize the performance of the tested frothers in terms of water recovery. Table 7 shows these results.

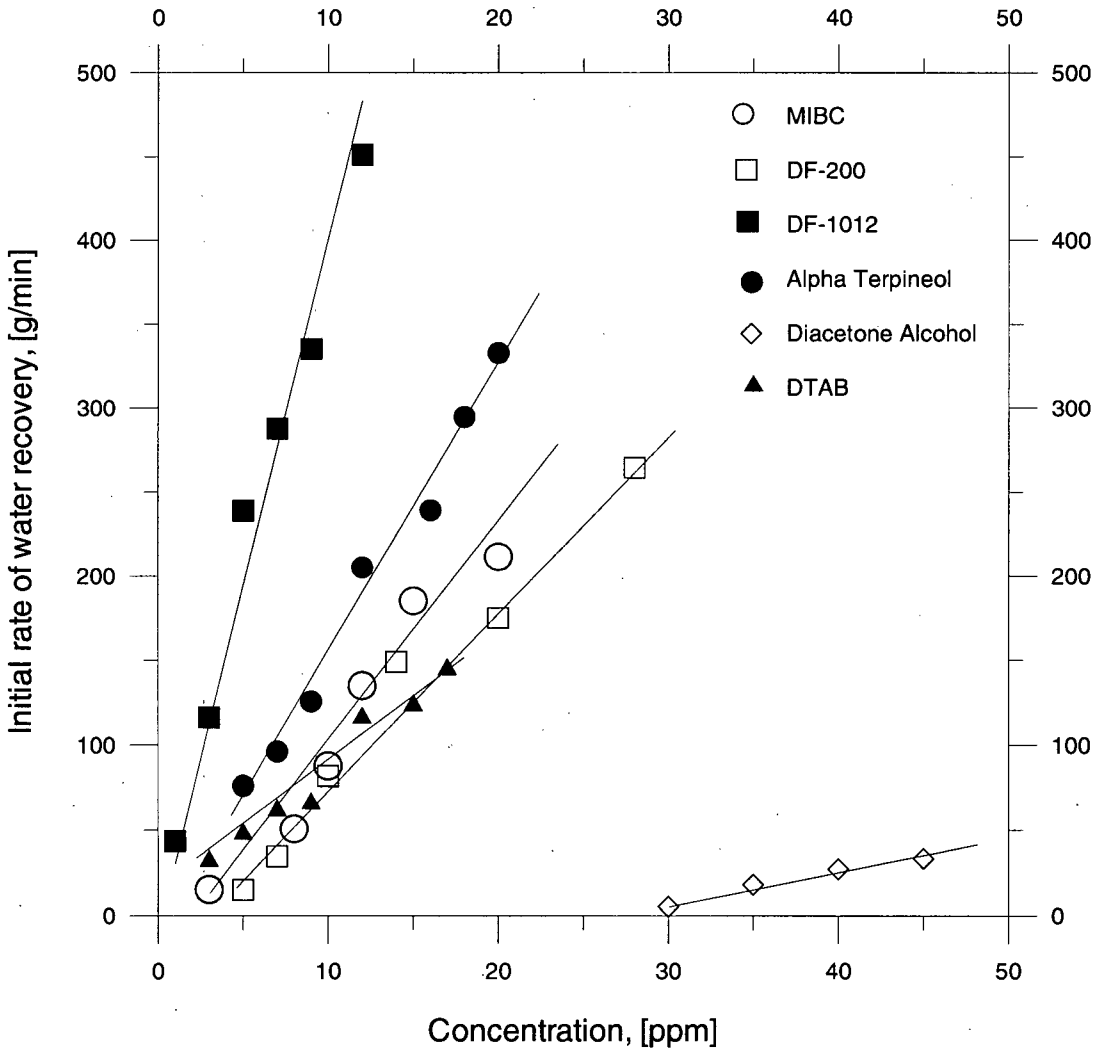

Figure 31: Initial rate of water recovery versus concentration (two-phase system) for different frothers.

Table 7: Water recovery constants calculated from Figure 30 for all the tested frothers.

Frother	Water recovery constant, [g/min/ppm]
DF-1012	36.5
α-terpineol	17.2
MIBC	12.8
DF-200	10.7
DTAB	8.2
Diacetone alcohol	1.8

From Figure 31 and Table 7 it can be observed that DF-1012 is the most active reagent with respect to the water recovery in the absence of solids, whereas in the case of diacetone alcohol, only at concentrations greater than 30 ppm some amount of water can be recovered at fairly low rates.

To relate the capability of each frother to transport water to the stability of the foam, the kinetic approach described in Section 3.3 was applied to the water recovery curves presented in Figures 25 to 29. Flotation rate constants were determined for all the concentrations tested. The calculated constants were then correlated to the DFI values for each frother at concentrations slightly exceeding the CCC in order to ensure that the coalescence of bubbles is entirely controlled. These concentrations are presented in Table 8.

As it can be seen from Figure 32, a very good correlation results between the flotation rate constants for water and the DFI values of the tested frothers.

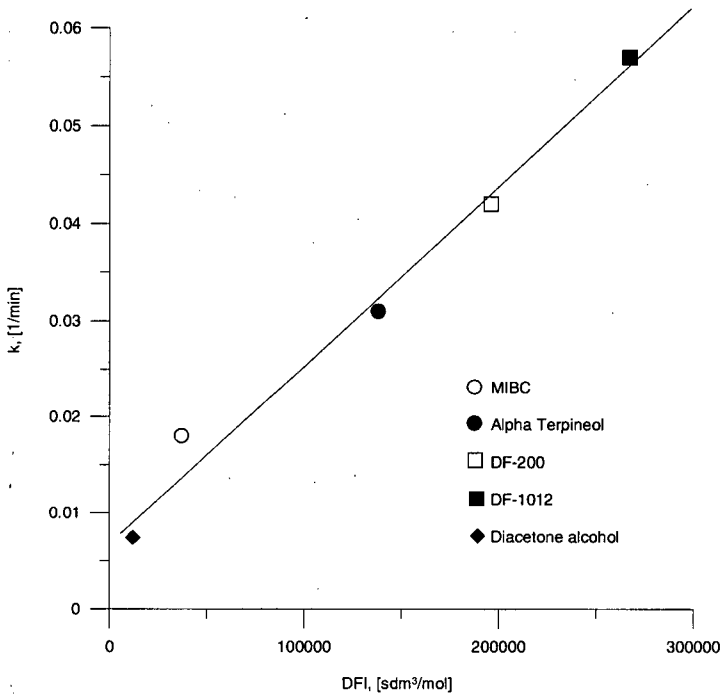

Figure 32: Correlation between the flotation rate constant for water (frother-water system) and DFI for the tested frothers.

Table 8: CCC values and concentrations used for the calculation of the water rate constants for the tested frothers.

Frother	CCC, [ppm]	Concentration used for the calculation of the water rate constant, [ppm]
MIBC	11.2	15
α-terpineol	Around 8-9	12
DF-200	18.4	28
DF-1012	6	12
Diacetone alcohol	Around 30-40	45

5.2. Batch Flotation Tests.

5.2.1. Forward Flotation.

5.2.1.1. Bituminous Coal (F4).

Figure 33 summarizes the results obtained in the forward flotation of the F4 coal-silica mixture. It can be observed that DF-1012 and diacetone alcohol are not efficient frothing agents for this coal. For these two frothers the yield is approximately constant (about 45 %) throughout the concentration range. The ash content curves follow the same trend.

Figure 33 also shows that α-terpineol and DF-200 performed similar in terms of yield and water recovery. The ash contents in the clean product were also similar and only at 100 g/t DF-200 performed slightly better than α-terpineol.

The water recoveries for MIBC, α-terpineol and DF-200 were higher compared to diacetone alcohol and DF-1012 at all concentrations, which correlates well with the ash content, confirming that there is a relationship between the amount of water recovered in the concentrate and the ash content in the clean product.

The kinetic curves shown in Figure 34 demonstrate that most of the product floats over the first two minutes. Figure 35 confirms that the material that floats in this period of time corresponds basically to fine coal, as the average particle size increases from about 20 microns for the concentrate obtained after one minute of flotation, to 50 microns for the concentrate obtained after 5 minutes.

It is clear that in this initial period of time (first two minutes), due to the high amount of material which is carried up to the froth collection zone, entrainment and entrapment are significant.

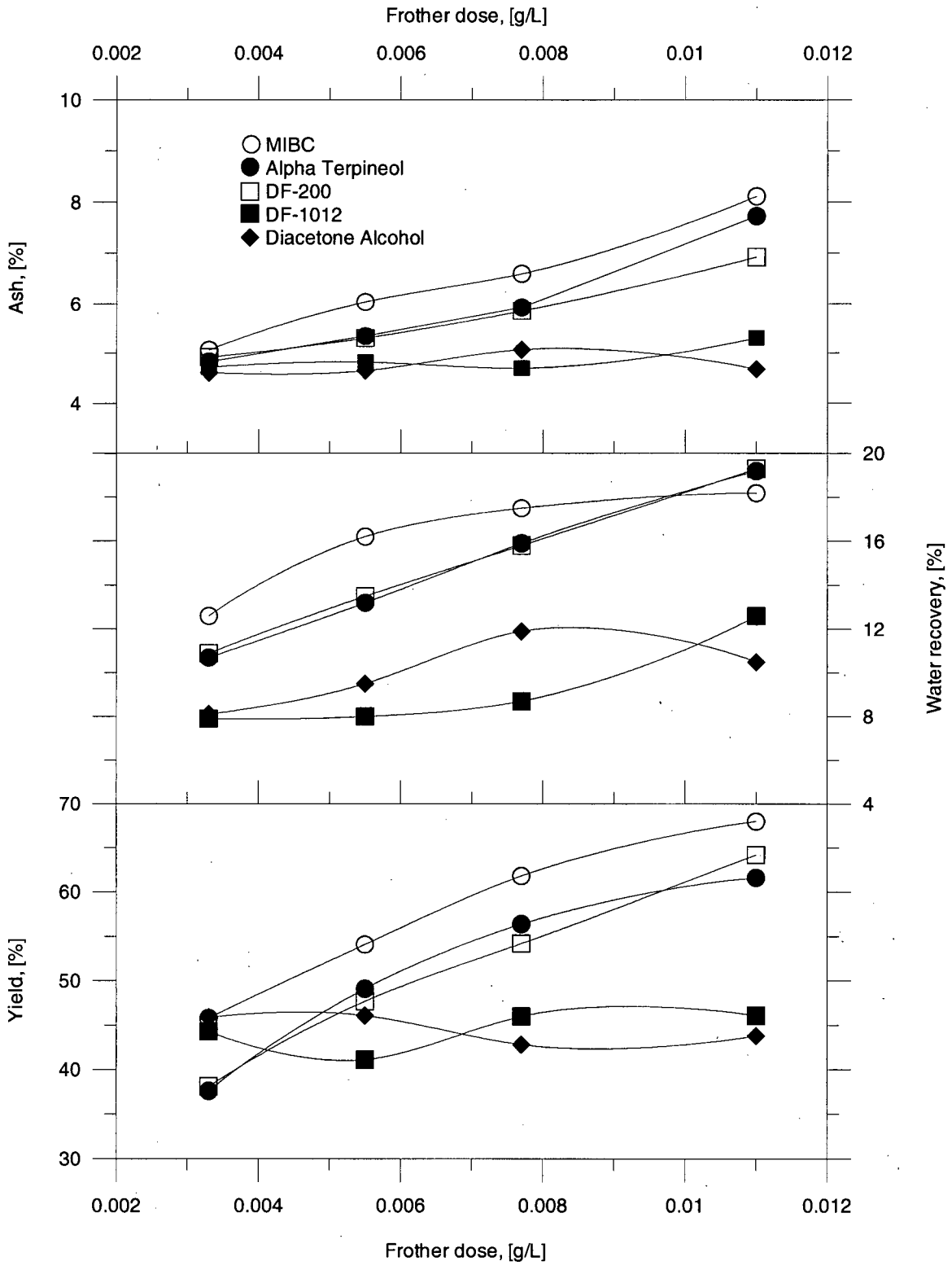

Figure 33: Effect of frother dose on yield, water recovery and ash content after 5 minutes of flotation (F4 coal-silica mixture, forward flotation)

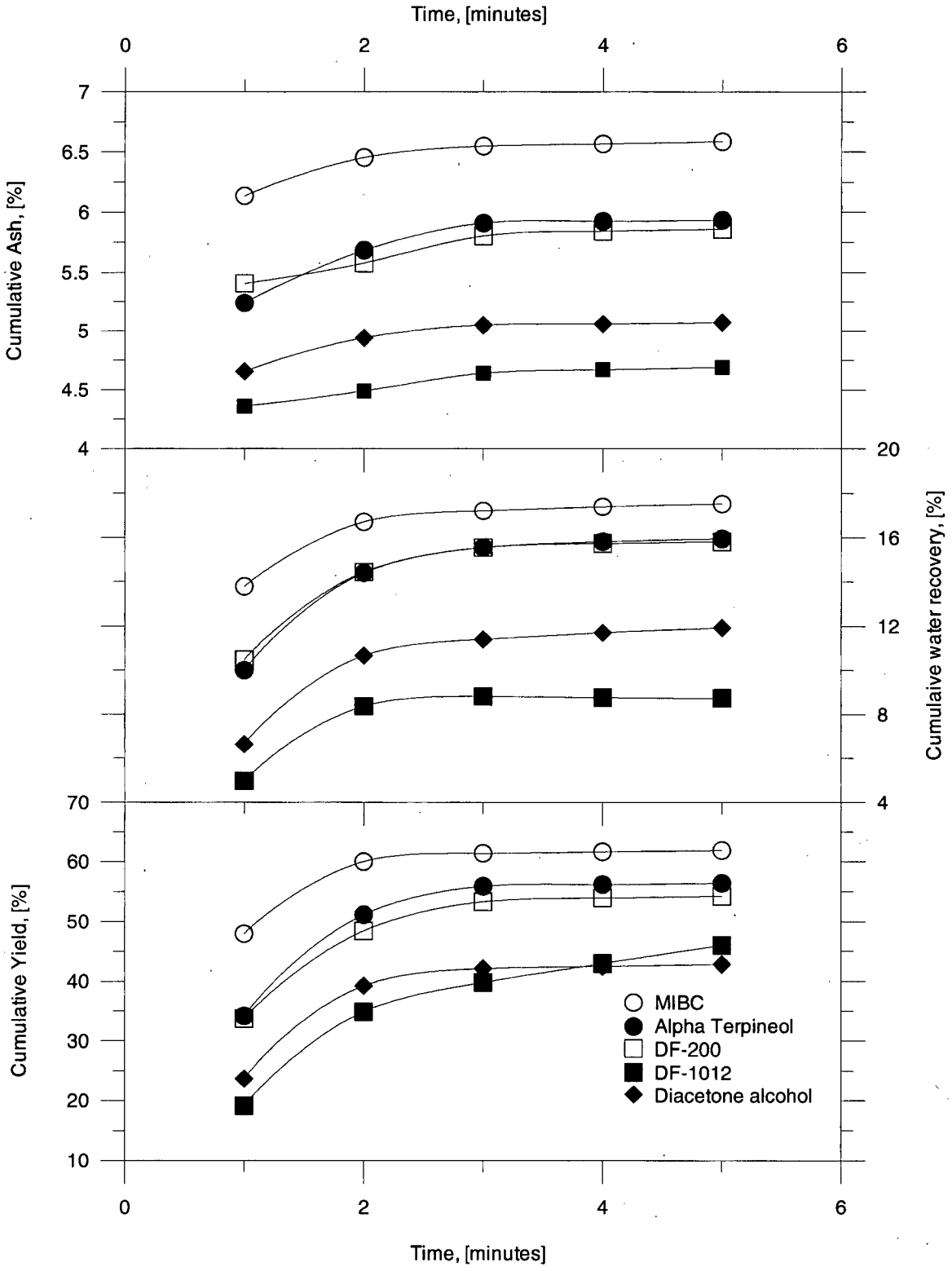

Figure 34: Flotation kinetics for F4 coal-silica mixture for all tested frothers at 7.7×10^{-3} g/L (forward flotation)

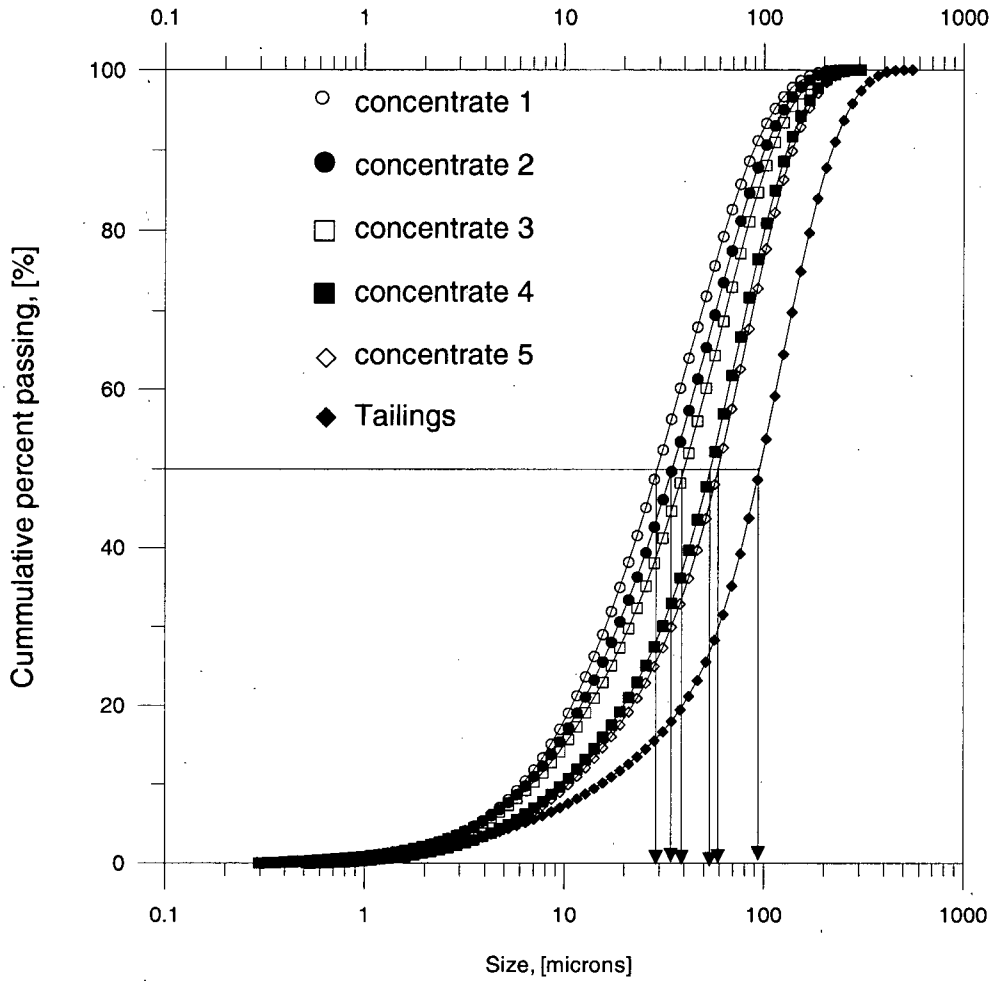

Figure 35: Particle size analysis for flotation products, forward flotation of F4-Silica mixture, in the presence of 3.3×10^{-3} g/L of α-terpineol.

Figure 36 shows the kinetic curves obtained for MIBC in terms of yield of coal versus time and log(100-yield) versus time. It is clear from the shape of the latter curves that more than one component is present in the feed, as one single straight line cannot be fitted to the curve. The plots for the rest of the tested frothers are presented in Appendix 3.

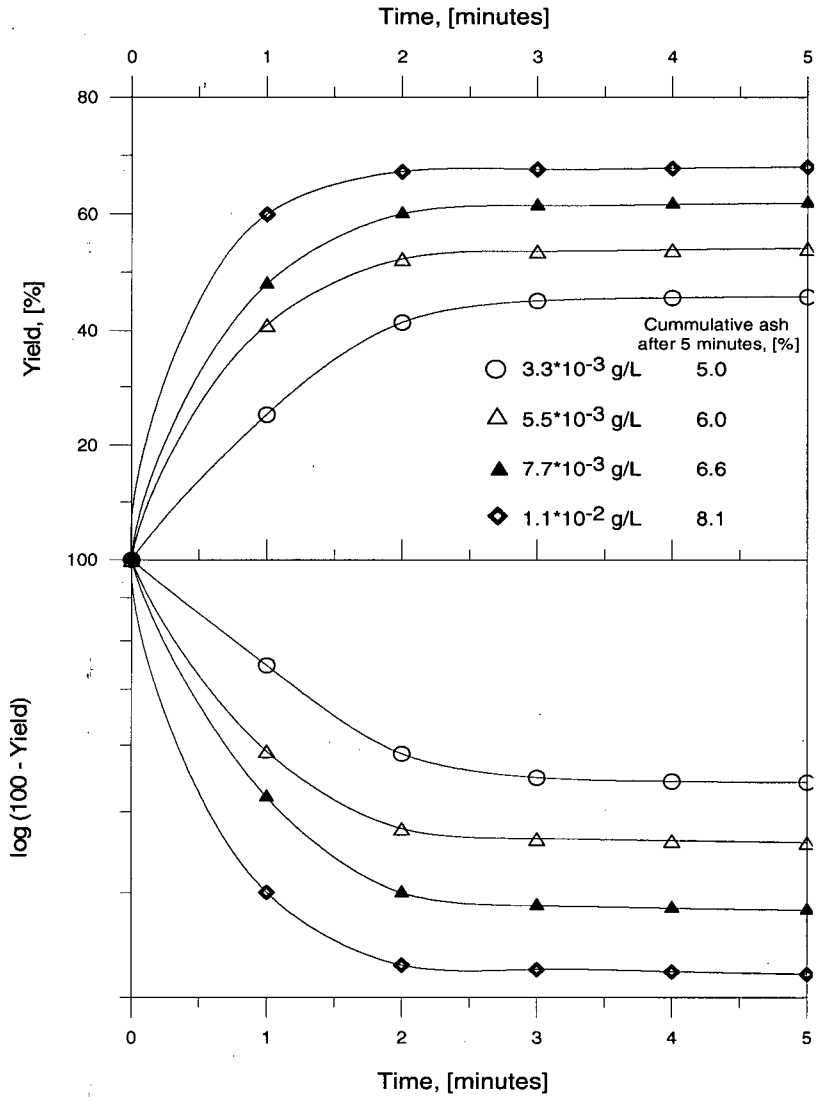

Figure 36: Yield versus time and log(100-yield) versus time for MIBC at different concentrations.

From the curves shown in Figure 36, flotation rate constants were determined for coal and the water recovered in the presence of coal. These constants were then correlated to each other. The results are presented in Figure 37.

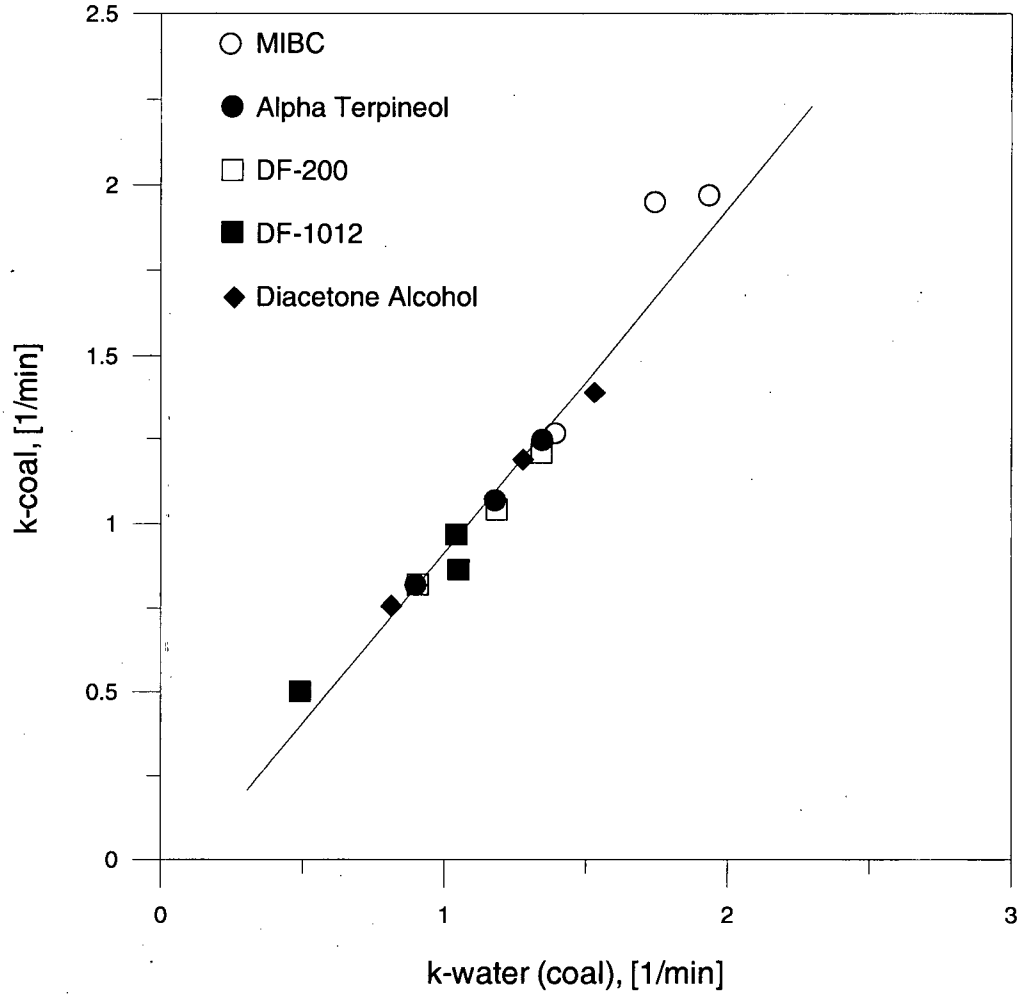

Figure 37: Correlation between the flotation rate constant for the coal fast floating component and flotation rate constant for water.

As Figure 37 reveals, there is a very good correlation between the flotation constants calculated for the fast floating coal particles and the water flotation rate constants obtained from the water contents of the froth products, which confirms that the flotation of fine particles should strongly depend on the content of water carried to the froth.

To compare the effect of the tested frothers on the flotation rate of the fast floating component, the k values were plotted versus DFI x C for each frother and each concentration (as suggested by Malysa et al., 1987). This plot unexpectedly displays two curves with the points for MIBC giving a different and very steep straight line (Figure 38). This implies that for MIBC the high flotation rate constants for fast floating coal were obtained at much lower equivalent MIBC concentrations.

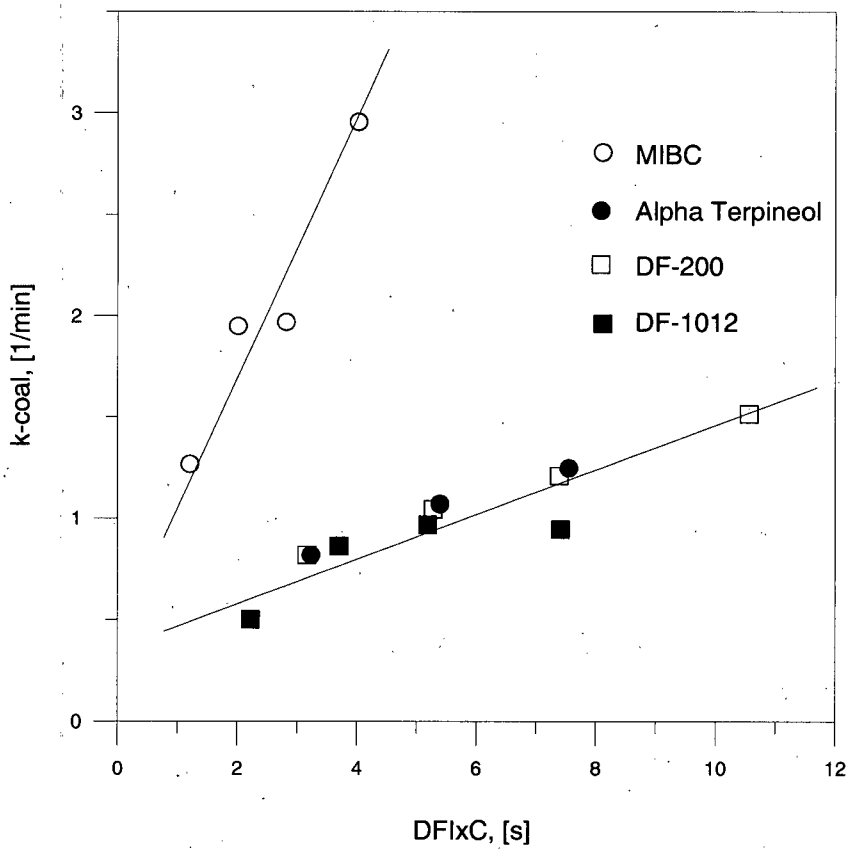

Figure 38: Correlation of flotation rate constants for coal fast floating component with DFI x C for MIBC, α-terpineol, DF-200 and DF-1012.

As pointed out before, coarse silica was used to increase the ash content of the F-4 coal sample utilized in these tests. Although the results obtained are valid for comparison purposes between the tested frothers, clearly the effect of entrainment is not significant under these conditions. In order to enhance the effect of entrainment in the results, two frothers, MIBC and DF-1012, were selected to carry out additional tests, this time using a mixture of a coal similar to F-4 (from here onwards "coal sample # 2") and fine silica.

The proximate analysis for the coal sample # 2 and the particle size distribution of the silica used in these additional tests are presented in Appendices 6 and 7, respectively.

The results are shown in Figure 39. The water recoveries with MIBC (about 20%) are higher in these tests than in Figure 33 (about 18%). This correlates well with much higher ash contents in Figure 39 (10-14%) compared with those shown in Figure 33 (5-8%). Similar trend is observed with DF-1012, but again this frother gave poorer flotation and less entrainment.

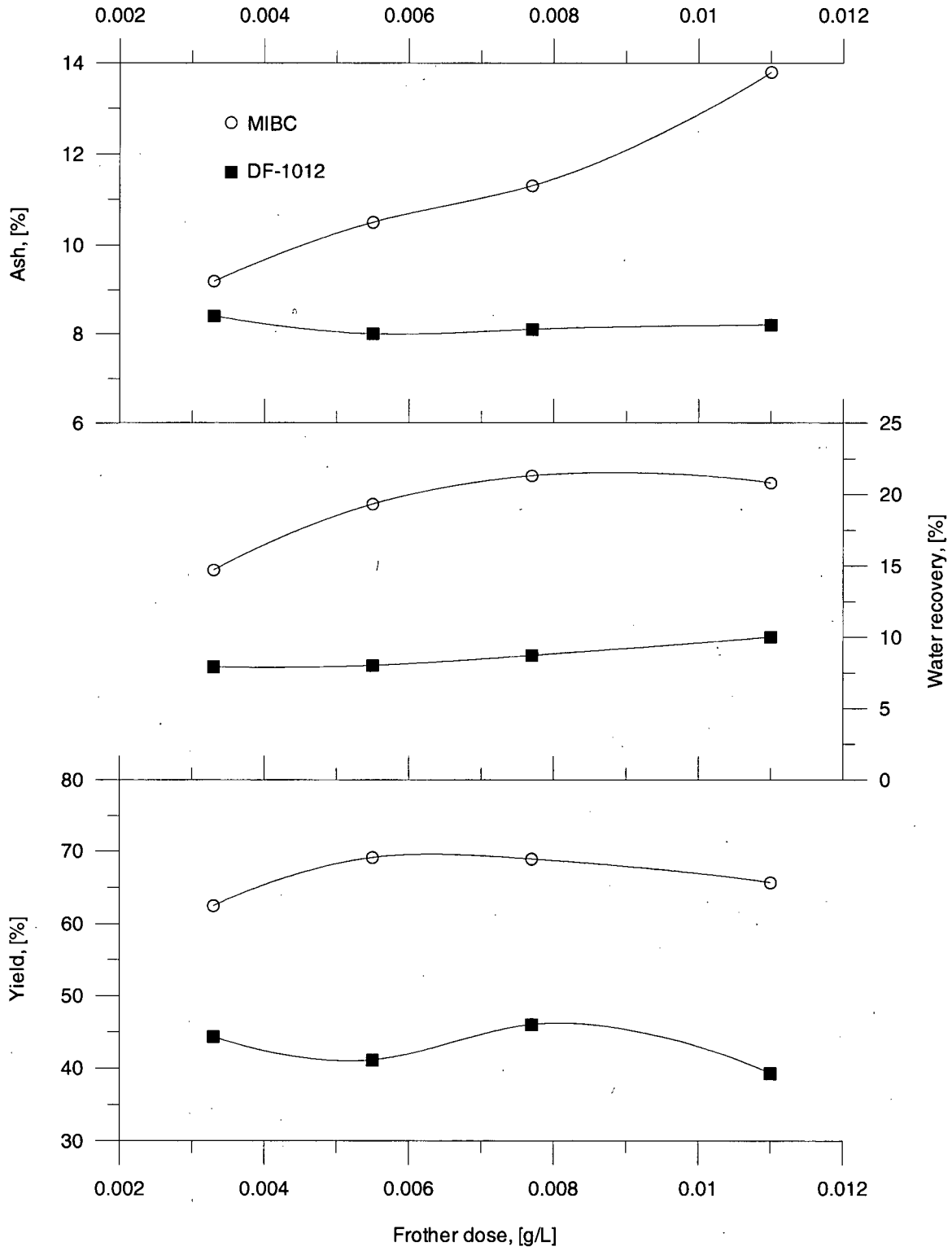

Figure 39: Effect of frother dose on yield, water recovery and ash content after 5 minutes of flotation, Forward flotation of coal sample # 2 + fine silica

5.2.1.2. *Sub-bituminous Coal (LS-20).*

Figure 40 shows the results of a series of preliminary tests conducted on LS-20 coal using $1.1x10^{-2}$ g/L (equivalent to 100 g/t) of MIBC and different Diesel oil dosages. The curve shows a clear effect on the yield, whereas the ash content in clean coal seems to be independent of the oily collector addition.

It is clear that the addition of Diesel oil improves the recovery of combustible matter in the flotation of LS-20. From Figure 40, a dosage of 3 kg/ton of Diesel oil was selected to conduct flotation tests at different frother dosages.

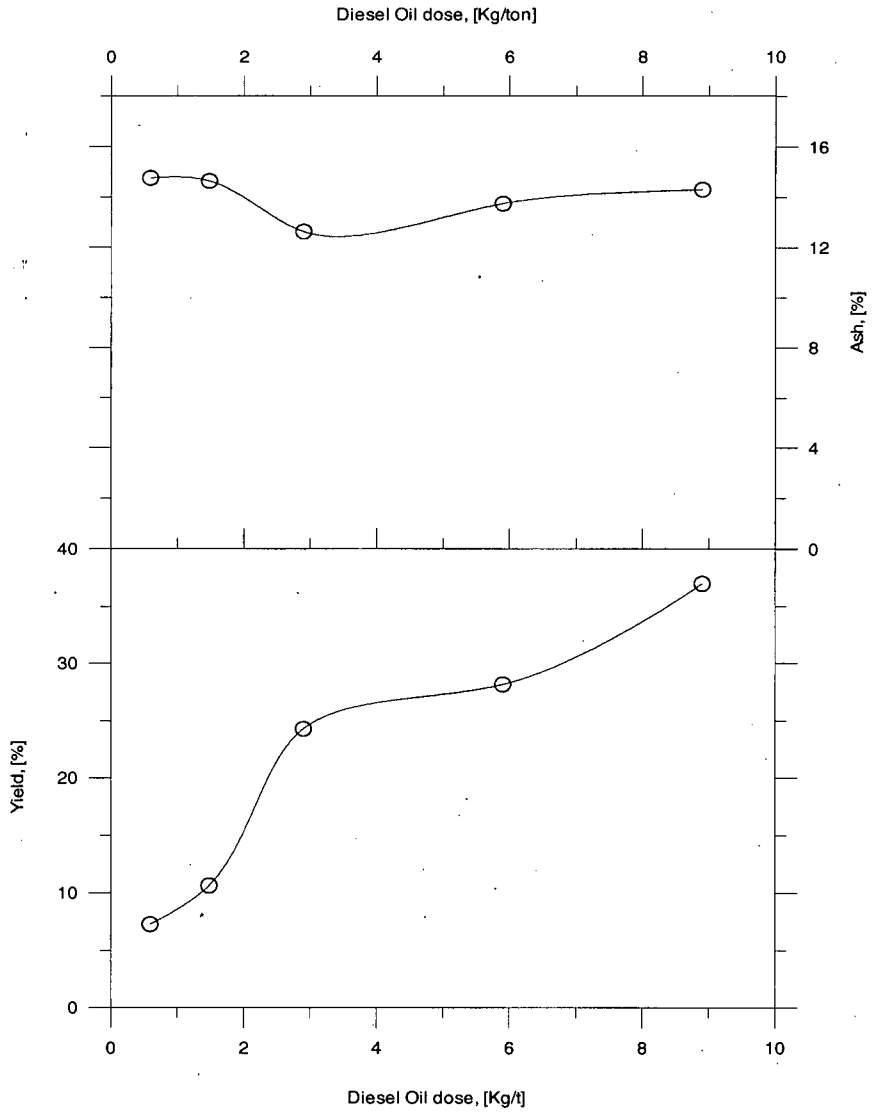

Figure 40: Effect of Diesel oil dosage on yield and ash content in clean product in the presence of $1.1x10^{-2}$g/L of MIBC, forward flotation of LS-20

Figure 41 shows the results of the flotation tests carried out on LS-20. Similarly to the case of F4, almost no flotation was observed in the presence of DF-1012 and diacetone alcohol. Figure 41 also indicates that in the flotation of LS-20 in the presence of Diesel oil, the measured water recoveries are quite low, compared to the flotation of the bituminous sample. It can be seen that the highest water recovery is about 12% at 2.2×10^{-2} g/L (200 g/t) of α-terpineol, whereas in the case of F-4, excepting the tests carried out with DF-1012 and diacetone alcohol, the water recoveries were always greater than 12 %, even at low frother concentrations.

It is quite obvious then that the presence of an oily collector contributes to the generation of "dry froths" that enhance the selectivity of the process.

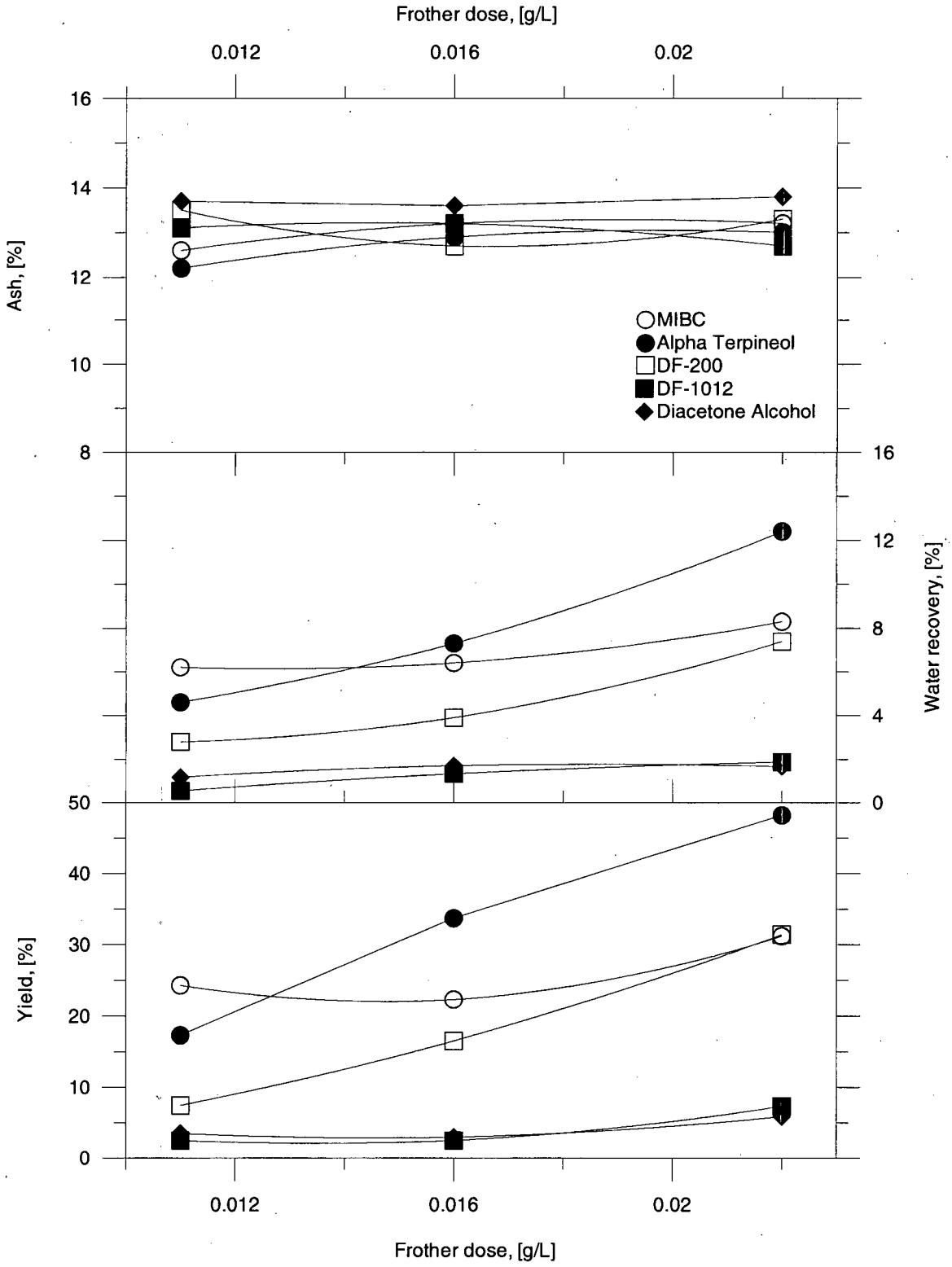

Figure 41: Effect of frother dosage on yield, water recovery and ash content in clean product after 5 minutes of flotation in the presence of 3 kg/ton of Diesel oil (LS-20 coal)

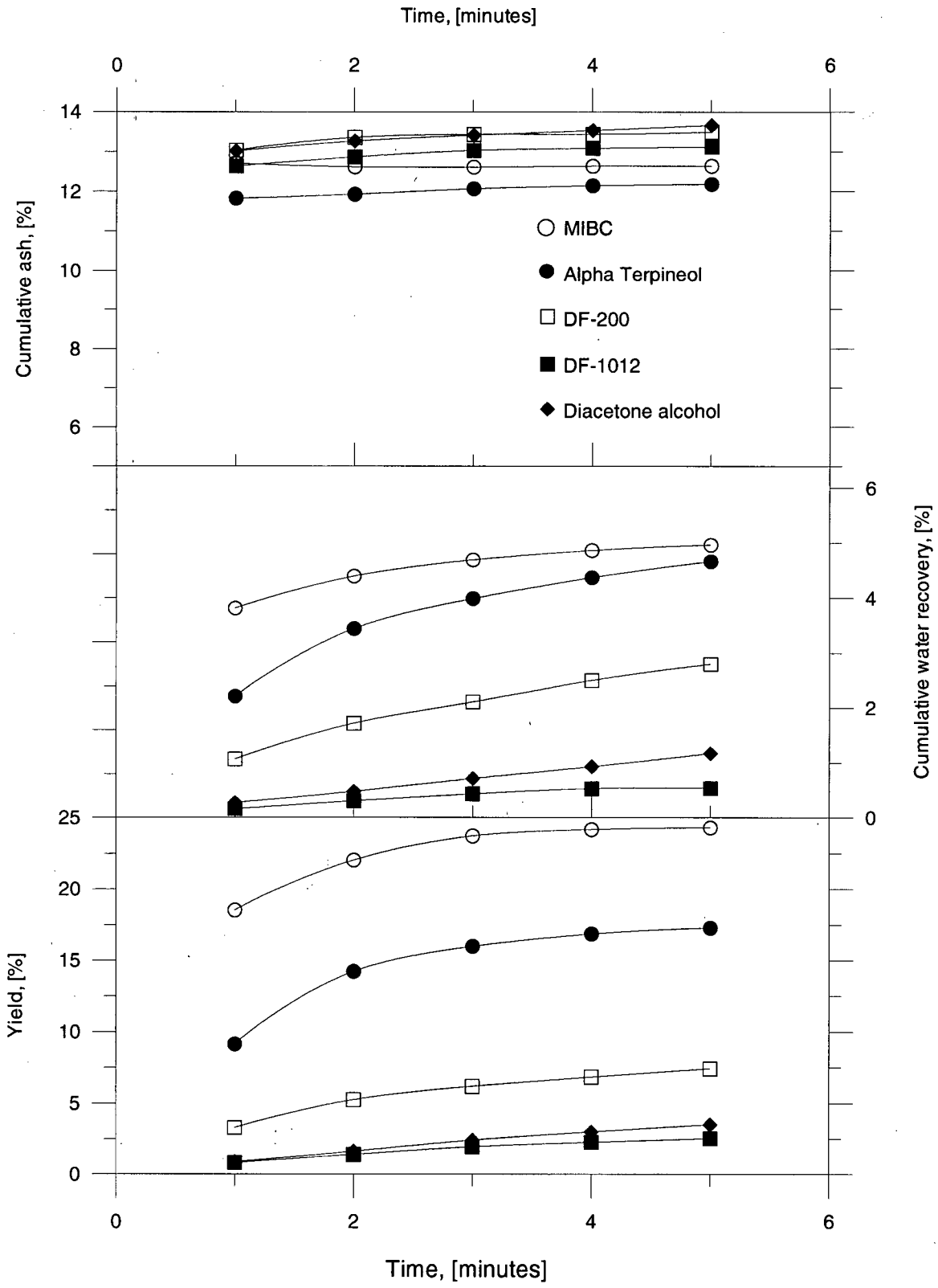

Figure 42: Flotation kinetics for LS-20 coal for all tested frothers at 1.1×10^{-2} g/L (100 g/t)

Similarly to the case of the flotation of the bituminous sample, a kinetic analysis was conducted in order to study the effect of frothers on the flotation rate constant of the solids. Figure 43 shows the results obtained for MIBC, DF-200 and α-terpineol. The results corresponding to DF-1012 and diacetone alcohol are not included since in the presence of these frothers almost no flotation was observed. The plot shows that the results for DF-200 and α-terpineol fall on the same straight line, whereas the results for MIBC are located on another line that is shifted to the left with respect to the first curve. This indicates that in the flotation of LS-20 in the presence of these frothers and Diesel oil, a given flotation rate can be achieved for MIBC at lower equivalent concentrations compared to α-terpineol and DF-200.

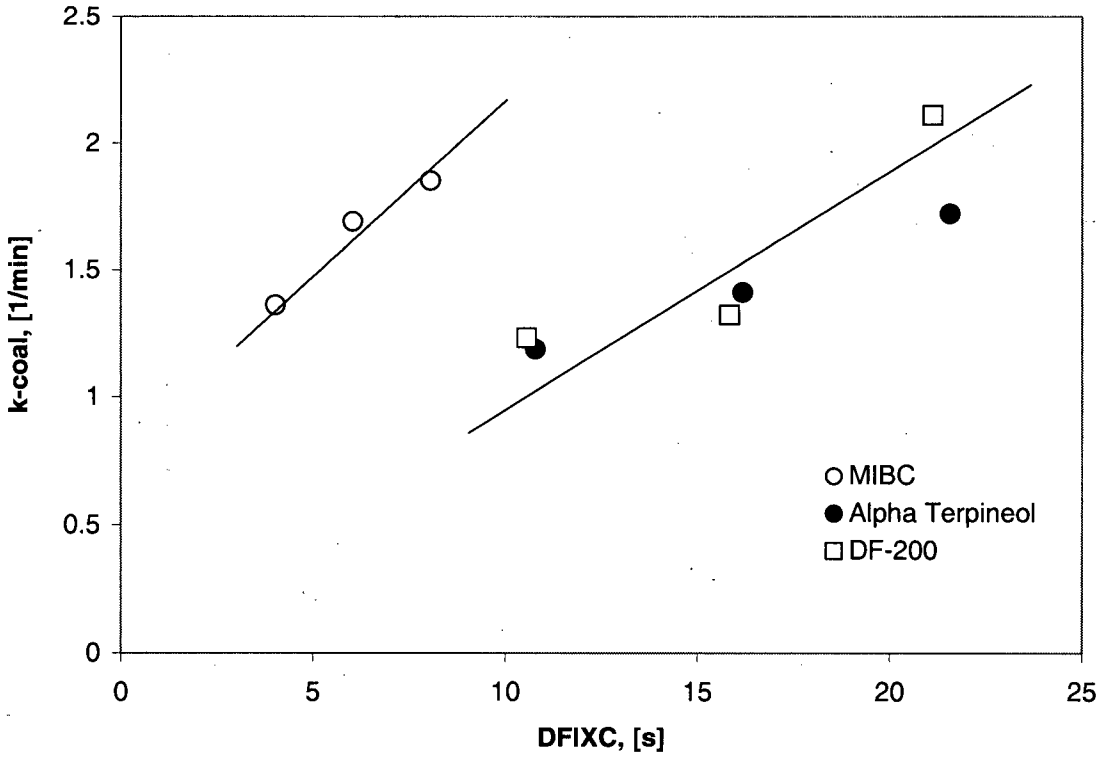

Figure 43: Flotation rate constant (coal) versus DFI x C, forward flotation of LS-20 coal

5.2.2. Reverse Flotation.

The reverse flotation tests were carried out on a sample of LS-20 (sub-bituminous) coal, mainly to relate the effect of DTAB on the water content in the froth, to the selectivity of the process.

It is worth pointing out that reverse flotation is a technology currently under development. The optimization of the process is therefore beyond the scope of the present work.

Figure 44 shows the results of the reverse flotation tests in terms of yield of clean coal (tailings) versus DTAB dosage. According to these results, high DTAB dosages (above 6 kg/t) are required in order to produce a stable froth that allows flotation to occur. Below this range, basically no flotation was observed.

From this curve it can also be seen that the addition of PAM, used in these tests to prevent the adsorption of DTAB onto coal, increases the amount of floating material.

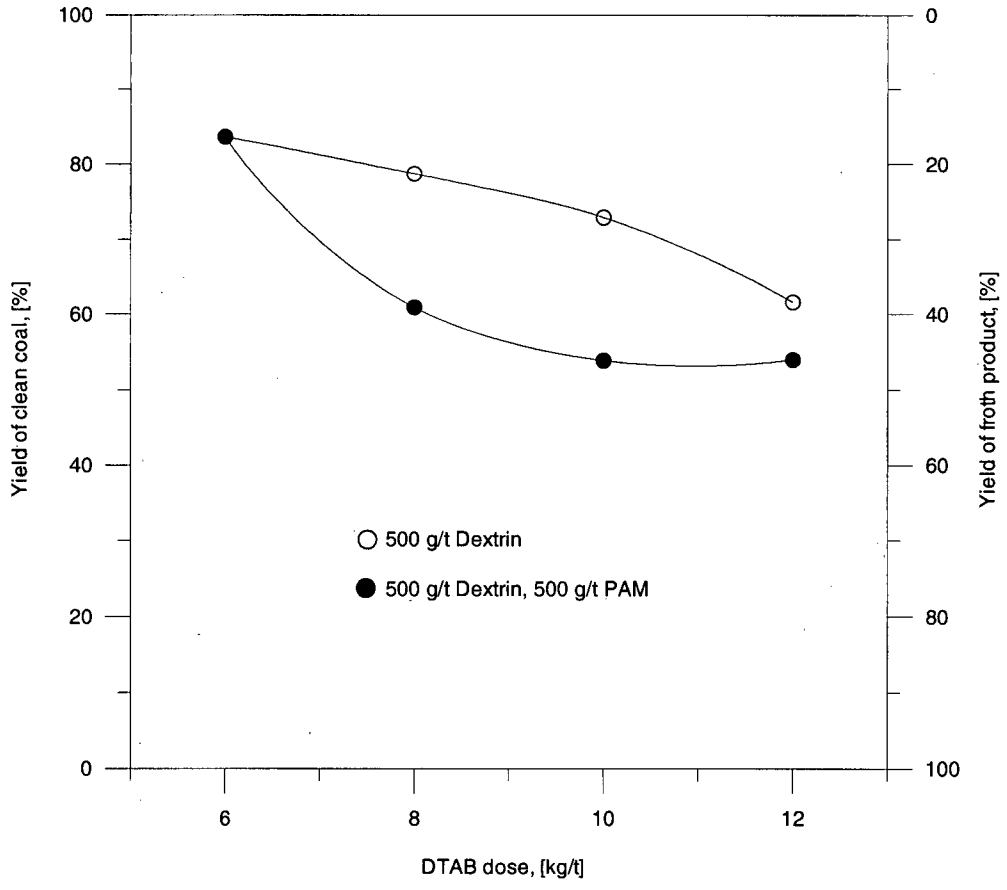

Figure 44: Yield of clean coal (tailings) versus DTAB dose in the presence of dextrin and PAM

Figure 45 shows the ash contents in the tests presented in Figure 44. In general, the results are quite poor, especially when only dextrin was used. The tests conducted in the presence of PAM yielded better results. The addition of this polymer allowed the ash content to decrease from 32% (ash content in feed) to about 22 %.

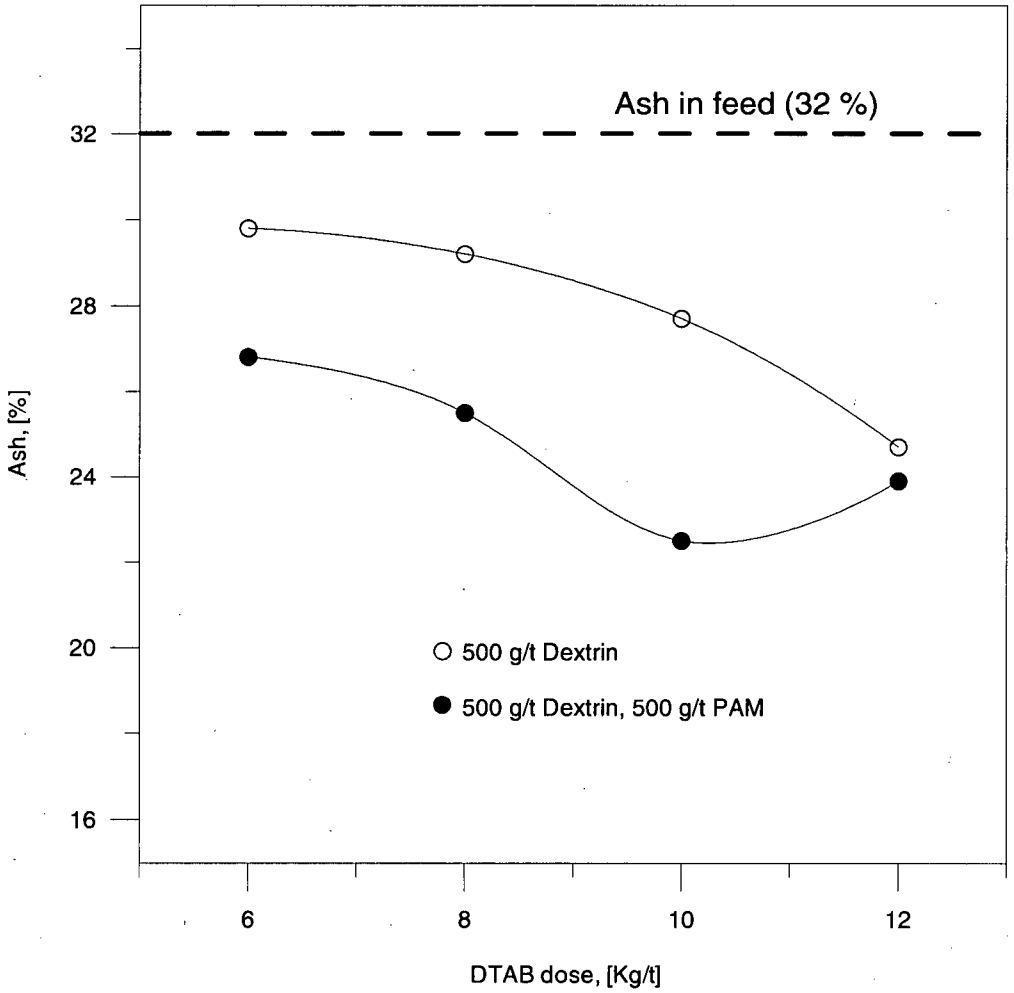

Figure 45: Ash content in clean coal (tailings) versus DTAB concentration, reverse flotation of LS-20

Figure 46 shows the amount of water recovered in the froth product as a function of the DTAB concentration in the presence of dextrin and PAM. It is clear from this plot that the water recovery increases sharply as the concentration of the amine increases. Figure 47 shows the flotation rate constants calculated for gangue and water. This plot confirms that if PAM is used in addition to DTAB and dextrin, both the rate of transfer of solids (gangue) and water to the froth increase significantly. This result correlates well with Figure 48, which shows the ash content of the froth product versus the water recovered in the froth. It can be seen that the ash

decreases with water recovery, and this diminution is more significant in the presence of PAM, which clearly indicates that more coal particles get entrained in the froth as a consequence of the higher rates of water recovery observed when PAM is used as a blinder.

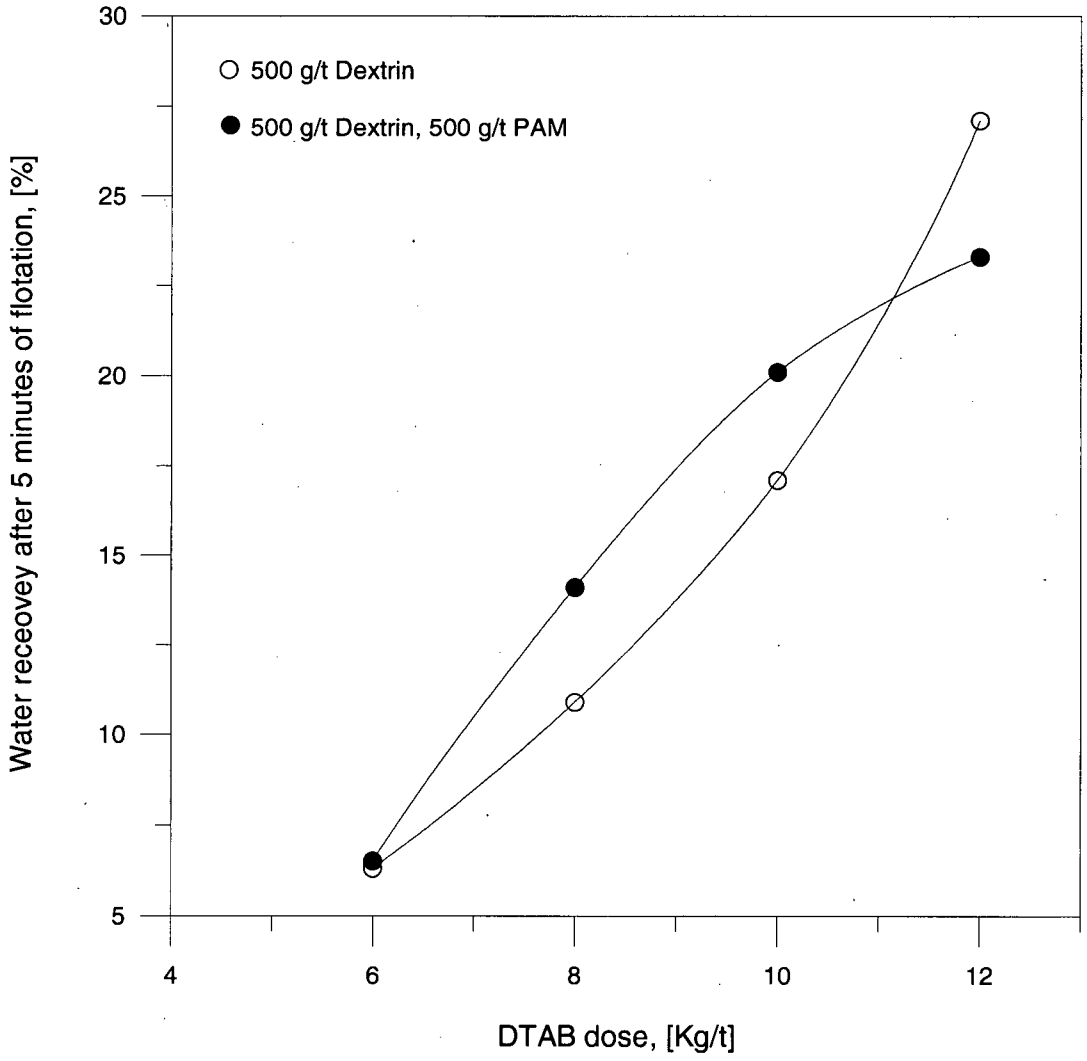

Figure 46: Water recovery versus DTAB dose in the presence of dextrin and PAM, reverse flotation of LS-20.

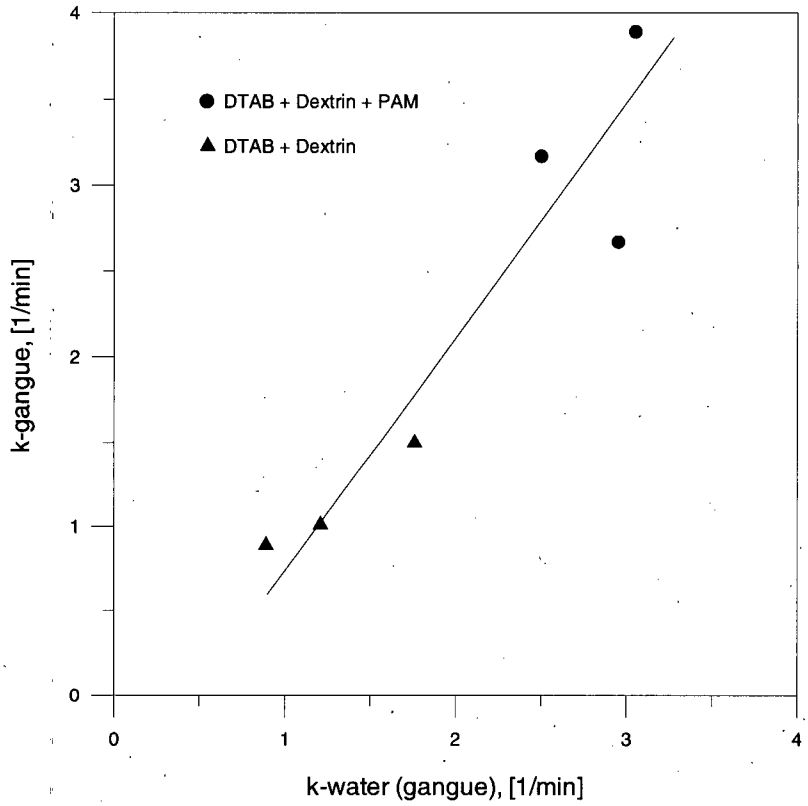

Figure 47: Flotation rate constant for gangue versus flotation rate constant for water in the presence of DTAB, dextrin and PAM, reverse flotation of LS-20 coal

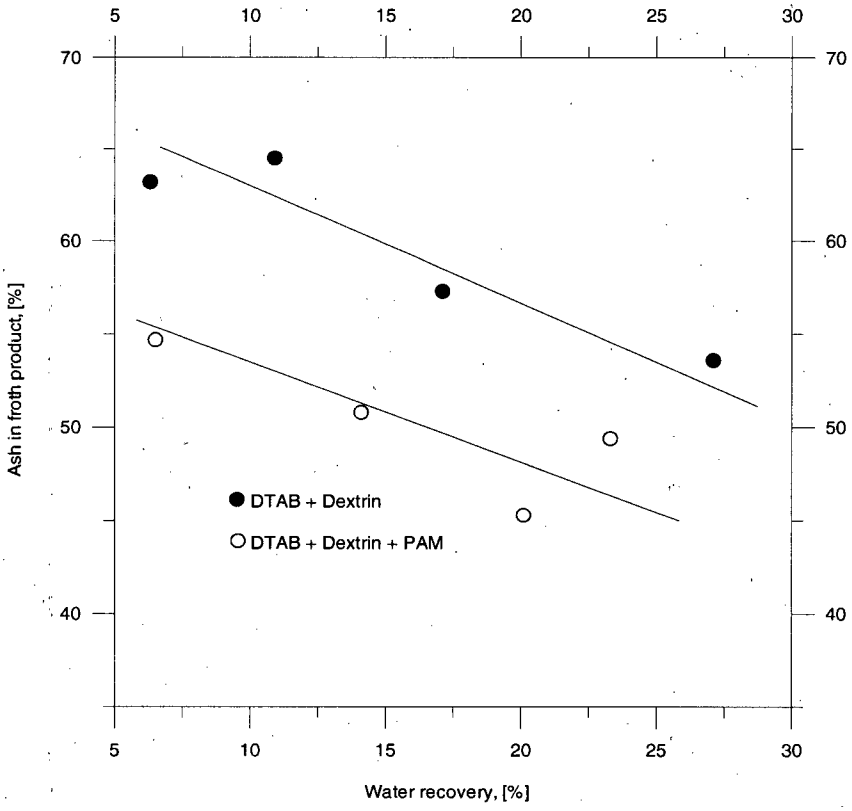

Figure 48: Ash content in froth product (reverse flotation) versus water recovery after 5 minutes of flotation in the presence of DTAB, dextrin and PAM.

6. DISCUSSION.

6.1. Measurements in the Two-Phase System (Water-Frother).

The results presented in Section 5.1 reveal that in general there is a good correlation between the surface activity of the tested frothers (Figure 22) and their ability to transport water in the absence of solids. As can be seen in Figures 22 and 31, it is clear that the most surface active frother tested (DF-1012) produced the highest initial rates of water recovery, whereas the least surface active frother (diacetone alcohol) exhibited frothing properties only at very high concentrations.

The results also proved that the stability of the foams generated in the presence of the investigated frothers correlates well with their ability to transfer water to the foam, as the correlation between the calculated flotation rate constants for water (in the absence of solids) and the DFI is linear (Figure 32). It is worth pointing out that the quality of this correlation is subject to the concentrations chosen for the calculation of the flotation rate constants. In Figure 32, the rate constants were calculated at concentrations exceeding the CCC values of the tested frothers, that is under the conditions under which bubble coalescence is prevented. If these water flotation rate constants are calculated at a given constant concentration for all the frothers, the resulting correlation is not linear, which indicates that coalescence plays a role in the transport of water to the foam.

6.2. Batch Flotation Tests.

6.2.1. Forward Flotation.

6.2.1.1. Flotation of F4 Coal.

As shown by the kinetic curves presented in Figure 34, the results obtained in the forward flotation of the F4 coal-silica mixture indicate that there is a large amount of material that floats over the first two minutes of flotation, which probably enhances significantly the effect of the entrapment of particles into the froth product.

Poor results were obtained in these tests when diacetone alcohol and DF-1012 were used as frothers. However, the same frothers performed the best in terms of ash content, following the lower water recoveries observed for these two frothing agents (Figure 33), which indicates that

the effect of entrainment in these two cases (DF-1012 and diacetone alcohol) was lower compared to the other tested frothers. Although MIBC produced the best results in terms of the yield, the ash contents in the froth products were also higher in comparison to the rest of the tested reagents, which again correlates well with the high water recoveries measured in the presence of this frother. This result indicates then that, in the case of MIBC, the effect of entrainment was more significant compared to the rest of the investigated frothers.

It is interesting to note that these experiments revealed that there is no correlation between the water recoveries measured in a two-phase system and the water recoveries obtained in a three-phase system. Figure 31 shows, for example, that the most surface active frother tested in this work (DF-1012), yielded the highest rates of water recovery when "floating" water from DF-1012 aqueous solutions, whereas in the presence of hydrophobic particles (F4 coal), MIBC exhibited the highest amounts of water recovered in the concentrate. This clearly indicates then that the water recovery in the froth product depends not only on the properties of the frother used, but also on the solid particles.

It is worth mentioning that the poor results observed in the presence of DF-1012 might be the consequence of the adsorption of this frother on coal.

6.2.1.2. Flotation of LS-20 Coal.

The results of the tests carried out with LS-20 using frothers and Diesel oil as a collector indicate that α-terpineol produced the best results in terms of yield, whereas in the presence of DF-1012 and diacetone alcohol, only a very small proportion of the feed floated (less than 10%). However, as far as the ash content is concerned, all the tested frothers yielded similar results throughout the concentration range. This is in good agreement with the preliminary tests conducted using MIBC (Figure 40), which confirms that the main effect of the addition of Diesel oil is to increase the selectivity of the process.

The water recoveries observed in the flotation of LS-20 in the presence of frothers and Diesel oil, were lower compared to the water recoveries recorded in the flotation of the F-4 coal, in which only frothers were used. Figure 49 clearly shows the difference between the two cases.

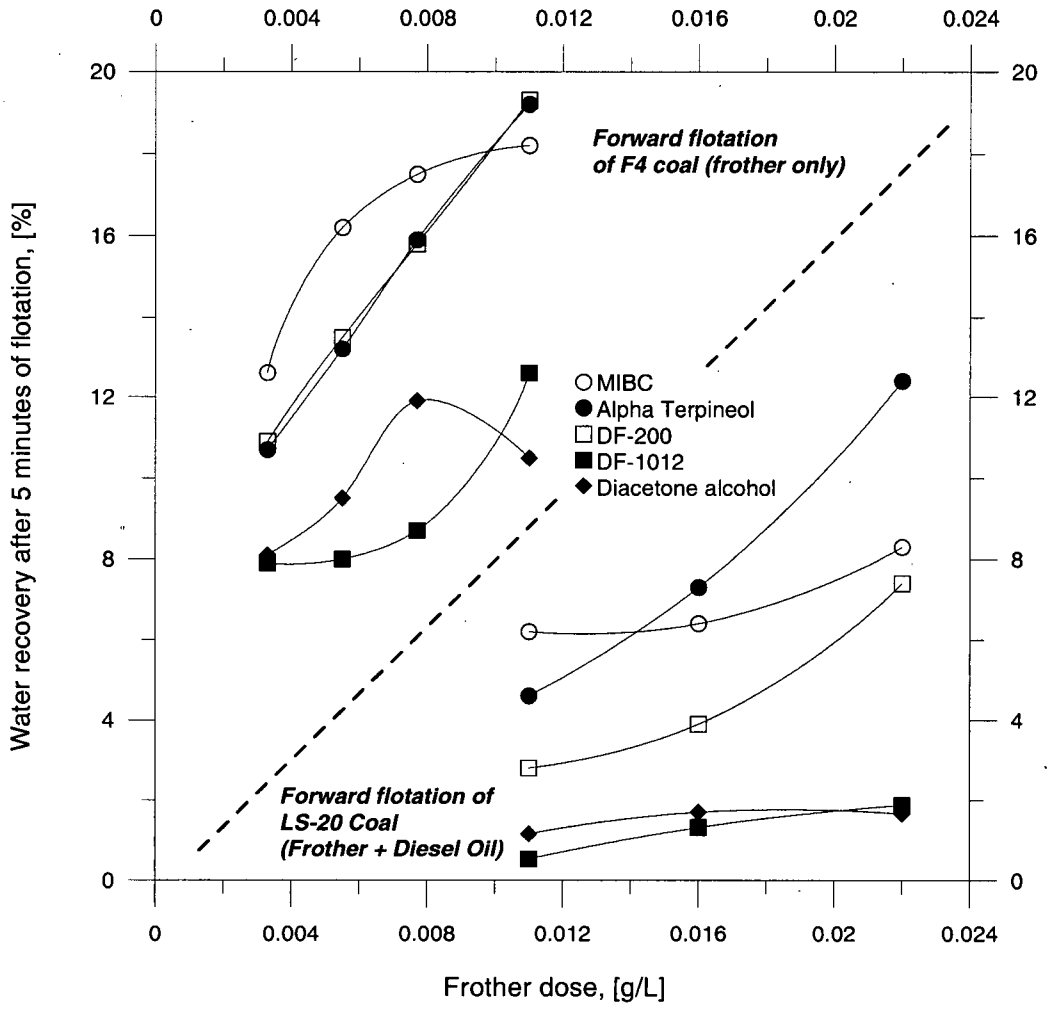

Figure 49: Comparison between water recoveries in the forward flotation of F-4 coal (frother only) and LS-20 coal (frother + Diesel oil)

Figure 50 also shows a comparison between the water recoveries observed in the flotation of the two coals, this time not in terms of frother dose but yield after five minutes of flotation. This plot demonstrates again that the water recoveries are higher in the case of the bituminous coal. However, it could be argued that this is so due to the higher yields observed in the flotation of the F-4 coal. Therefore, the comparison should be made at the same yield in both cases. This is shown in Figure 51, which presents the results of water recoveries calculated over the same yield range for the F-4 coal and the LS-20 coal, in the presence of MIBC and α-terpineol. For the rest of the tested frothers, this comparison could not be made since the yields observed in the flotation of LS-20 coal were consistently lower compared to the flotation of F-4 coal. From this curve (Figure 51) it can be seen that, for example, in the case of MIBC, the curve obtained for

the bituminous sample is shifted upwards compared to the curve corresponding to LS-20 in the presence of MIBC, which indicates that, at a given yield, the water recovery is lower when an oily collector is used.

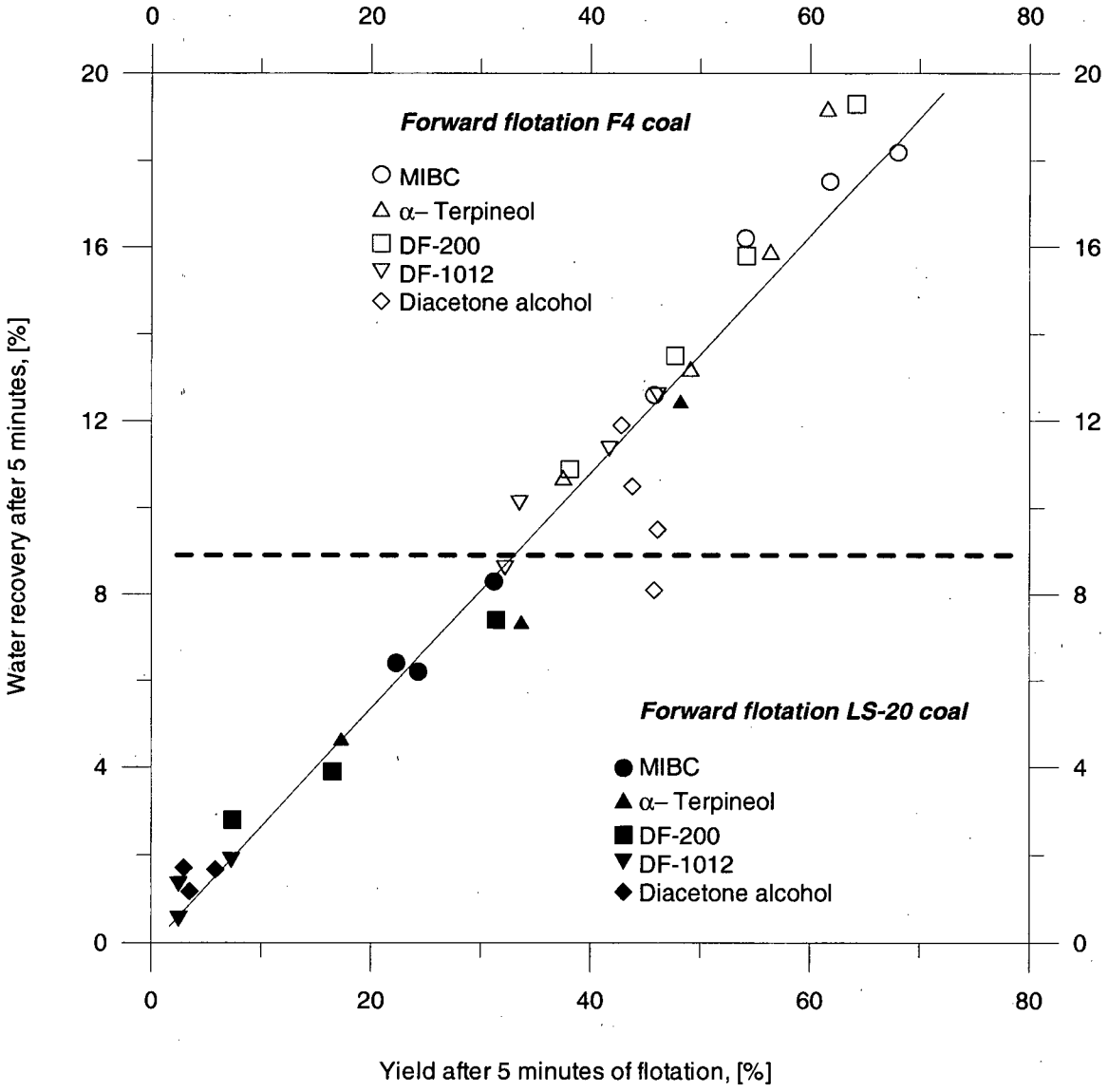

Figure 50: Water recovery versus yield after five minutes of flotation for F4 coal and LS-20 coal (3 kg/t of Diesel oil) in the presence of the tested frothers.

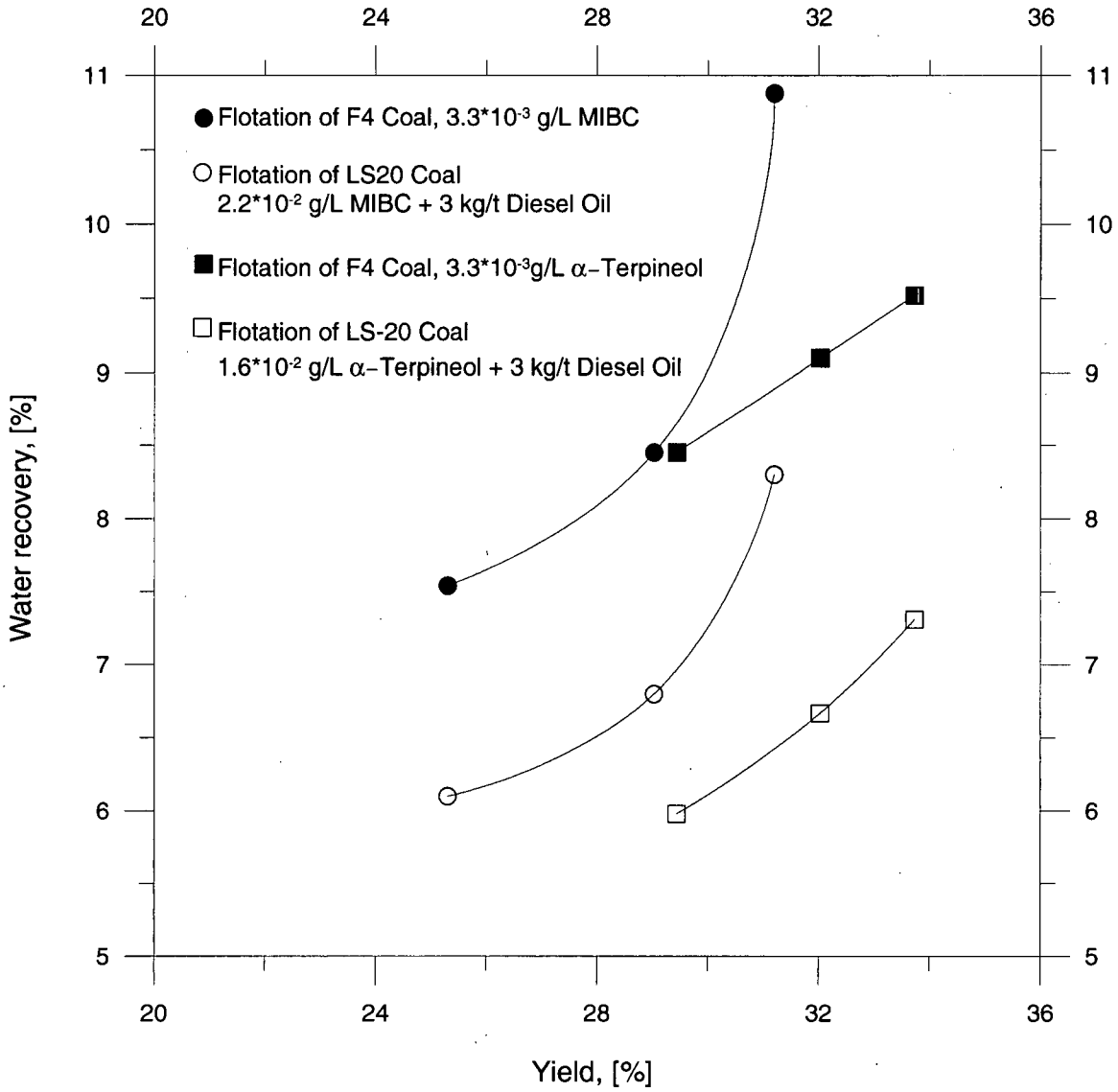

Figure 51: Water recovery versus yield for F4 coal and LS-20 coal (3 kg/t of Diesel oil) in the presence of MIBC and α-terpineol.

It is interesting to point out that in the case of LS-20, although the water recoveries increase with frother dose, the ash content in the clean product seems to be constant throughout the concentration range, as opposed to the case of the F-4 coal, which indicates that the effect of entrainment in the flotation of LS-20 in the presence of Diesel oil is not significant.

Finally, similarly to the case of the F-4 coal, the performance of the tested frothers in terms of the amount of water transferred to the froth in the presence of the LS-20 coal did not follow the trend found in the tests conducted with two-phase systems (aqueous solutions of different frothers).

6.2.2. Frother Performance: Differences in Water Recovery between a Two-Phase System and a Three-Phase System.

The differences between the results observed in the two-phase system and in the three-phase system are summarized in Figure 52. As it was mentioned in Section 6.1, in a two-phase system (water-frother), DF-1012 performed the best in terms of initial rates of water recovery, followed by α-terpineol, MIBC, DF-200 and diacetone alcohol (These results were presented in Figure 31, which is shown again in Figure 52a for comparison purposes). However, the results presented in Figures 33 and 41 revealed that in a three-phase system (water-coal-frother), the trend is different:

- In the case of the F-4 coal, clearly MIBC performed the best in terms of initial rates of water recoveries, followed by α-terpineol and DF-200. DF-1012, as opposed to the results observed in the two-phase system, yielded low initial rates of water recovery, same as diacetone alcohol (Figure 52b).

- The results obtained in the flotation tests carried out with the LS-20 coal also showed that, in the presence of solids particles, the performance of the tested frothers is different. In this case, both MIBC and α-terpineol yielded similar results, whereas DF-1012 and diacetone alcohol again gave poor results (Figure 52b).

These results indicate that characterization of flotation frothers in a two-phase experiment is not adequate since the water transport results obtained in the two-phase and three-phase experiments were different.

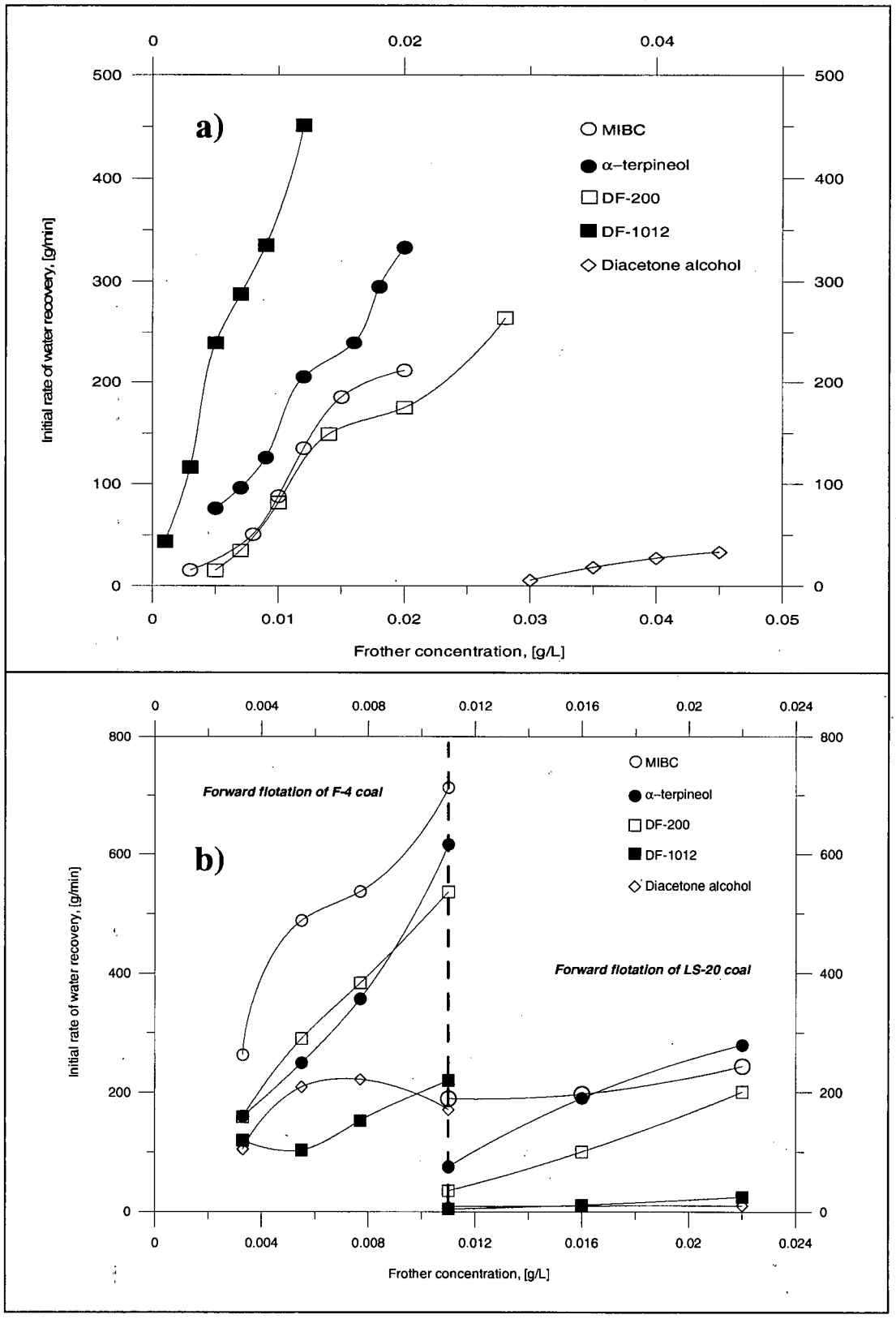

Figure 52: a) Initial rates of water recovery in a two-phase system (water-frother) b) Initial rates of water recovery in a three-phase system (water-frother-coal)

6.2.3. Reverse Flotation (LS-20).

In general, poor flotation results were obtained in the reverse flotation tests conducted in this project. One of the major problems to be solved is the high consumption of DTAB needed to achieve some degree of separation. According to Figure 44, only in the presence of 6 kg/t of the amine, about 15 % of the feed floated. Below this concentration, no frothing effect was observed, probably due to the excessive adsorption of DTAB onto coal. It is interesting to note that this phenomenon took place even when no conditioning time was given to this reagent, as flotation started immediately after it was added. In order to overcome this problem, a blinder (PAM) was utilized to prevent the adsorption of the amine onto coal. As Figure 44 shows, in the presence of 500 g/t of this polymer, the yield of concentrate (gangue) increases, which clearly indicates that there is a higher amount of DTAB available in solution to be adsorbed onto the gangue particles.

The PAM addition also improved the results in terms of selectivity, as the ash contents in the clean product (tailings) dropped significantly throughout the DTAB concentration range tested in this work (Figure 45). The most successful experiment conducted in the presence of dextrin, PAM and DTAB allowed to decrease the ash content from 32% to about 22%.

It is worth pointing out that the results presented in the patent by Evesson (1961) on reverse flotation in terms of ash contents of the clean products are not satisfactory.

Figure 46 shows the water recovery curves corresponding to the results shown in Figures 44 and 45. As these figures reveal, the amount of water present in the froth product ranges from about 5 to 27 % and it strongly depends on the DTAB concentration. As shown in Figure 47, the addition of PAM increases the rates of transfer of solids and water to the concentrate, which translates into a more significant effect of the entrainment of coal particles in the froth product. This can be observed in Figure 48, in which the ash content decreases as the water recovery increases. This reduction of the ash content is explained because of the transport of coal to the froth by entrainment.

It is interesting to note that, as it was mentioned in previous sections, DTAB generates metastable froths, which is confirmed by Figure 53, which shows the froth generated in a reverse flotation test carried out in the presence of dextrin, PAM and DTAB. This Figure clearly shows that in the presence of the latter reagent, the bubbles acquire the polyhedral shape that characterizes this kind of froth, as opposed to the spherical bubbles observed in the presence of a traditional flotation frother such as MIBC (Figure 54).

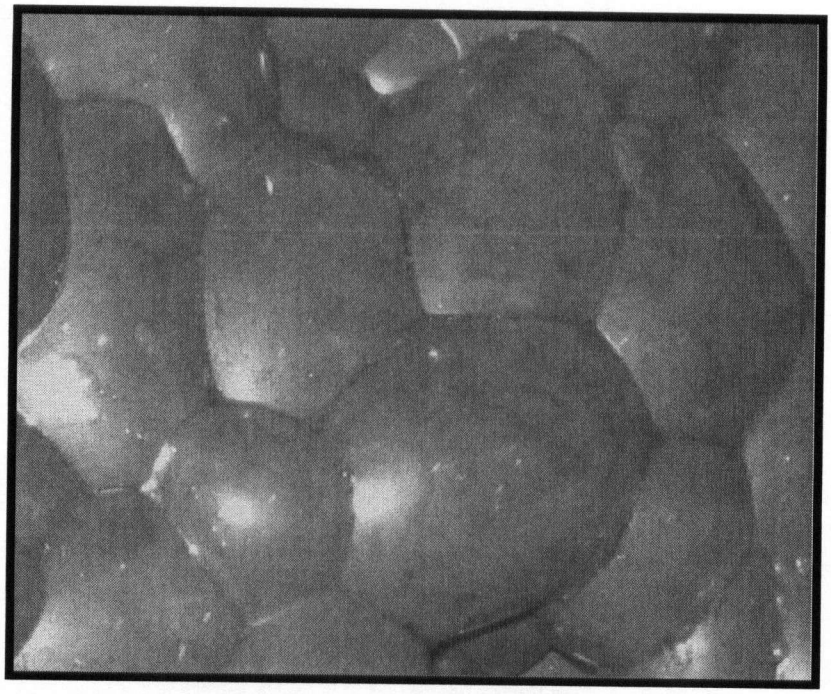

Figure 53: Froth in the reverse flotation (LS-20 coal, 8 kg/t DTAB, 500 g/t dextrin, 500 g/t PAM)

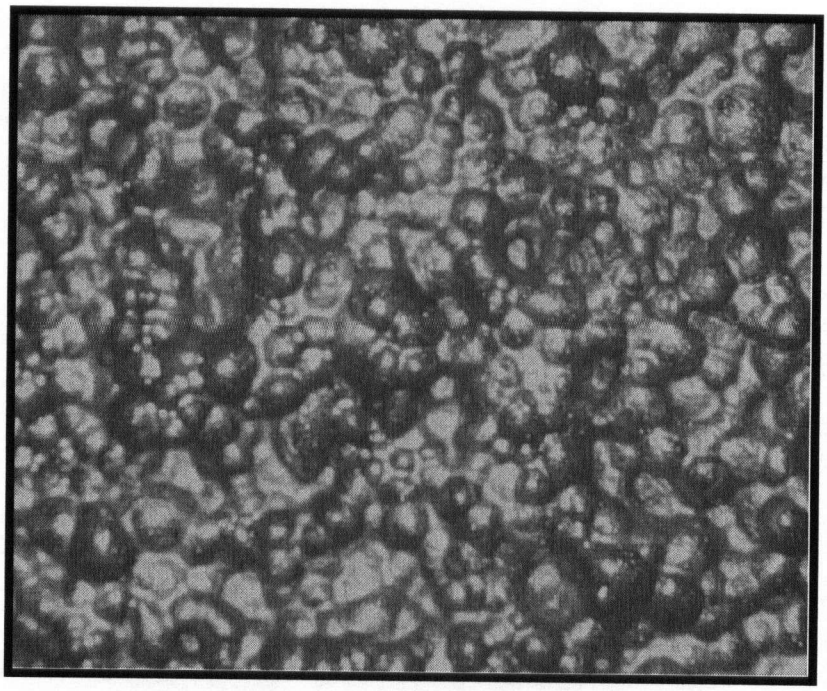

Figure 54: Froth in the forward flotation (F4 coal $5.5x10^{-3}$ g/L MIBC)

The results presented in Figure 31 also confirm that DTAB generates foams with low water contents. This plot indicates that the initial rates of water recovery observed for DTAB solutions are in general lower compared to the rest of the tested frothers, except in the case of diacetone alcohol. However, the comparison of the ranges of water recovery observed for DTAB in the presence of solid particles (5 to 27% recovery) indicates that they are higher than those observed for the other frothers in the forward flotation of F4 (10 to 20% recovery) and LS-20 (below 12 % recovery) coals. To explain this phenomenon, it should be borne in mind that the DTAB concentrations used in the reverse flotation tests are several times higher than the concentrations tested with the rest of the investigated frothers, and therefore, it is not possible to make a direct comparison. In addition, DTAB operates both as a gangue collector and as frother, which complicates even more a straight comparison with conventional flotation frothers.

7. CONCLUSIONS.

7.1. Frother Characterization and Frother Performance in Forward Flotation.

This work demonstrates that there is a good correlation between the surface activity of five different flotation frothers and their ability to transport water towards the foam formed when gas is pumped through their aqueous solutions. The stability of the foams generated in the presence of the tested frothers, which was quantified in terms of the DFI values, also correlated well with the rates of water recovery measured in aqueous solutions. In general, the more stable the foam, i.e. the higher the DFI value, the higher the rate of water recovery. However, the relationships between frother concentration and water recovery obtained in the two-phase experiments turned out to be different in the presence of solid particles. This indicates that in a real flotation system, a frother characterized by a high DFI does not necessarily yield high water recoveries, since the properties of the solids can influence the effect of the frother on the amount of water transferred to the froth.

In the particular case of this project, the adsorption of frothers onto solid particles can be mentioned as one of the interactions that can strongly affect the water recovery and the degree of entrainment in the froth product. Although no measurements of residual frother concentration were done in this research, it is likely that a significant amount of DF-1012 was adsorbed by the coal samples used in this project, which explains the poor performance of this reagent in the forward flotation of the F-4 and LS-20 samples, in terms of yield and water recovery.

Frother adsorption onto coal particles might also have occurred in the presence of the other tested frothers, but to a much lesser extent compared to DF-1012.

7.2. Reverse Flotation.

This research also showed that the use of DTAB in the reverse flotation process strongly affects the recovery of water. The selectivity observed in the tests conducted in this work improved when a blinder (PAM) was used in addition to the gangue collector (DTAB) and coal depressant (dextrin). However, the results were still poor, probably due to the high stability of the froth formed in the presence of DTAB, which does not allow a proper drainage of unwanted particles from the froth back to the pulp.

The high DTAB consumption observed in the reverse flotation tests, which is a consequence of the adsorption of the amine onto the sub-bituminous sample used in this work, could be reduced in the presence of PAM. However, the dosages of DTAB required to both render gangue particles hydrophobic and to generate a stable froth are still considerably high. It is clear that this problem needs to be addressed in order to ensure the applicability of the reverse flotation technology on an industrial scale.

8. RECOMMENDATIONS FOR FUTURE WORK.

The results of this project demonstrate that the water recovery into the froth is strongly affected by the presence of solid particles. Since the parameters developed over the last years for the characterization of flotation frothers are measured in the two-phase tests carried out with frother aqueous solutions, these indices should be further investigated and quantified in the presence of solid particles with varying degrees of hydrophobicity.

REFERENCES.

1. **Ata, S., Ahmed, N. and Jameson, G.J.** *" Gangue drainage in flotation froths"*, Proceedings of the XXII International Mineral Processing Congress, Cape Town, South Africa (2003)

2. **Cho, Y.S. and Laskowski, J.S.** *"Effect of flotation frothers on bubble size and foam stability"*, International Journal of Mineral Processing, vol. 64, pp. 69-80 (2002)

3. **Cilek, E.C. and Umucu, Y.** *"A statistical model for gangue entrainment into froths in flotation of sulphide ores"*, Minerals Engineering, vol. 14, pp. 1055-1066 (2001)

4. **Cocks, B. & McPherson, J.** *"An investigation into the role of frothers in the recovery of water in froth flotation"*, Undergraduate Thesis, University of Cape Town, South Africa (1999)

5. **Comley, B. A.** *" Dynamic surface tension as a means of characterizing flotation frother performance"*, M.Sc. Eng Thesis, Department of Chemical Engineering, University of Cape Town (2001)

6. **Czarnecki, J., Malaysa, K. and Pomianowski, A.** *"Dynamic frothability index"*, Journal of Coll. Interf. Sci., vol. 86, pp. 570-572 (1982)

7. **Ding, K.** Private communication, Department of Mining Engineering, University of British Columbia (2004)

8. **Ekmekci, Z., Bradshaw, D.J., Allison, S.A., Harris, P.J.** *" Effects of frother type and froth height on the flotation behavior of chromite in UG ore"*, Minerals Engineering, vol. 16, pp. 941-949 (2003)

9. **Engelbrecht, J.A. and Woodburn, E.T.** *"The effects of froth height, aeration rate and gas precipitation on flotation"*, Journal of the South African Institute of Mining and Metallurgy, pp. 125-132 (1975)

10. **Eveson, G.F.** *"Removing shale particles from coal or from coal-washing effluent by froth flotation"*, British Patent 863,805 (1961)

11. **Firth, B. A., Swanson, A.R. and Nicol S.K.** *"The influence of feed size distribution on the staged flotation of poorly floating coals"*, Proc. Australas. Inst. Min. Metall., no. 267, pp. 49-53 (1978)

12. **Fuerstenau, D.W and Pradip.** *"Adsorption of frothers at coal/water interfaces"*, Colloids and Surfaces, vol. 4, pp. 229-243 (1982)

13. **Govindarajan, B., Vanangamudi, M. and Rao, T.C.** *"Batch coal flotation model based on water recovery concept"*, Mineral & Metallurgical Processing, May 1991, pp. 105-109.

14. **Gurses, A., Bayrakceken, S. and Sahin, M.** *" Adsorption of o-cresol from aqueous solution on coal"*, Colloids and Surfaces, vol. 64, pp. 7-13 (1992)

15. **Iglesias, E., Anderez, J., Forgiarini, A. and Salager, J.L.** *"A new method to estimate the stability of short-life foams"*, Colloids and Surfaces, vol. 98, pp. 167-174 (1995)

16. **Johnson N.W., McKee D.J. and Lynch, A.J.**, Trans. Soc. Min. Eng. AIME, vol. 256, 204 (1974)

17. **Khristov, Khr., Malysa, K. and Exerowa, D.** *"Steady-state foams: Influence of the type of liquid films"*, Colloids and Surfaces, vol. 11, pp. 39-49 (1984)

18. **Kirjavainen, V.M.** *" Review and analysis of factors controlling the mechanical flotation of gangue minerals"*, International Journal of Mineral Processing, vol. 46, pp. 21-34 (1996)

19. **Kitchener, J.A. and Cooper, C.F.** *"Current concepts in the theory of foaming"*. Q. Rev. (London), 13, 71 (1959)

20. **Laplante, A.R., Kaya, M. and Smith, H.W.** *"The effect of froth on flotation kinetics: A mass transfer approach"*, Frothing in Flotation (J.S. Laskowski, ed.), Gordon and Breach, pp. 147-169 (1989)

21. **Laskowski, J.S.** *"Fundamental properties of flotation frothers"*, Proc. 22nd Int. Mineral Processing Congress (L. Lorenzen and D.J.Bradshaw, eds.), Cape Town, vol. 2, pp.788-797 (2003)

22. **Laskowski, J.S., Tlhone, T., Williams, P. and Ding, K.** *"Fundamental properties of the polyoxypropylene alkyl ether flotation frothers"*, Int. Journal of Mineral Processing, vol. 72, pp. 289-299 (2003)

23. **Laskowski, J.S.** *"Flocculation in mineral processing circuits"*, Proceedings of the "Strategic Conference and Workshop on Flotation and Flocculation: From Fundamentals to Applications", pp. 303-310 (2002)

24. **Laskowski, J.S.** *"Does it matter how coals are cleaned for CWS"*, Coal Preparation, vol. 21, pp. 105-123 (1999)

25. **Laskowski, J.S.** *"Frothers and frothing"*, Frothing in Flotation II (J.S. Laskowski and E.T. Woodburn, eds.), Gordon and Breach, pp. 1-49 (1998)

26. **Lekki, J. and Laskowski, J.S.** *"A new concept of frothing in flotation systems and general classification of flotation frothers"*, Proceedings of the 11th International Mineral Processing Congress, Cagliari, Italy (1975)

27. **Lynch, A.J., Johnson, N.W., Manlapig, E.V., Thorne, C.G.** *" Mineral and coal flotation circuits: Their simulation and control",* Developments in Mineral Processing (Elsevier), vol. 3 (1981)

28. **Malysa, E., Malysa K. and Czarnecki, J.** *"A method of comparison of the frothing and collecting properties of frothers",* Colloids and Surfaces, vol. 23, pp. 29-39 (1987)

29. **Miller, J.D., Lin, C.L. and Chang, S.S.** *" MIBC adsorption at the coal/water interface",* Colloids and Surfaces, vol. 7, pp. 351-355 (1983)

30. **Mohanty, M., Honaker, R., Patwardhan, A. and Ho, K.** *" Coal flotation washability: An evaluation of the traditional procedures",* Coal Preparation, vol. 19, pp. 33-49 (1997)

31. **Nazier, A.** *"The effect of particle hydrophobicity on froth stability and metallurgical performance*", Undergraduate Thesis, Department of Chemical Engineering, University of Cape Town (2002)

32. **Pawlik, M., Laskowski, J.S. and Melo, F.** *"Effect of coal surface wettability on aggregation of fine coal particles",* Coal Preparation, vol. 24, pp. 233-248 (2004)

33. **Pawlik, M. and Laskowski, J.S.** *"Coal reverse flotation: Part I. Adsorption of dodecyltrimethyl ammonium bromide and humic acids onto coal and silica",* Coal Preparation, vol. 23, pp. 91-112 (2003)

34. **Pawilik, M. and Laskowski, J.S.** *"Coal reverse flotation: Part II. Batch flotation tests",* Coal Preparation, vol. 23, pp. 113-127 (2003)

35. **Pawlik, M.** *"Reverse flotation as a method of coal cleaning for preparation of coal-water slurries",* PhD Thesis, University of British Columbia (2002)

36. **Pawlik, M., Laskowski, J.S. and Liu, H.** *"Effect of humic acids and coal surface properties on rheology of coal-water slurries",* Coal Preparation, vol. 18, pp. 129-149 (1997)

37. **Rahal, K., Manlapig, E. and Franzidis, J-P.** *"Effect of frother type and concentration on the water recovery and entrainment recovery relationship",* Minerals & Metallurgical Processing, vol. 18, pp. 138-141.(2001)

38. **Rastogi, R.C. and Aplan, FF.** *"Coal flotation as a rate process",* Minerals and Metallurgical Processing, pp.137-145 (1985)

39. **Saleh, A. and Iskra, J.** *"The influence of frother type on the flotation kinetics of low rank coal",* Fizykochemiczne Problemy Mineralurgii, vol. 27, pp. 107-116 (1993)

40. **Savassi, O.N.** *"Direct estimation of the degree of entrainment and the froth recovery of attached particles in industrial flotation cells*", PhD Thesis, University of Queensland (1998)

41. **Savassi, O.N., Alexander, D.J., Franzidis, J.P. and Manlapig, E.V.** *"An empirical model for entrainment in industrial flotation plants"*, Minerals Engineering, vol. 11, pp. 243-256 (1997)

42. **Smith, P.G., Warren, L.J.** *"Entrainment of particles into flotation froths"*, Mineral Processing and Extractive Metallurgy Review, vol. 5, pp. 123-145.(1989)

43. **Stonestreet, P. and Franzidis, J-P.** *"Reverse flotation of coal – A novel way for the beneficiation of coal fines"*, Minerals Engineering, vol. 1, pp 343-349 (1998)

44. **Stonestreet, P. and Franzidis, J-P.** *"Development of the reverse coal flotation process: Application to column cells"*, Minerals Engineering, vol. 5, pp 1041-1051 (1992)

45. **Stonestreet, P.** *" Reverse flotation as a method for beneficiation of fine coal"*, PhD Thesis, Department of Chemical Engineering, University of Cape Town (1991)

46. **Strydom, P.J., Spitzer, D.P. and Goodman, R.M.** *"Fine coal flotation with alcohol: dialkyl sulfosuccinate frothing systems"*, Colloids and Surfaces, vol. 8, pp. 175-185 (1983)

47. **Szatkowski, M.** *"Effects of air usage on flotation of coal"*, Minerals and Metallurgical Processing, February 1987, pp. 37-40 (1987)

48. **Szatkowski, M.** *"Factors influencing behavior of flotation froth"*, Trans. Instn Min. Metall, Section C: Mineral Process. Extractive Metallurgy, vol. 96, pp. 115-122 (1987)

49. **Tlhone, T. and Williams, P.** *"Fundamental properties of flotation frothers blends"*, Undergraduate Thesis, Department of Chemical Engineering, University of Cape Town (2001)

50. **Tuteja, R.K., Spottiswood, D.J. and Misra, V.N.** *"Column parameters: Their effect on entrainment in froth"*, Minerals Engineering, vol. 8, pp 1359-1368 (1995)

51. **Vera, M.A., Mathe, Z.T., Franzidis, J.P., Harris, M.C., Manlapig, E.V., O'Connor, C.T.** *"The modeling of froth zone recovery in batch and continuously operated laboratory flotation cells"*, International Journal of Mineral Processing, vol. 64, pp. 135-151.(2001)

52. **Vera, M.A., Franzidis, J.P. and Manlapig, E.V.** *"Simultaneous determination of collection zone rate constant and froth zone recovery in a mechanical flotation environment"*, Minerals Engineering, vol. 12, pp. 1163-1176. (1999)

53. **Vera, M.A. and Franzidis, J.P.** *"The upgrading process across the froth phase and its relationship to the recovery – enrichment ratio curve"*, Flotation and Flocculation, from Fundamentals to Applications, Strategic Conference and Workshop, Hawaii, Proceedings, pp. 229-240 (2002)

54. **Warren, L. J.** "*Determination of the contributions of true flotation and entrainment in batch flotation tests*", International Journal of Mineral Processing, vol. 14, pp. 33-44 (1985)

55. **Wheeler, T.A.** "*Coal floats by itself, doesn't it?*", Reagents for Better Metallurgy, Chapter 14. Published by Society of Mining, Metallurgy and Exploration Inc., Littleton, Colorado (1994)

APPENDIX 1

Nomenclature

CCC	Critical Coalescence Concentration, [ppm]
CF^i, CFM^i	Classification factors for particle size i
DFI	Dynamic Foamability Index, [sdm^3/mol]
d.m.m.f.	Dry-Mineral Matter Free Basis
DTAB	Dodecyl-Trimethyl-Ammonium-Bromide
ENT	Degree of entrainment (empirical partition curve)
e_v^i	Entrainment factor for hydrophobic valuables (size i)
e_g^i	Entrainment factor for hydrophilic gangue (size i)
F_v^i	Recovery of solids due to "true flotation" (size i), [%]
H	Height of the foam column, [cm]
H_0	Initial height of the foam column, [cm]
HLB	Hydrophile-Lipophile-Balance Number
k	Flotation rate constant, [1/min]
k-coal	Flotation rate constant for coal, [1/min]
k_f	Flotation rate constant (fast floating component), [1/min]
k_s	Flotation rate constant (slow floating component), [1/min]
k-water (coal)	Flotation rate constant for water in the presence of coal, [1/min]
MIBC	Methyl-Isobutyl-Carbinol
PAM	Polyacrylamide
R_v^i	Recovery of hydrophobic valuables (size i), [%]
R_g^i	Recovery of hydrophilic gangue (size i), [%]
R_w	Water recovery, [%]
rt	Retention time, [min]
rt_∞	Limiting value for the retention time, [min]
$t_{1/2}$	Time required to decrease the height of a foam column to half of the initial value, [min]
x_i	Particle size i (empirical partition curve), [microns]

δ	Drainage parameter
ξ	Entrainment parameter
ϕ	Amount of slow floating component in the flotation feed, [%]

APPENDIX 2

Determination of the Dynamic Foamability Index (DFI) for Diacetone Alcohol

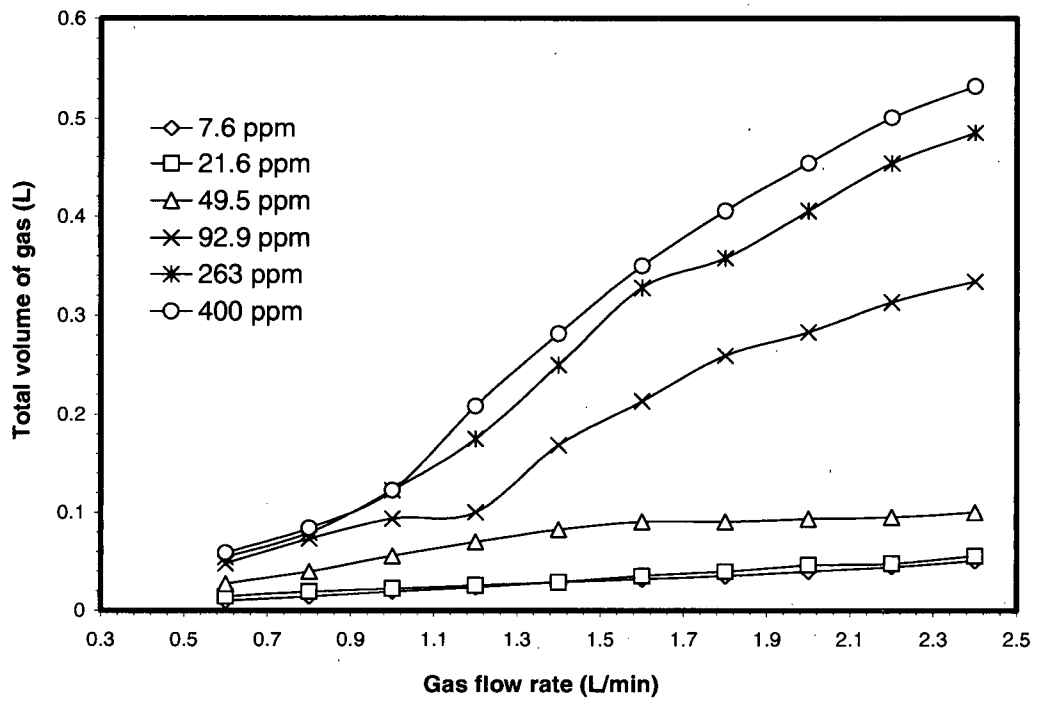

Figure 2a: Total volume of gas versus gas flow rate at different concentrations of diacetone alcohol

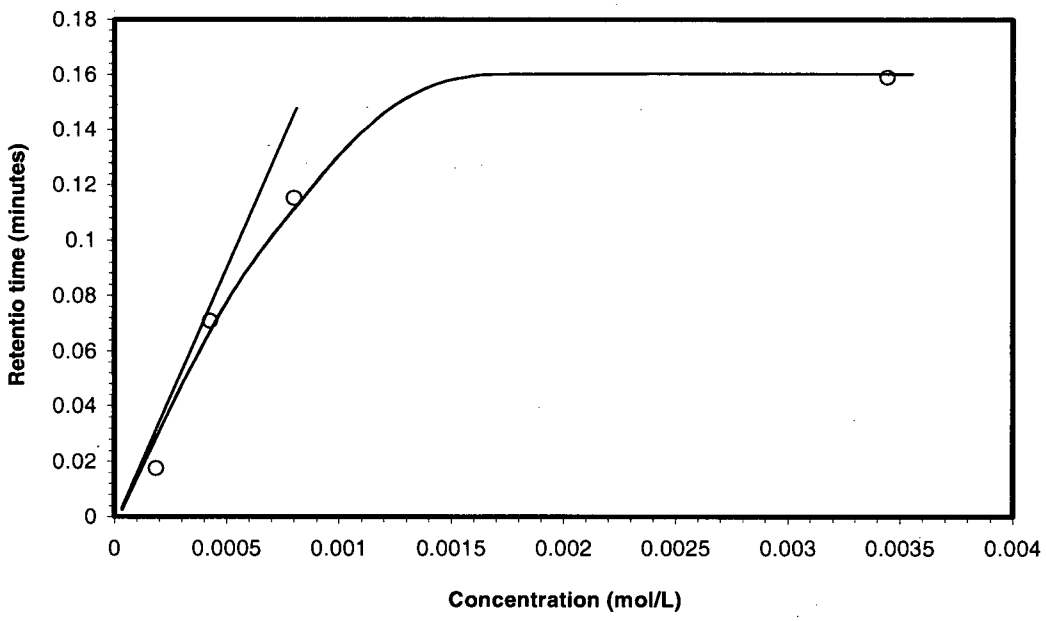

Figure 2b: Retention time versus concentration

APPENDIX 3

Cumulative yield versus time and log(100-yield) versus time curves for all the tested frothers (Forward flotation of F4 coal)

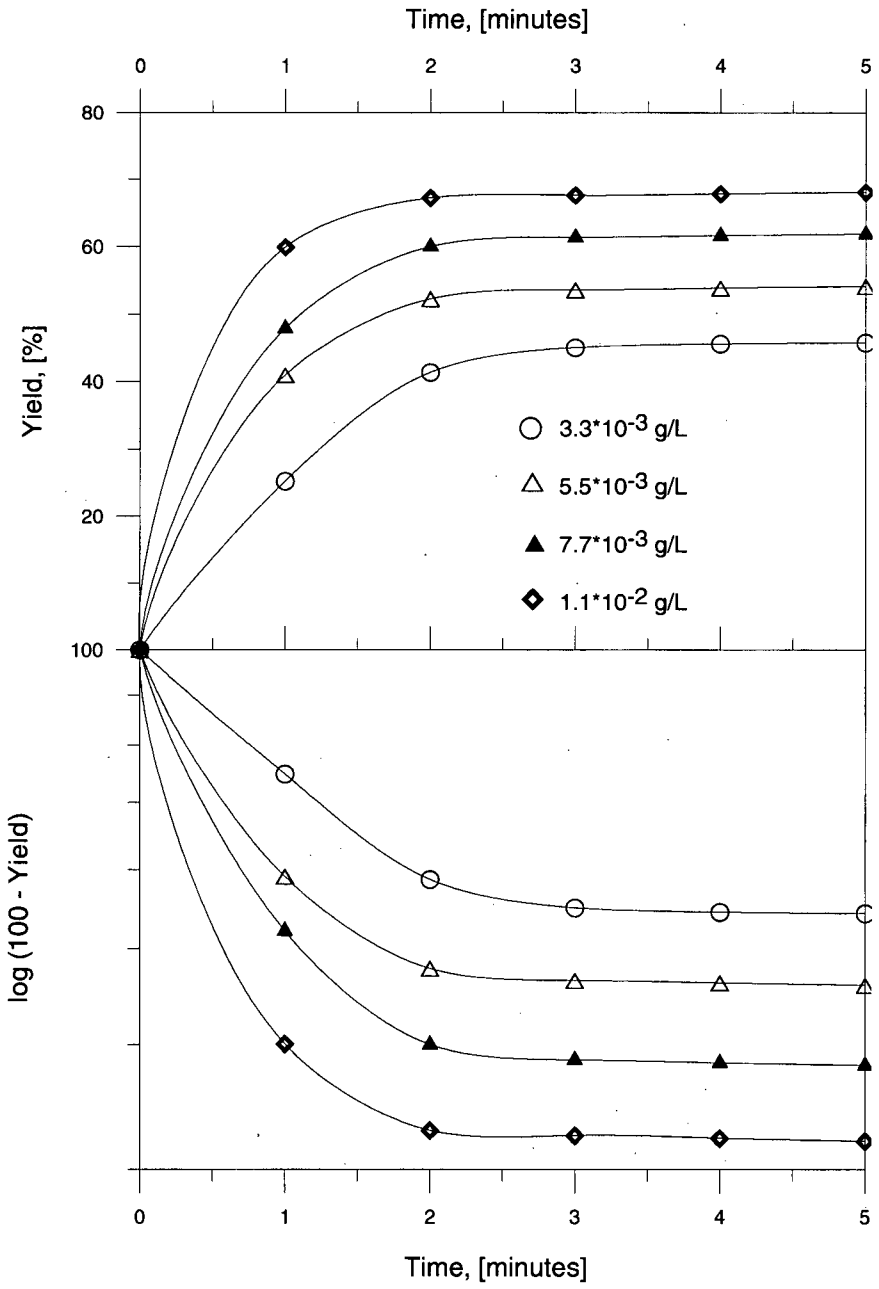

Figure 3a: Cumulative yield versus time and log(100-yield) versus time curves for MIBC at different concentrations.

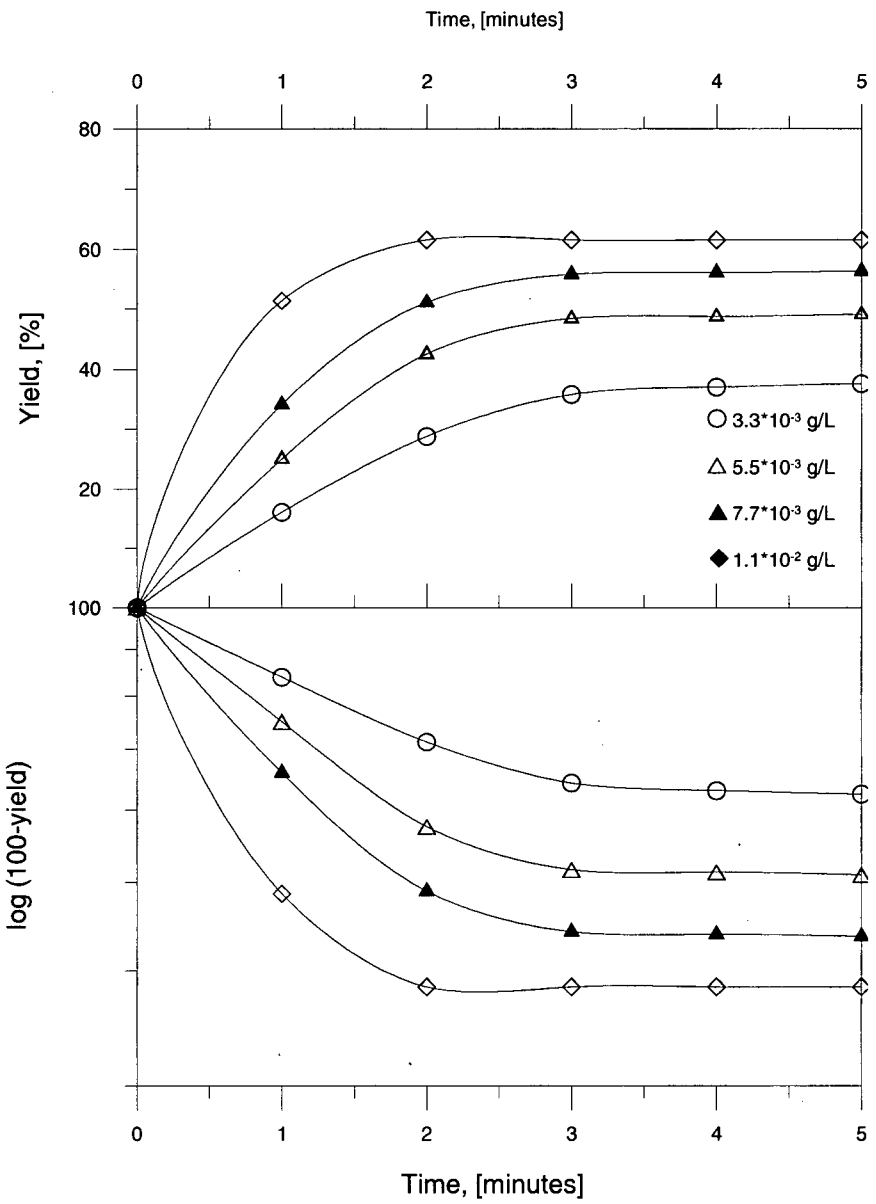

Figure 3b: Cumulative yield versus time and log(100-yield) versus time curves for α-terpineol at different concentrations.

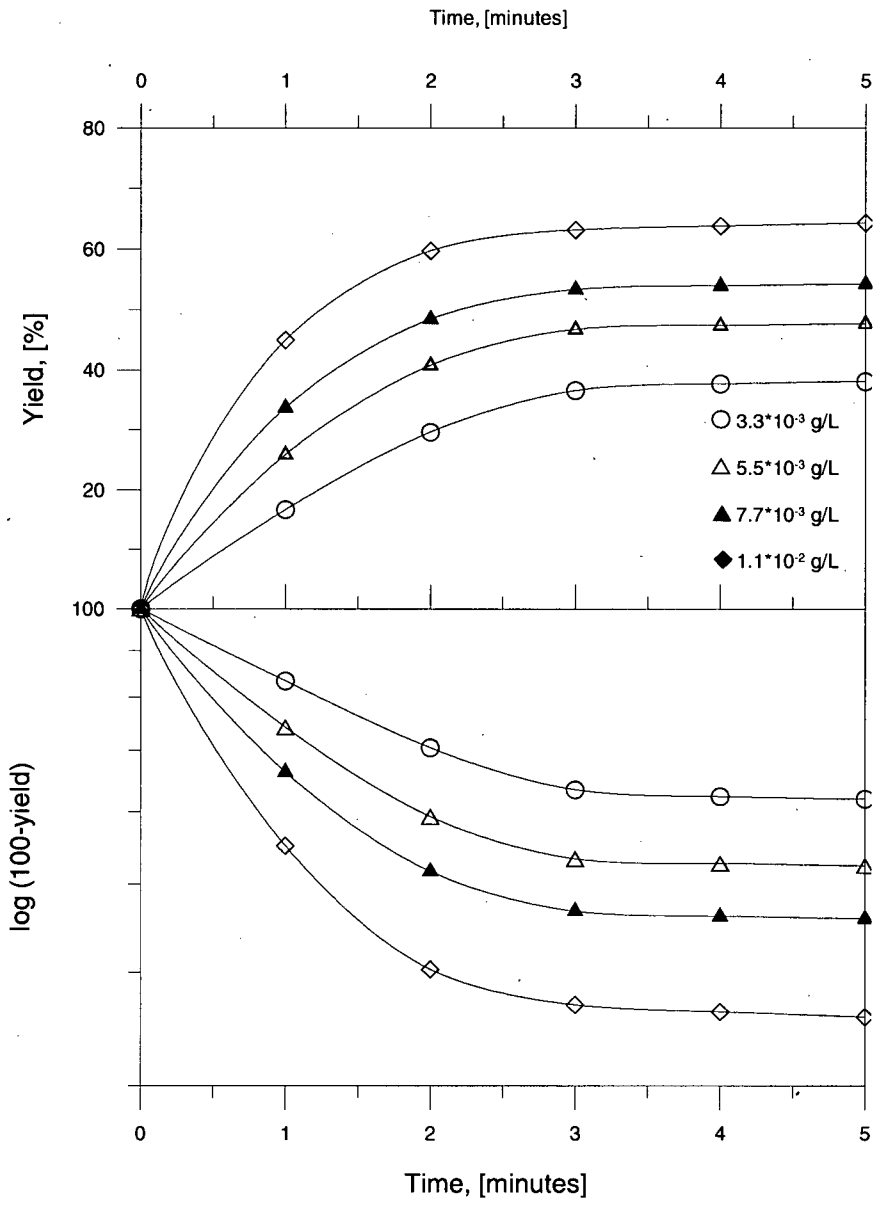

Figure 3c: Cumulative yield versus time and log(100-yield) versus time curves for DF-200 at different concentrations.

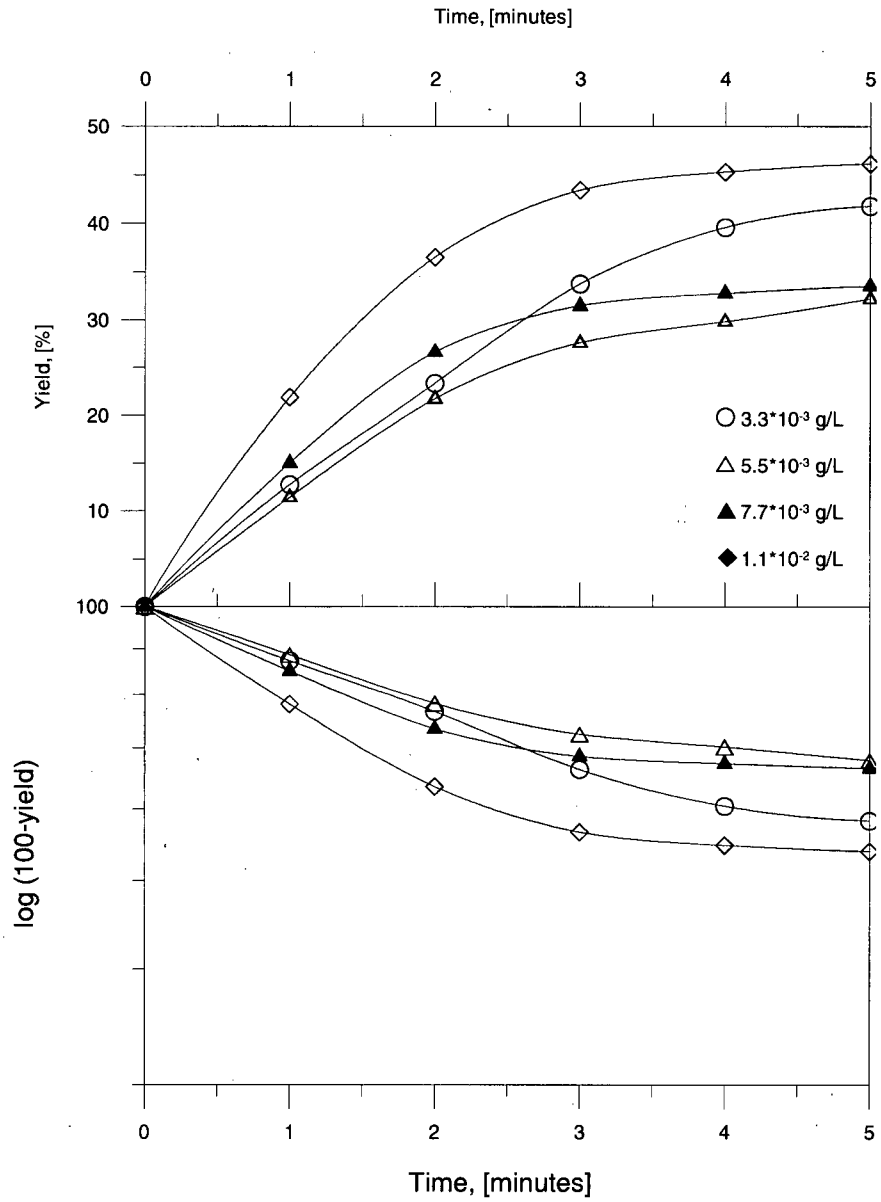

Figure 3d: Cumulative yield versus time and log(100-yield) versus time curves for DF-1012 at different concentrations.

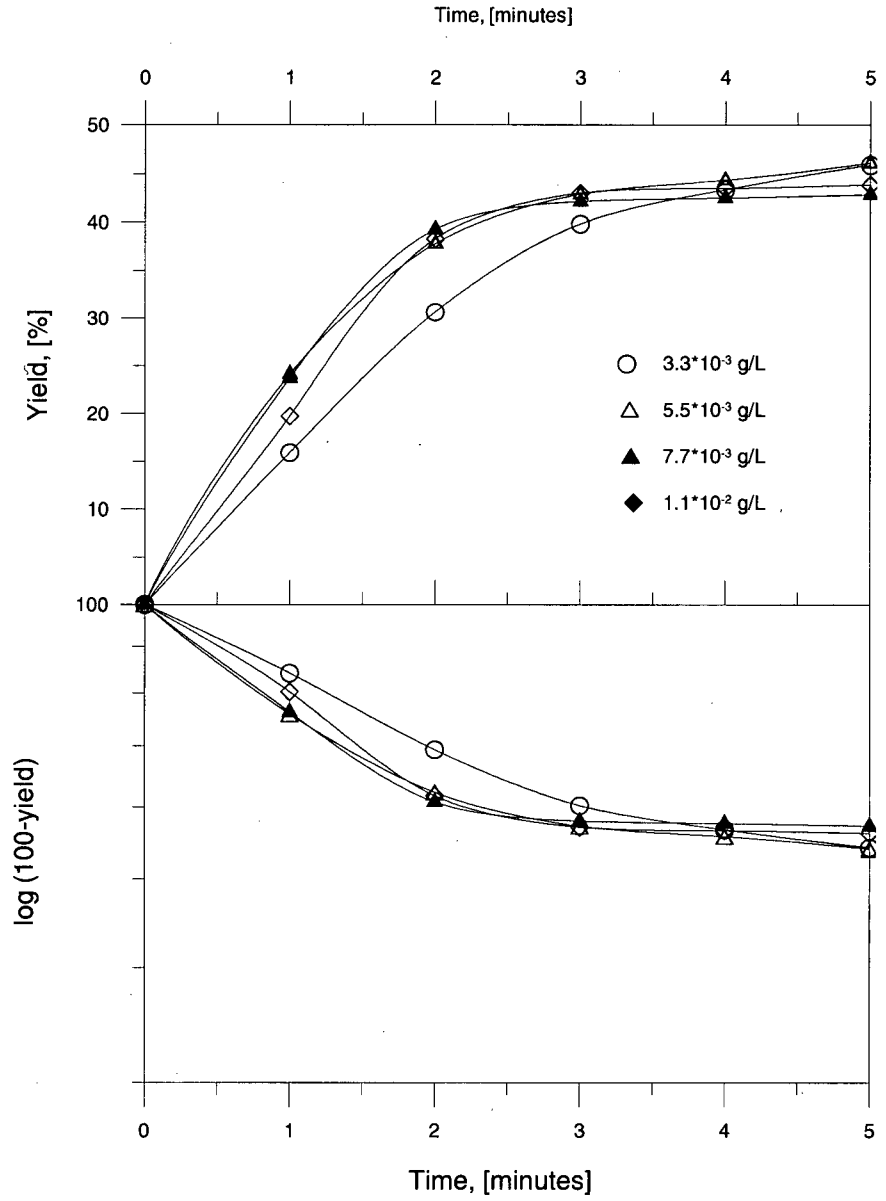

Figure 3e: Cumulative yield versus time and log(100-yield) versus time curves for diacetone alcohol at different concentrations.

APPENDIX 4

Rate of water recovery versus time curves for all the tested frothers.

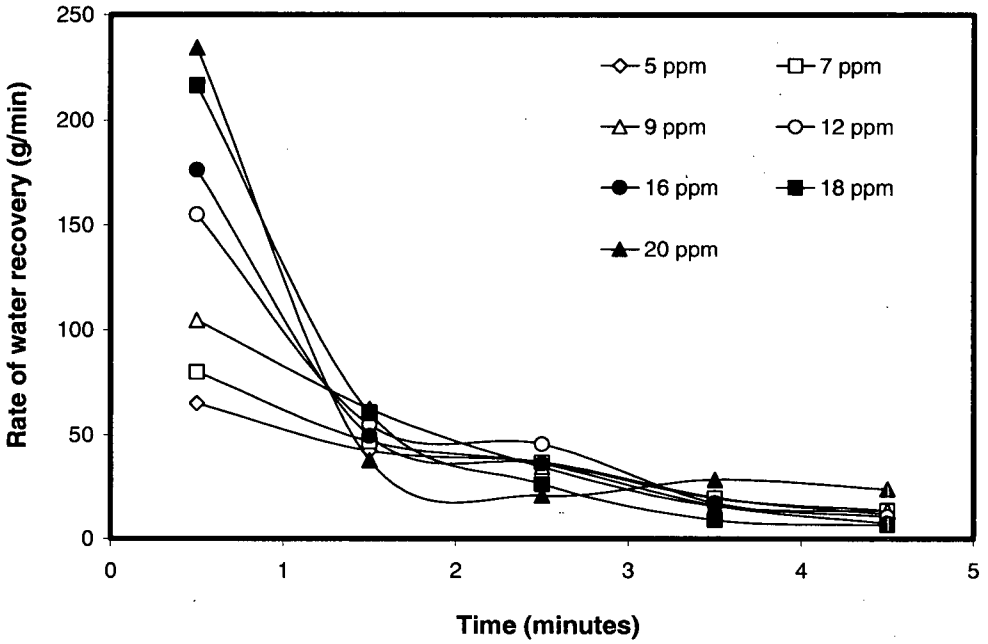

Figure 4a: Rate of water recovery versus time for α-terpineol solutions.

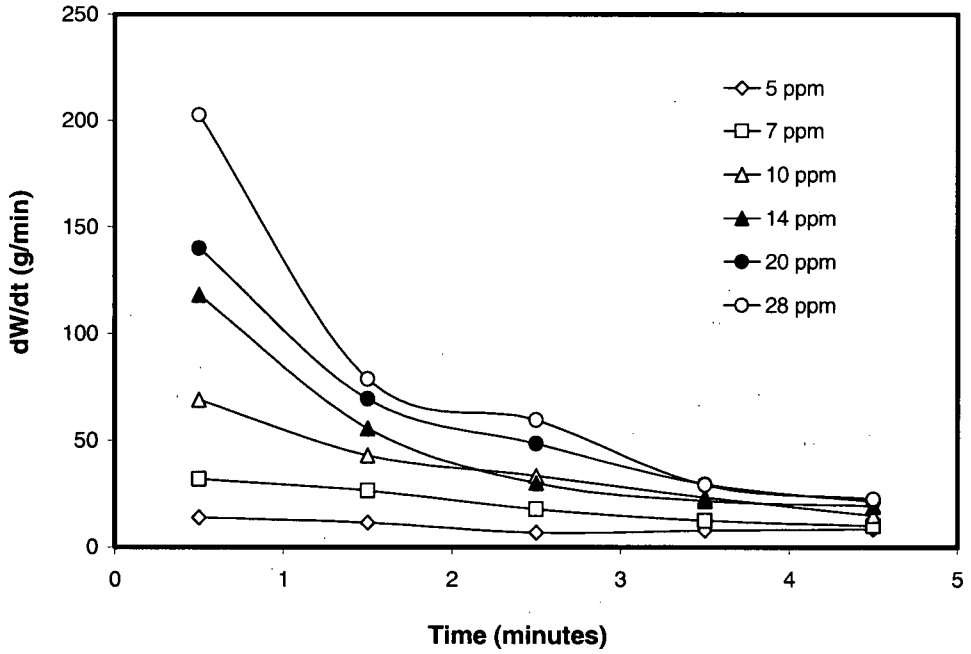

Figure 4b: Rate of water recovery versus time for DF-200 solutions.

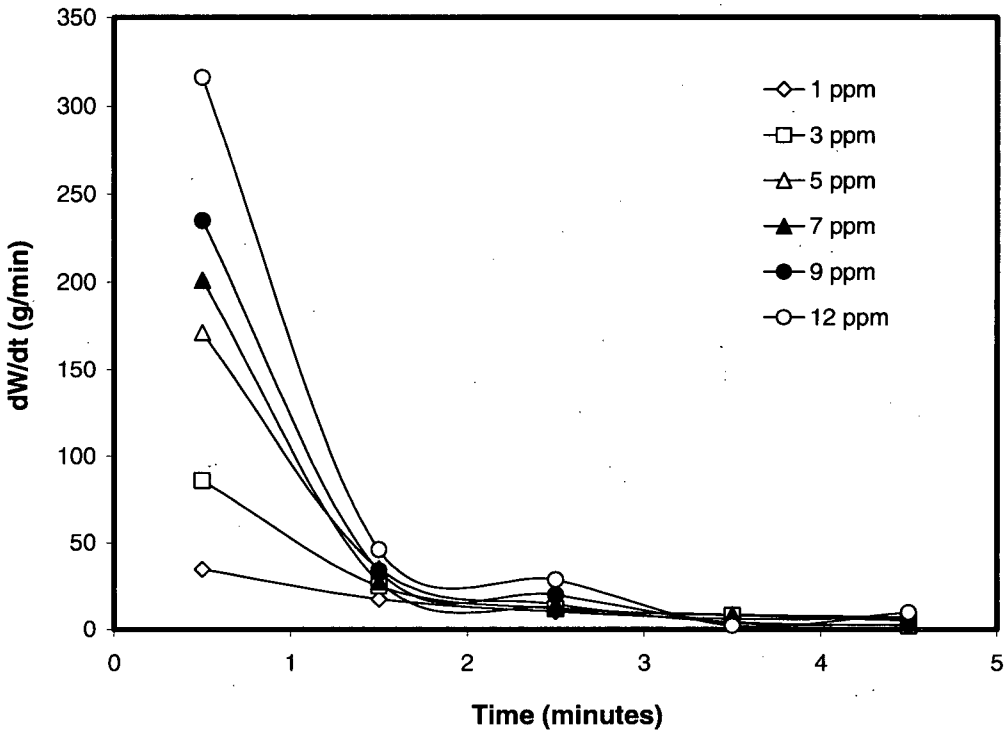

Figure 4c: Rate of water recovery versus time for DF-1012 solutions

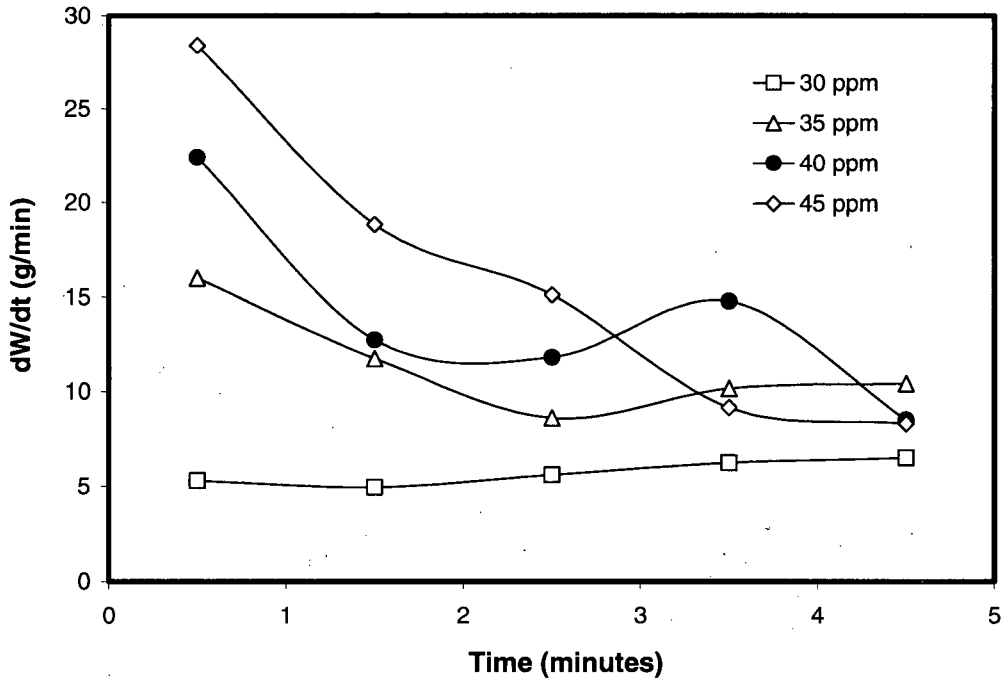

Figure 4d: Rate of water recovery versus time for diacetone alcohol solutions.

APPENDIX 5

Particle size distribution for silica (F4 coal-Silica mixture)

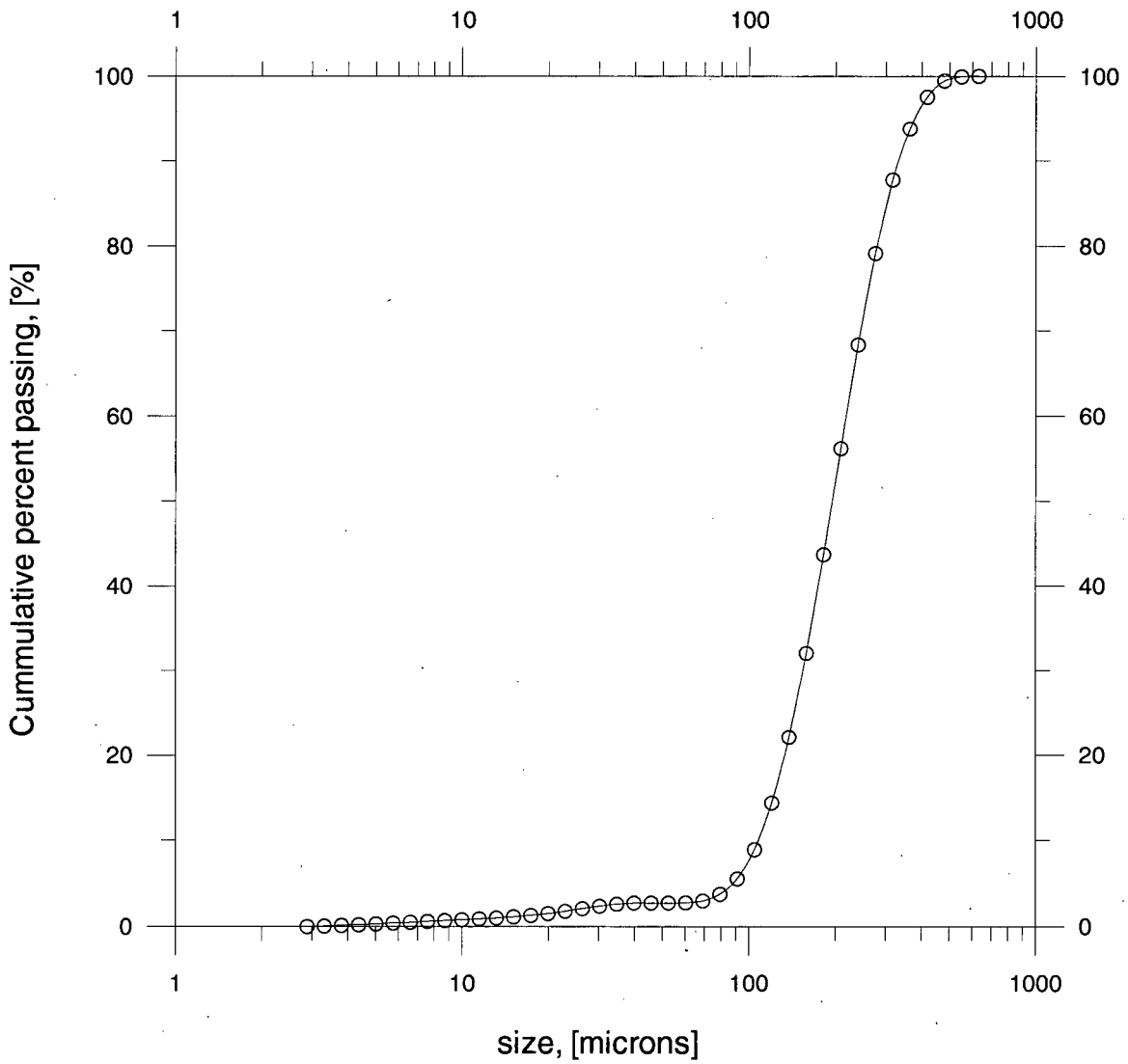

APPENDIX 6

Proximate analysis for bituminous coal used in additional tests with MIBC and DF-1012

Moisture, [%]	Ash, [%]	Volatile matter, [%]	Volatile Matter, d.m.m.f., [%]	Fixed Carbon, d.m.m.f., [%]
0.48	12.1	22.24	25.4	75.6

APPENDIX 7

Particle size distribution for fine silica used in additional tests with MIBC and DF-1012